AD-A048 823 LOUISIANA STATE UNIV BATON ROUGE COASTAL STUDIES INST F/G 8/3
A COLLECTION OF REPRINTS.(U)
DEC 77
UNCLASSIFIED TR-239 N00014-75-C-0192
NL

1 OF 1
AD A048823

END
DATE FILMED
2-78
DDC

(14) TR-239, TR-240

(1) U.S.

A COLLECTION OF REPRINTS.

(12) 93 p.

Coastal Studies Institute
Center for Wetland Resources
Louisiana State University
Baton Rouge, Louisiana 70803

Technical Report No. 239

WAVE ACTION AND SEDIMENT TRANSPORT ON FRINGING REEF

Joseph N. Suhayda and Harry H. Roberts

December 1977

Reprint from
Proceedings, 3rd International
Coral Reef Symp., University
of Miami, May 1977, pp. 65-70.

Office of Naval Research
N00014-75-C-0192
Project No. NR 388 002

Proceedings, Third International Coral Reef Symposium
Rosenstiel School of Marine and Atmospheric Science
University of Miami
Miami, Florida 33149, U.S.A.
May 1977

WAVE ACTION AND SEDIMENT TRANSPORT ON FRINGING REEFS

Joseph N. Suhayda and Harry H. Roberts
Coastal Studies Institute
Louisiana State University
Baton Rouge, Louisiana 70803

ABSTRACT

Measurements of wave processes, wave-driven currents, and sediment distribution have been made in several fringing reef systems. Wave height and wave period are typically reduced by about 50% as waves pass over the reef crest. This decrease depends primarily upon reef crest water depth, so that wave conditions in the back-reef lagoon show s[illegible]ficant changes over a single tide cycle. Wave-driven currents tend to flow continuously onsh[illegible] the reef crest. Their velocity is greatest near low tide, when wave breaking is most intense. [illegible] in the lagoon moat generally showed a tendency to drain the lagoon except during brief int[illegible] near flooding tide when a weak current reversal occurred. Sediment distribution in the lagoon displays a pattern that reflects current patterns in the lagoon and wave characteristics at the lagoon shoreline.

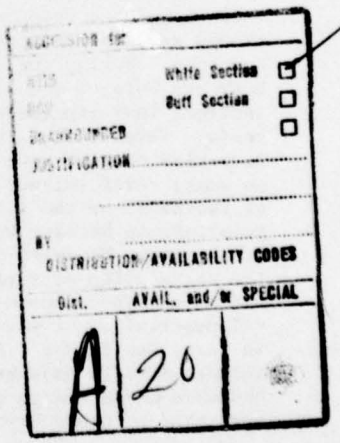

KEY WORDS: Waves, Fringing Reef, Wave-Driven Currents, Sediment Dispersal Patterns

WAVE ACTION AND SEDIMENT TRANSPORT ON FRINGING REEFS

Joseph N. Suhayda and Harry H. Roberts
Coastal Studies Institute, Louisiana State University
Baton Rouge, Louisiana 70803

Introduction

Recent investigations (1), (2), (3) continue to demonstrate the importance of waves and wave-driven currents to coral reef ecosystems. These studies have indicated that several effects result from wave action, including the direct physical force on coral branches and the movement of water and sediment within the reef system. There are, however, problems with making accurate field measurements of wave action and with relating these measurements to coral growth (or destruction). The variability of reef geometries worldwide implies that many studies will be required even to assess wave characteristics on reefs. A detailed quantitative understanding of wave processes occurring on reefs will develop only after acquisition of these field data. This study presents the results of direct measurements of waves and wave-driven currents in natural reef systems. The measurements were limited to fringing reefs where a well-developed shallow lagoon was present shoreward of the reef crest. Although this system is somewhat specialized, it does contain many of the features and processes occurring on reefs in general.

Few field measurements of wave action on reefs have been reported in the literature, even though studies relating to wave action have been numerous. During the late 1940s and early 1950s Munk and Sargent (4) and von Arx (5) initiated indirect investigations of wave processes on reefs. Several studies followed, including investigations of wave refraction and wave energy on small coral islands of the Campeche Bank (6); of the swell on the island of Aruba (7); of the relationship between wave power and island landforms on the Windward Caribbean Islands (8); of the correlation of reef variability and wave action on Grand Cayman (3); and of the theoretical description of wave-induced set-up of water on coral reefs (9). Direct measurements of wave thrust on reefs have been reported (10), (11), and wave measurements on a fore-reef shelf have been made on Grand Cayman (12).

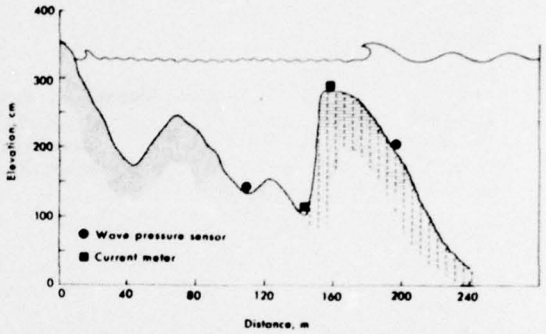

Figure 1. Profile view of reef and lagoon system on Great Corn Island, Nicaragua, and the location of wave and current instruments.

Wave Processes

A typical example of the type of reef system in which the wave measurements were made is shown in Figure 1. The reef is located on the northern coast of Great Corn Island, Nicaragua. The reef system includes a fringing reef barrier that slopes gently seaward and a steep landward-facing scarp. The reef encloses a lagoon having a sediment-covered floor and a well-developed moat immediately behind the reef. This segment of the fringing reef extends approximately 300 m along shore to a point where inlet channels occur and separate this reef from other extensions of the reef system. Waves typically break on the reef crest and continue breaking until they reach the moat. At the moat the breakers reform into nonbreaking waves and propagate shoreward with a height and period that are lower than offshore wave conditions. Wave-driven currents sweep across the reef crest, and the landward-facing scarp is formed by large ($\sim$0.5 m) pieces of coral rubble transported from the reef crest. Field sites having essentially the same reef crest and lagoon characteristics were studied on Grand Cayman, B.W.I.; Barbados, W.I.; and the northeastern coast of Brazil.

The shallow fringing reef crest is a critical zone for wave processes on reefs because

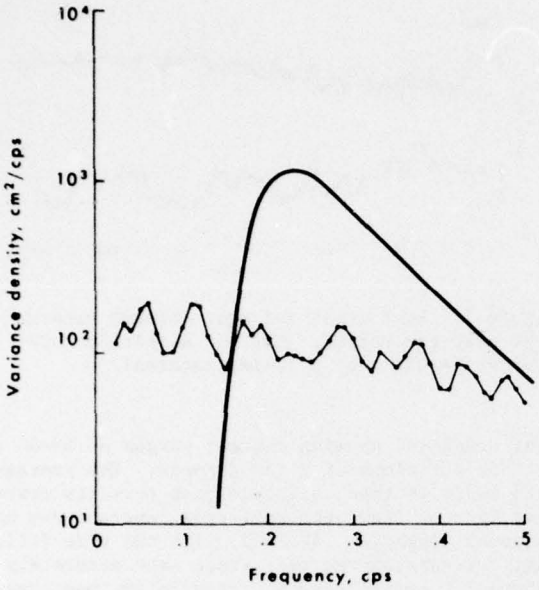

Figure 2. Wave spectra from a measurement inside the reef crest (dotted line) compared to Pierson-Moscowitz input spectrum (solid line) inferred from 6 m/sec trade wind, illustrating the extreme modification due to wave breaking [after (13)].

interactions there cause extreme modification of the incoming waves. The main feature of the reef crest affecting the waves is its shallow depth, typically 1 m, which normally causes wave breaking. Tide, of course, causes the actual depth to vary throughout the day. Waves may break continually as they transect the reef crest until reaching the deeper lagoon water, or they may propagate unbroken until secondary wave crests are formed. Observations at the point of reformation, taken in a fringing-reef-formed windward lagoon on Barbados, are shown in Figure 2. For comparison, the deepwater Pierson-Moscowitz (PM) spectrum for a typical trade wind speed [6 m/sec (13)] is also shown because no actual measurements were made on the fore-reef shelf. Two features are obvious: there has been a substantial loss of wave energy, and the wave spectrum has significantly changed shape. The estimated energy loss, calculated from the change in wave height, for the observed conditions is about 75%. This result is in rough agreement with laboratory measurements of wave transformation over a submerged shoal (14). This energy loss has not been uniform because the observed spectrum shows that considerable energy remains at low frequencies. Thus breaking has flattened the spectrum peak and perhaps transferred energy to low frequency. The exact amount of energy loss and the spectral change induced depend upon the depth of water over the reef crest and the input wave conditions. The reef crest did not contain surge channels, which have been observed in Pacific reefs (4) to significantly

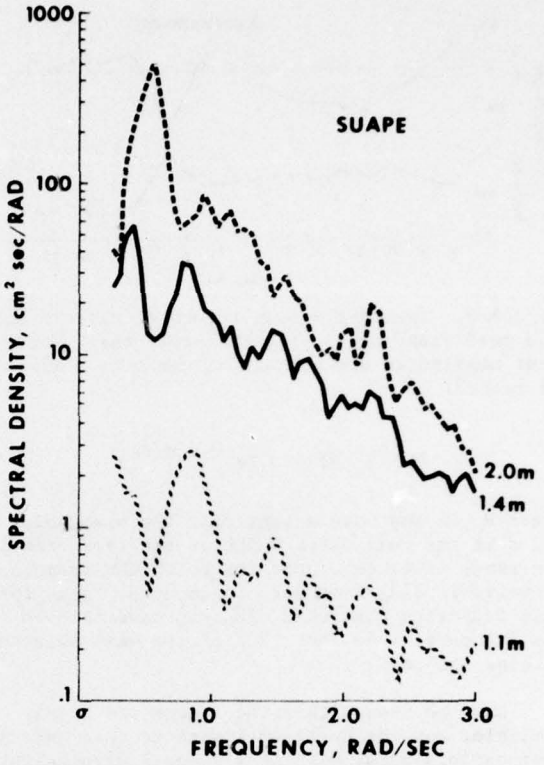

Figure 3. Measured wave spectra in the Suape Lagoon at different stages of the tide.

modify the incoming waves.

Measurements of waves near the shoreline at Suape, Pernambuco, Brazil, behind a beach rock barrier are summarized as wave spectra and are shown in Figure 3. Geomorphically, the beach rock barrier has the same basic components as most well-developed fringing coral reef systems: a seaward-sloping barrier, back-barrier moat, back-barrier lagoon, and occasional breaks in the barrier trend (inlets). The measurements shown are for three tide stages and show the effect of water level changes at the reef crest. At a tide datum of 1.1 m the water level was at the crest of the barrier. Wave height was 7 cm and the spectrum showed several peaks. At a tide level of 1.4 m the wave height had increased to 28 cm, and the height at a tide level of 2.0 m had increased to 56 cm. The offshore wave height was about 1 m.

The process of wave breaking is, at present, not well described by hydrodynamic theory. The decrease in wave height across a reef crest resulting from breaking can, however, be given empirically. Using the data of this study and published data (14), wave height at the point of reforming H is given by

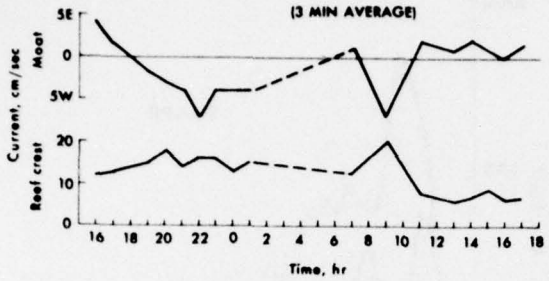

Figure 4. Twenty-six-hour record of current on the reef crest and in the back-reef moat. Current magnitudes are average values over 3 min of record.

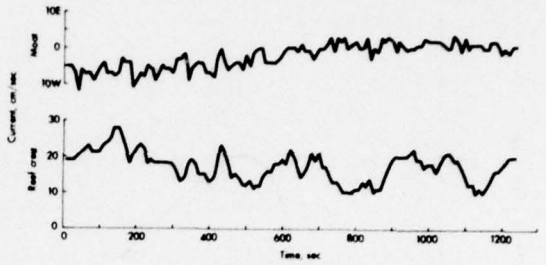

Figure 5. Reef crest and moat current records over a 20-min period. Current magnitudes are average values over a 10-sec interval.

$$H = H_o\ (1 - 0.8e^{-0.6\ d/H_o})$$

where H_o is the wave height near the breakpoint and d is the mean water depth at the reef crest. The range of water depths for which the formula is valid is d/H_o from zero to about 5. This formula indicates that when $d/H_o = 0$ wave heights in the lagoon will be about 20% of the wave heights outside the reef.

Wave periods within the lagoon are highly variable, and the spectrum indicates that several wave periods occur with nearly equal wave height. Generally, the mean wave period in the lagoon is smaller by about 50% to 75% than the wave period offshore.

Wave-Driven Currents

Waves that break on the reef crest drive water shoreward into the lagoon. This shoreward flow provides the mechanism for transporting water and sediment from the fore-reef shelf environment into the back-reef lagoon. Water brought across the reef crest has been shown to exit the lagoon through channels in the fringing reef (15), (16). Previous studies have suggested that tidal currents may reverse the direction of flow of water on the reef crest and in the reef channels. Current measurements were made at two locations on Great Corn Island to document the characteristics of reef crest and moat currents (Fig. 1).

The reef crest current meter was oriented in an onshore-offshore direction, and the moat current meter was aligned parallel to the alongshore dimension of the reef. The position of the moat current meter was near a break in the reef crest and probably reflects flow in the inlet channel.

Figure 4 shows current observations on the reef crest and in the moat over a 26-hour period. Data represent average current over a 3-min section of record. Actual instantaneous measurements show the effect of each wave transiting the reef crest and causing current surges of 50-80 cm/sec for durations of a few seconds. The average data indicate that, although moat currents reverse direction of flow, the reef crest current was continuously onshore. At 1600, with the tide falling, currents on the reef crest were moderately strong (10 cm/sec) and the flow in the moat was changing from east (or filling the lagoon) to strongly westward (draining the lagoon). Near low tide (0000), the reef crest current reached a maximum and currents in the moat reach a maximum. As the tide rose, the westward flow in the moat was reversed to eastward and reef crest currents generally decreased. Near high tide (~1200) reef currents are minimal and the current in the lagoon is eastward. This change in reef crest current flow results from the fact that at low tide wave breaking is more complete on the reef crest and more of the wave energy goes to driving the current over the crest and into the back-reef lagoon.

Figure 5 shows a sample of the averaged reef crest and moat current values over a 20-min period (1200 sec). At this time scale more detail of the time changes in the record is noticeable. The data show the importance of variations in speed at a period of about 100-150 sec on the reef crest. These variations may be related to long-period gravity waves generated on the reef face by the breaking waves and/or the effect of groups of high waves. The data indicate that variations about the mean speed of up to 50% can occur within 1 or 2 min. The moat current record shows no corresponding variations at 100-200 sec period; however, variations at approximately a 50-sec period do occur.

Sediment Movement

It has been suggested that circulation of water and sediment distribution within a fringing reef lagoon are determined by lagoon geometry and the input of water across the reef crest (15), (16). The inflow of water may be wave or tide induced, although wave input has been reported to dominate (5), (11). Wave-induced input results from wave breaking and set-up on the reef crest.

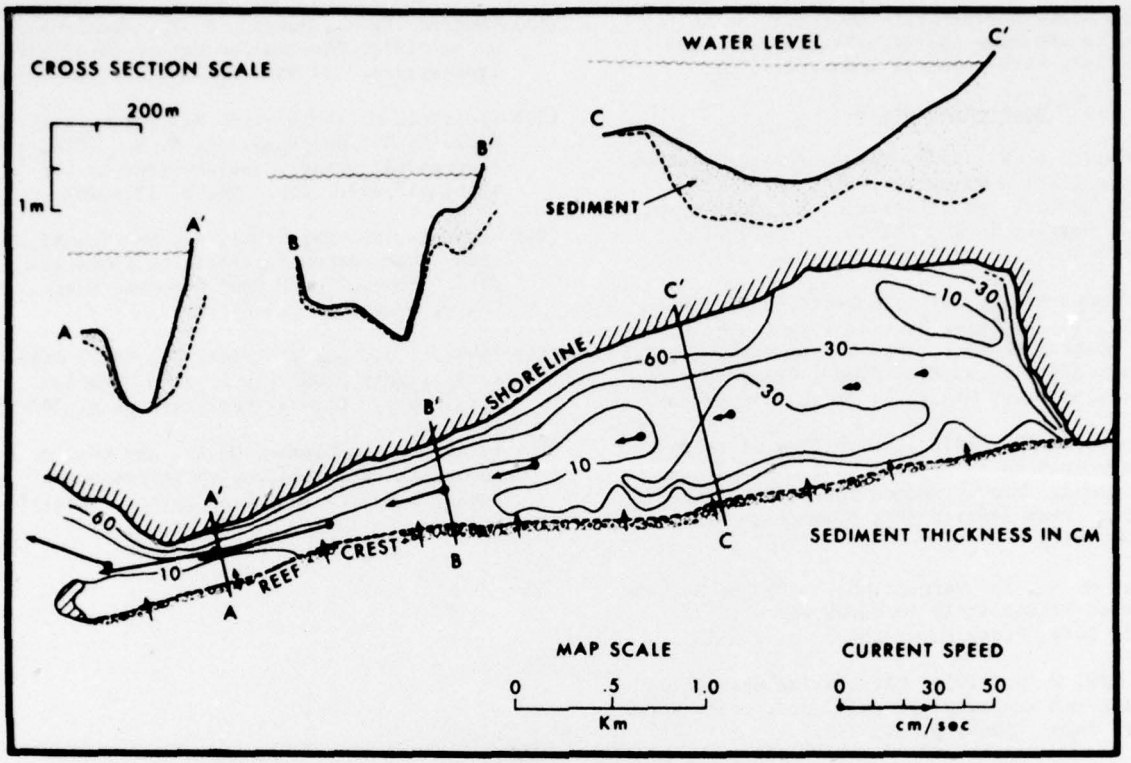

Figure 6. Sediment thickness distribution in South Sound shown in plan view and cross section, and the lagoon axis current speed (shown by arrows). Note the correspondence of the thick sediment accumulations and low speed, and thin sediment accumulation and high speed [after (12)].

which are enhanced as water depth on the reef crest decreases. Using the wave data taken during the Cayman experiment (12), the influx of water across the reef crest at South Sound, Grand Cayman, can be calculated. Conservation of this mass flux allows the average transport within South Sound to be calculated as a function of position down the axis of the lagoon. As a result of the geometry of South Sound (Fig. 6), the influx of water over the reef crest is funneled to the west. Currents in the lagoon calculated for an input current across the reef crest of 10 cm/sec are shown in Figure 6. Lagoon current speeds range from 2 to 45 cm/sec, being lowest in the eastern part. Examination of sediment thickness within the lagoon (Fig. 6), as determined by probe stations in a gridded array, indicates a distribution in accordance with the current field. Thick, fine-grained sediment accumulations occur in the eastern part of the lagoon (see section C-C'), and as the lagoon narrows and currents increase sediments become coarser and thickness decreases abruptly (section A-A', B-B'). Thick accumulations of relatively coarse sediments occur along the island coast as a result of beach building by wave action in the lagoon. For the given volume flux of water (400 m^3/sec) over the reef crest, the lagoon volume (3.3 x $10^6 m^3$) could be replaced in about 2.5 hours; the implication is rapid renewal of lagoon water. Thus it appears that sediment distribution and nearshore wave and current fields are linked in a system to reef crest and lagoonal morphology.

Conclusions

Measurements of waves and wave-driven currents at several field sites indicate that wave processes at the reef crest are intense and important to the movement of water and sediment in a fringing reef system. Wave height is reduced by breaking to a fraction (i.e., 40%) of input wave height. Wave breaking drives currents across the reef crest into the back-reef lagoon, and these currents appear to control circulation and sediment dispersal in the lagoon. Tidal variations in water level on the reef crest cause diurnal variations in both lagoon wave heights and wave-driven currents.

Acknowledgments

The research presented in this paper was supported by the Geography Programs, Office of Naval Research, Arlington, Virginia 22217, under a contract with the Coastal Studies Institute,

Louisiana State University. Appreciation is extended to the many individuals who made the foreign field work possible and successful.

References Cited

(1) Stoddart, D. R., 1973, Port-hurricane changes on the British Honduras reefs; re-survey of 1972. Proc., Second Inter. Coral Reef Symp., Great Barrier Reef Committee, Brisbane, p. 473-483.

(2) Hernandez-Avila, M. L., Roberts, H. H., and Rouse, L. J., 1977, Hurricane-generated waves and coastal boulder rampart formation. Proc., Third Inter. Coral Reef Symp., Great Barrier Reef Committee, Miami, in press this volume.

(3) Roberts, H. H., 1974, Variability of reefs with regard to changes in wave power around an island. Proc., Second Inter. Coral Reef Symp., Great Barrier Reef Committee, Brisbane, p. 497-512.

(4) Munk, W. H., and Sargent, M. S., 1954, Adjustment of Bikini Atoll to ocean waves. U.S. Geol. Surv. Prof. Paper 260-C, p. 275-280.

(5) von Arx, W. S., 1954, Circulation systems of Bikini and Rongelap lagoons. U.S. Geol. Surv. Prof. Paper 260-B, p. 265-273.

(6) Walsh, D. E., Reid, R. O., and Bader, R. G., 1962, Wave refraction and wave energy on Cayo Arenas, Campeche Bank. Texas A & M Res. Foundation Project 286(a), p. 1-62.

(7) Wilson, W. S., Wilson, D. G., and Michael, J. A., 1973, Analysis of swell near the island of Aruba. J. Geophys. Res. 78, p. 7834-7844.

(8) Hernandez, M. L., and Roberts, H. H., 1974, Form-process relationships on island coasts. Tech. Rept. 166, Coastal Studies Inst., Louisiana State Univ., 76 pp.

(9) Tait, R. J., 1972, Wave set-up on coral reefs. J. Geophys. Res. 77, p. 2207-2211.

(10) Shinn, E. A., 1963, Formation of spurs and grooves on the Florida reef tract. J. Sediment. Petrol. 33, p. 291-303.

(11) Storr, J. F., 1964, Ecology and oceanography of the coral-reef tract, Abaco Island, Bahamas. Geol. Soc. Amer. Special Paper 79, p. 1-98.

(12) Roberts, H. H., Murray, S. P., and Suhayda, J. N., 1975, Physical processes in a fringing reef system. J. Mar. Res. 33, p. 233-260.

(13) Garstang, M., LaSeur, N. E., Warsh, K. L., Hadlock, R., and Peterson, T. R., 1970, Atmospheric-oceanic observations in the tropics. Amer. Sci. 58, p. 482-495.

(14) Nakamura, M., Shiraishi, H., and Sasaki, Y., 1966, Wave dampening effect of submerged dike. Proc., Tenth Conf. Coastal Engr., Tokyo, Japan, p. 254-267.

(15) Kohn, A. J., and Helfrich, P., 1957, Primary organic productivity of a Hawaiian coral reef. Limnol. Oceanogr. 2, p. 241-251.

(16) Inman, D. L., Gayman, W. R., and Cox, D. C., 1963, Littoral sedimentary processes on Kauai, a subtropical high island. Pacific Sci. 17, p. 106-130.

Unclassified
Security Classification

DOCUMENT CONTROL DATA - R & D

(Security classification of title, body of abstract and indexing annotation must be entered when the overall report is classified)

1. ORIGINATING ACTIVITY (Corporate author) Coastal Studies Institute Louisiana State University Baton Rouge, Louisiana 70803	2a. REPORT SECURITY CLASSIFICATION Unclassified 2b. GROUP Unclassified

3. REPORT TITLE

WAVE ACTION AND SEDIMENT TRANSPORT ON FRINGING REEFS

4. DESCRIPTIVE NOTES (Type of report and inclusive dates)

5. AUTHOR(S) (First name, middle initial, last name)

Joseph N. Suhayda and Harry H. Roberts

6. REPORT DATE	7a. TOTAL NO. OF PAGES	7b. NO. OF REFS
December 1977	6	16

8a. CONTRACT OR GRANT NO.	9a. ORIGINATOR'S REPORT NUMBER(S)
N00014-75-C-0192 b. PROJECT NO. NR 388 002 c. d.	Technical Report No. 239 9b. OTHER REPORT NO(S) (Any other numbers that may be assigned this report) A043 695

10. DISTRIBUTION STATEMENT

Approved for public release; distribution unlimited.

11. SUPPLEMENTARY NOTES	12. SPONSORING MILITARY ACTIVITY
Reprint from: Proceedings, 3rd International Coral Reef Symp., University of Miami, May 1977, pp. 65-70.	Geography Programs Office of Naval Research Arlington, Virginia 22217

13. ABSTRACT

Measurements of wave processes, wave-driven currents, and sediment distribution have been made in several fringing reef systems. Wave height and wave period are typically reduced by about 50% as waves pass over the reef crest. This decrease depends primarily upon reef crest water depth, so that wave conditions in the back-reef lagoon show significant changes over a single tide cycle. Wave-driven currents tend to flow continuously onshore over the reef crest. Their velocity is greatest near low tide, when wave breaking is most intense. Current in the lagoon moat generally showed a tendency to drain the lagoon except during brief intervals near flooding tide when a weak current reversal occurred. Sediment distribution in the lagoon displays a pattern that reflects current patterns in the lagoon and wave characteristics at the lagoon shoreline.

14. KEY WORDS	LINK A		LINK B		LINK C	
	ROLE	WT	ROLE	WT	ROLE	WT
Waves						
Fringing reefs						
Wave-driven currents						
Sediment dispersal patterns						

Coastal Studies Institute
Center for Wetland Resources
Louisiana State University
Baton Rouge, Louisiana 70803

Technical Report No. 240

PHYSICAL PROCESSES IN A FORE-REEF SHELF ENVIRONMENT

Harry H. Roberts, Stephen P. Murray, and Joseph N. Suhayda

December 1977

Reprint from
Third International Coral Reef
Symposium, Miami,
Florida, May 1977, pp. 507-515.

Office of Naval Research
N00014-75-C-0192
Project No. NR 388 002

Proceedings, Third International Coral Reef Symposium
Rosenstiel School of Marine and Atmospheric Science
University of Miami
Miami, Florida 33149, U.S.A.
May 1977

PHYSICAL PROCESSES IN A FORE-REEF SHELF ENVIRONMENT

Harry H. Roberts, Stephen P. Murray, and Joseph N. Suhayda
Coastal Studies Institute
Louisiana State University
Baton Rouge, Louisiana 70803

ABSTRACT

Wave and current measurements were made across a rough-bottomed fore-reef shelf along the south coast of Grand Cayman Island. Wave heights attenuated 20% and current speeds 30% from the shelf margin (≈ 22-meter depth) to a depth of approximately 8 meters, a distance of ≈ 0.4 km. Strong, rectilinear tidal currents ($\sim$ 50 cm s^{-1}) dominated the deep shelf margin, but weak, directionally variable currents were characteristic of the shallow shelf. Attenuation of wave heights and current speeds across the shelf is attributed to frictional effects resulting from strong interactions with the unique boundary conditions of the extremely rough bottom.

A dye experiment illustrated that strong ($\approx$ 35 cm s^{-1}) on-shelf flow is directed up the deep coral reef grooves at the shelf margin. High levels of turbulence (turbulence intensity ≈ 23 cm s^{-1} diffusion coefficient ≈ 2.4 x 10^{3} cm^{2} s^{-1}) characterize this process.

Wave force-dominated versus current force-dominated portions of the fore-reef shelf were defined from *in situ* measurements. Variations in organic communities, growth forms, and reef structure are consistent with these zones.

KEY WORDS: Waves, Currents, Bottom Roughness, Fore-Reef Shelf, Turbulence, Tidal Current, Wave-Dominated Zone, Current-Dominated Zone

PHYSICAL PROCESSES IN A FORE-REEF SHELF ENVIRONMENT

Harry H. Roberts, Stephen P. Murray, and Joseph N. Suhayda
Coastal Studies Institute, Louisiana State University
Baton Rouge, Louisiana 70803

Introduction

General understanding of the magnitudes and spatial-temporal variations of physical processes (in particular waves and currents) on the seaward shelves of well-developed reefs is based on very few actual measurements. Recent work (1) has shown that the concept of tranquil conditions below the effective wave base on fore-reef shelves is not well founded. On the contrary, the margins of island shelves are commonly exposed to strong, periodic currents. The present paper is designed to present results of physical process studies conducted on the fore-reef shelf of Grand Cayman Island and to relate what we have learned about the physical environment to the reef and some of its constituents.

Figure 1 illustrates the central Caribbean location of Grand Cayman Island, where in situ data on waves and currents, as well as reef morphology, were collected. A site along the south coast was selected for study because of its well-developed reef morphology on the fore-reef shelf, its adequate exposure to dominant ocean waves, and its accessibility from our docking facility near Georgetown. As is characteristic of all fore-reef areas around the island, the shelf in the study area has a general stepped configuration and is very narrow (≈0.6 km wide). An abrupt break in slope at approximately 8 meters delineates the seaward edge of the shallow fore-reef terrace, and a second break in slope at approximately 20-22 meters marks the shelf edge and seaward margin of the deep fore-reef terrace. Along the south coast it is common for the shelf edge to display overhanging reef lobes or a near-vertical seaward-facing reef wall. This seaward reef face extends to various depths (commonly near 700-800 meters) where the deep island slope is encountered. Both the shallow and deep fore-reef terraces support coral communities that are viable but of somewhat different composition. The shallow terrace is dominated by Acropora palmata. Other corals, such as Diploria strigosa, Dichocoenia stokesii, Agaricia agaricites, Porites astreoides, and Montastrea annularis, are also common. In addition, Gorgonians and various alcyonarians are important members of the community. The deep fore-reef terrace can be divided into two zones based on composition of the coral communities: (1) an Acropora cervicornis zone and (2) a Montastrea annularis zone. Coral-covered ridges extend from the seaward extent of the shallow terrace to the buttress zone or shelf margin reef (2) at the shelf edge. These coral spurs are separated by sediment-floored grooves and larger open areas of sediment accumulation. Acropora cervicornis and Agaricia agaricites compose the dominant coral growth on the coral ridges, whereas Montastrea annularis, M. cavernosa, and Agaricia are the most important corals of the shelf margin reef.

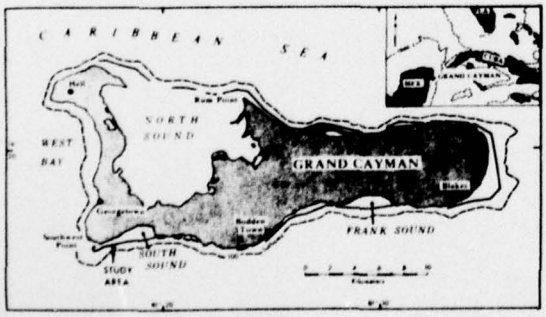

Figure 1. Location map of Grand Cayman Island and the area of study.

Bottom roughness of both the shallow and the deep terraces is primarily the result of coral-covered spurs oriented at a high angle to the coastline and separated by linear areas of sediment accumulation. The spurs and grooves of the shallow terrace generally have a shorter wavelength and smaller amplitude than similar features on the deep fore-reef terrace. Figure 2 quantitatively illustrates this relationship in the form of two bottom roughness spectra derived from the two bathymetric profiles run across the structural grain of the shelf at the approximate midpoints of the shallow and deep fore-reef terraces.

Because Grand Cayman is located in the central Caribbean region, it is sheltered by other land masses from strong storm swells that originate in high latitudes. Therefore, the trade wind system is the driving force behind the wave regime. The process climate in which Grand Cayman resides can be characterized as follows: (1) a

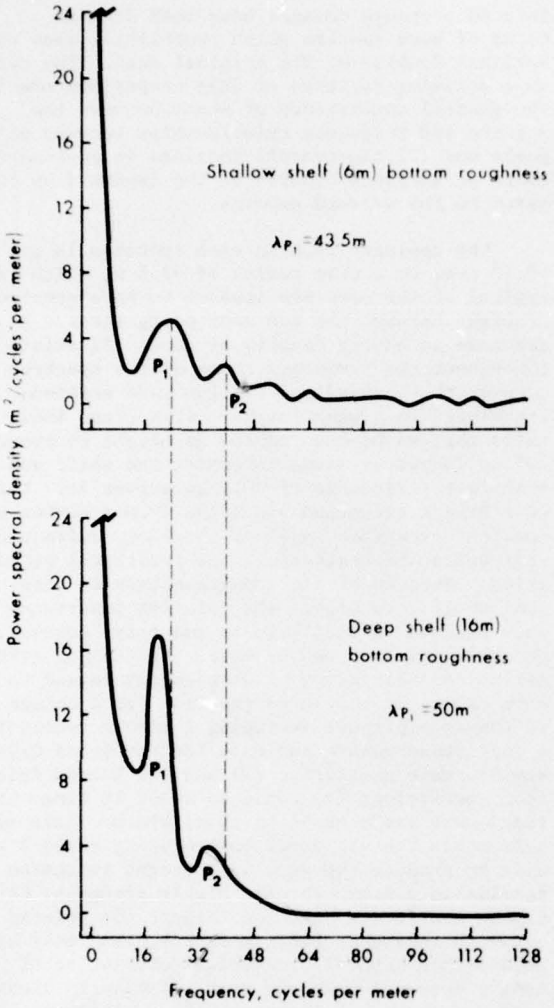

Figure 2. Bottom roughness spectra of the shallow and deep fore-reef terraces in the study area. Note the longer wavelengths and greater amplitude (related to peak heights) of the forms on the deep shelf terrace.

mixed diurnal and semidiurnal microtidal regime, (2) a moderately strong unidirectional trade wind and wave field, (3) moderate-strong oceanic currents, (4) a sheltered position with regard to high-latitude storm swell, and (5) occasional hurricane winds and waves.

Data Collection Methods

Wave and current data were collected from the instrument array shown in Fig. 3. Instrument positions are plotted on a bathymetric profile of the fore-reef shelf that illustrates the extreme irregularity of the bottom--i.e., the spur and groove morphology oriented across the

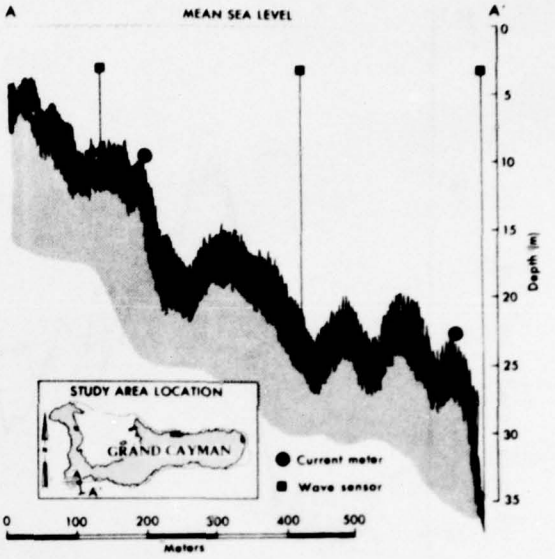

Figure 3. Bathymetric profile across the fore-reef shelf in the study area adjacent to South Sound (see Fig. 1). Note the extreme bottom roughness resulting from coral-covered spurs and intervening sand-floored grooves. Locations of wave and current sensors are plotted on the shelf profile.

shelf, plus the two submarine terraces positioned along the shelf. Instruments were positioned so that the modification of both waves and currents could be assessed as they impinged on the shelf and propagated over a surface of unusual bottom roughness. Tide measurements were made with a capacitance tide gage installed in the back-reef lagoon adjacent to the shelf study area.

In situ continuously recording, bottom-mounted current meters (Marine Advisors Q-16) were used. One current meter was deployed at the seaward margin of the shallow fore-reef terrace (≈8 meters). A second current meter was positioned on top of a coral spur at the shelf edge (≈21 meters), where unobstructed on-shelf currents could be monitored. Data collection was continuous over a 2-week period.

Current meters were not deployed in the deep grooves at the shelf margin. In order to measure the hydrodynamic activity levels in this environment, a dye experiment was designed. Time-lapse photographs were taken as dye (Rhodamine B) was diver released at a depth of ≈33 meters on the groove floor. The experiment was conducted during a peak in the current cycle to assess whether the grooves were active or passive structures with regard to the on-shelf movement of oceanic water.

Wave data were collected from three absolute

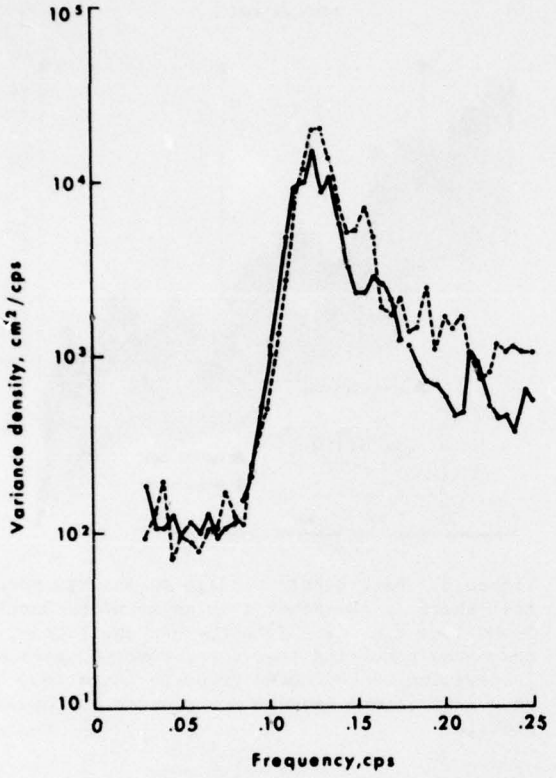

Figure 4. Wave spectra (variance density) from wave measurements at the shelf edge (dashed line) and near the shallow reef crest (dotted solid line).

pressure sensors buoyed at the shelf edge, mid-shelf, and mid-shallow fore-reef terrace positions. The output from each sensor was corrected to give surface measurements. Pressure changes caused by passing waves were registered on a boat-based Brush analog recorder. Sensor depth was read before each measurement by employing a low-pass filter. Data collection periods were ≈20 min at each sensor site. Multiple readings were taken. Data from the pressure sensors were used to define wave spectra at three locations on the shelf.

Results

Comparison of wave data collected at three points on the fore-reef shelf of Grand Cayman Island (Fig. 3) indicates that deepwater wave characteristics are significantly modified by reef morphology. An interesting point concerning these modifications is that changes occur over a very short lateral distance (≈0.4 km). Figure 4 illustrates data taken from the seaward (shelf edge) and landward (near the shallow reef crest) wave monitoring stations. In this figure, wave-induced pressure changes have been defined in terms of wave spectra which essentially show the variance density of the original data. The two most striking features of this comparison are (1) the general consistency of shape between the spectra and frequency relationships between major peaks and (2) the overall decrease in peak amplitudes or variance density of the landward as compared to the seaward spectra.

The dominant peak in each spectrum is at ≈0.13 cps, or a wave period of ≈7.6 s, which is typical of the area and appears to have remained constant between the two monitoring sites. A decrease in energy density of about 45% exists throughout the frequency range of the spectrum between the seaward and the landward stations. Translated into wave heights, this trend indicates that waves are reduced in height by about 20% as deepwater waves intersect the shelf and translate a distance of ≈0.4 km across it. This wave height reduction can arise from a number of combined processes, such as shoaling, refraction, reflection and scattering, and frictional attenuation. Because of the complex nature of fore-reef shelf morphology, the relative importance of each process is difficult to quantify; however, general estimates can be made. Frictional attenuation and scattering of wave energy depend to some extent on bottom roughness. For a bottom roughness amplitude averaging 2 meters (which is a very conservative estimate for the Grand Cayman shelf), wave scattering (3) and the bottom friction coefficient (4) would be about 10 times that found on a sandy shelf of equal width. This estimate means that it would take a sandy shelf 4 km wide to produce the same wave height reduction as results in 0.4 km over the highly irregular Grand Cayman shelf. As Munk and Sargent (5) pointed out with regard to Pacific atolls, the reefs are molded into natural breakwaters consisting of long ridges and channels that efficiently dissipate the energy of incoming waves. Although Munk and Sargent were primarily referring to shallow surge channels and their seaward extensions, the concept is valid for all depths where waves feel bottom and is the configuration common to the entire Grand Cayman shelf. Wave reflection could be significant in some circumstances, but because of the extreme complexity of the shelf morphology it is difficult to estimate. Taking the seaward face of the shallow fore-reef terrace alone, the reflection coefficient (4) is about 0.1 or 10%. Refraction and shoaling can also result in reduced wave heights. For the example given in Fig. 4 a reduction of about 10% is estimated; however, roughness of the fore-reef shelf may cause changes in the wave phase speed. Because of energy losses resulting from percolation and water movement into the reef matrix and sediment, this process cannot be estimated at the present time. Several studies (5), (2) have shown that the wave field plays a major role in determining reef morphology. From the present study it is also apparent that the reef morphology or bottom roughness strongly affects wave processes. Therefore, variability

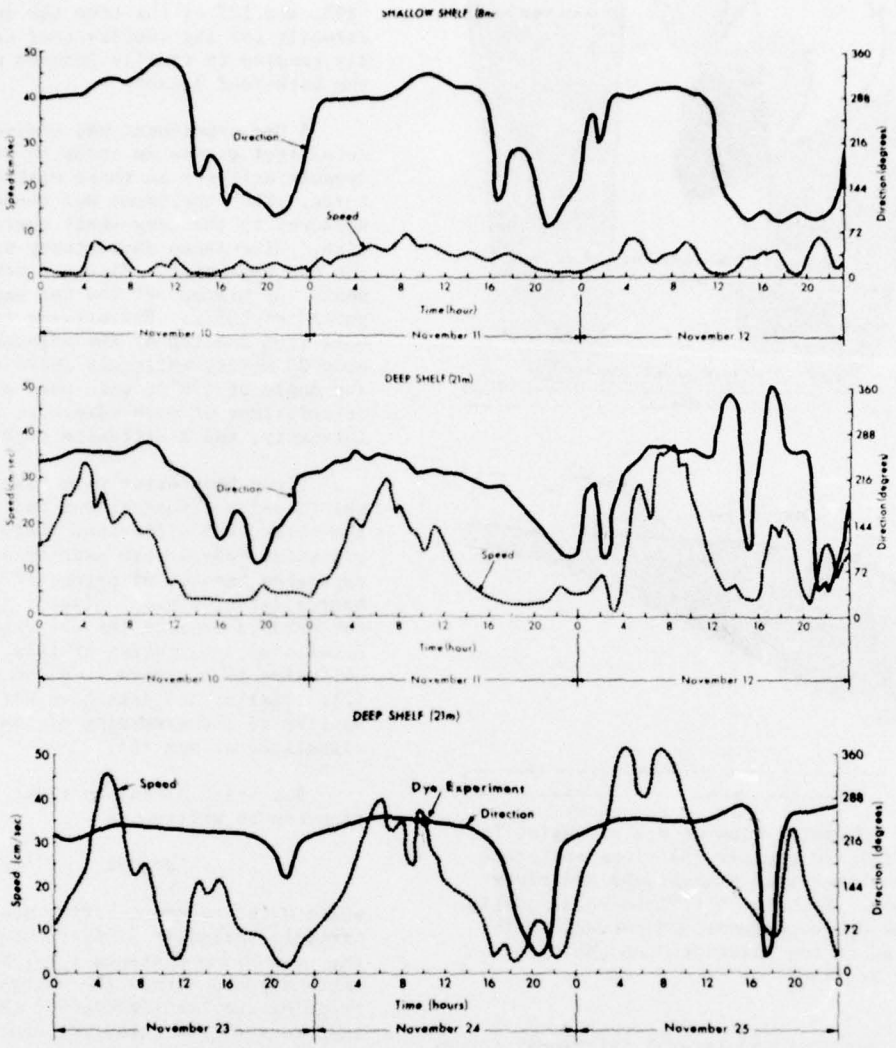

Figure 5. Time-series plot of current speed and direction from both shallow and deep fore-reef shelf current meter stations. Note the position in the current cycle when the deep coral reef groove dye experiment was conducted.

in reef morphology implies a correspondingly strong variability in the rate of the aforementioned wave processes.

Figure 5 illustrates the time-dependent behavior of currents monitored at both the edge of the shelf and the margin of the shallow fore-reef terrace (Fig. 3). Although these and other records from the Cayman shelf were collected in a region strongly influenced by the steady trade winds, currents display very distinct variations in both speed and direction. Records from the deep shelf current meter station clearly show periodicities in current magnitude and direction that are near the diurnal tidal frequency. Shallow fore-reef terrace data sets generally illustrate the same basic trend; however, currents are greatly reduced and more directionally variable. Current speeds at the shelf edge commonly were in excess of 50 cm s^{-1} at the peak in the current cycle, whereas currents on the shallow shelf rarely exceeded 15 cm s^{-1} and generally were <7.5 cm s^{-1}. Current speeds at the deep terrace are distinctly higher, averaging 21.9 cm s^{-1} over a selected 6-day period. A comparison of current speeds at the two monitoring sites over the same time period discloses a 60-70% speed reduction from the deep-shelf station, a distance of ≈0.4

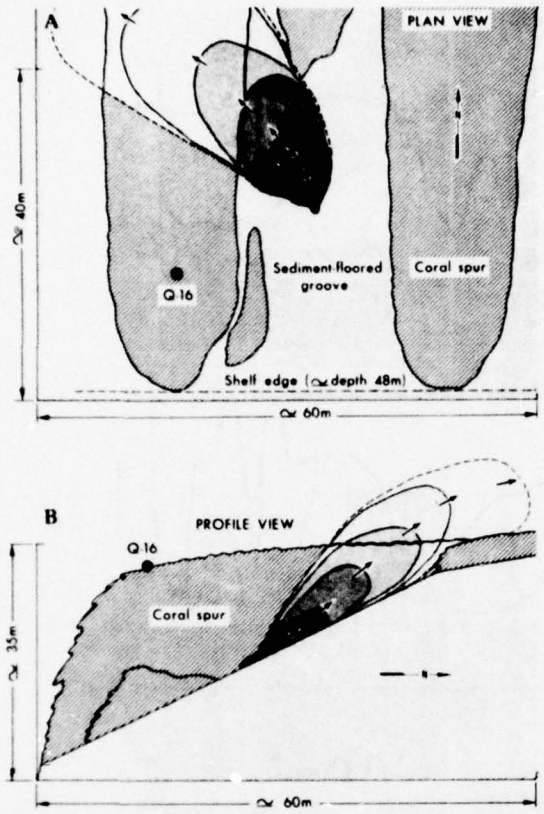

Figure 6. Schematic view of dye expansion in both plan (A) and profile (B) views as interpreted from time-lapse photographs and diver observations. See Fig. 5 for the relationship between the dye experiment and current cycle as monitored at the adjacent deep shelf current meter station.

km. Large vertical and lateral frictional forces associated with the shelf's reef induced extreme bottom roughness and wall roughness, which are probably responsible for the remarkable attenuation of the current speed over such a short expanse of shelf.

In addition to being considerably stronger, currents on the deep fore-reef shelf are much more unidirectional. West- (on-shelf) and slightly southwest- (along-shelf) setting currents account for ≈85% of the total bottom currents at this site. As can be seen in Fig. 5, the directional trace is characterized by long periods of unidirectional flow that are interrupted by short intervals of current reversal accompanied by minimums in the speed record. Currents on the shallow shelf are generally much more directionally variable, although this trend is not especially clear in the record selected for Fig. 5. As might be expected, the dominant shallow current is to the west (≈60%). A secondary east to southeast direction accounts for ≈29%, and 10% of the time the current flows south, directly off the shallow reef crest, and is probably related to tidally induced water exchange with the back-reef lagoon.

A dye experiment was conducted in a deep coral reef groove in order to determine the hydrodynamic activity in these distinct shelf-edge features. The experiment was conducted in a groove adjacent to the deep-shelf current meter mooring site. Time-lapse photography was used to track the dye expansion. Figure 6 schematically represents the history of the dye expansion over a time period of 105 s. Photographs taken at 15-s intervals from the top of the adjacent coral spurs, some 20 meters obliquely above the injection point (an angle of ≈70°), were used as a data base for calculations of mean advection speed, turbulence intensity, and a diffusion coefficient.

Plume boundaries were traced from the original time-lapse photographs and used to quantify the horizontal diffusion. Only the first four exposures (60-s) were used to quantify plume expansion because of perspective problems and source deterioration. Taylor (6) diffusion theory was used to analyze the dye expansion behavior. Details of application of this theory to the dye diffusion in a groove is given by Roberts et al. (7). Similar analyses have been successfully applied to the spreading of continuously emitted oil slicks at sea (8).

For brief diffusion times Taylor's (6) relation can be written as

$$d\sigma_y/dx = \langle V'^2 \rangle^{1/2}/U \qquad (1)$$

where σ is the cross-stream standard deviation of particle spread (≈ visible outline of plume), x is the down-plume distance = Ut, U is the constant ambient speed across the source, measured by tracking the leading edge of the dye plume, V' is the cross-stream turbulent speed, and the angle bracket is the averaging operator. Long diffusion times can be expressed by

$$d\sigma_y^2/dx = 2\langle V'^2 \rangle^{1/2}\, \ell^*/U \qquad (2)$$

where ℓ^*, the Lagrangian scale length, commonly is considered a representative eddy size. Thus $d\sigma_y/dx$ for short distances and $d\sigma_y^2/dx$ for long distances should be constants (all terms on the right side of eqs. 1 and 2 are known to be approximately constant). The tangent of half the angle of expansion of the plume ($d\sigma_y/dx$) can now be measured from the photographs, which give a turbulent intensity $\langle V'^2 \rangle^{1/2} \approx 24$ cm s^{-1} from eq. 1, as U is already known from movement of the plume front (≈35 cm s^{-1}). Average values of the relative turbulent intensity, $\langle V'^2 \rangle^{1/2}/U$, from both field and laboratory studies varies between 0.05 and 0.20. Murray (9) reported a value as high as 0.25 during a hurricane. An extremely high value of ≈0.7 was obtained from this study and appears to be the result of current and/or wave inter-

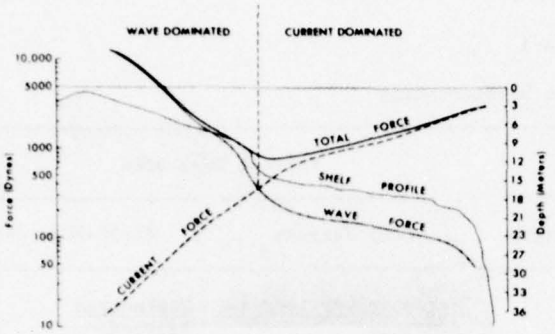

Figure 7. Distribution of wave and current forces across the fore-reef shelf calculated for a vertical surface oriented directly into the flow. Basic zonation of the reef is shown in relation to the force curves.

actions with the unusual wall roughness of the confining coral spurs. Other published values are from situations of unconfined flow.

A diffusion coefficient, K_y, can be expressed as

$$K_y = U/2\ (d\sigma_y^2/dx) = \langle V'^2 \rangle^{1/2}\ \ell^* \qquad (3)$$

For the groove experiment a value of 2.4×10^3 $cm^2\ s^{-1}$ was calculated. This value is an order of magnitude greater than might be expected from previous studies, summarized in Okubo's (10) diffusion diagram, if a 12-meter groove spacing is used as a diffusion scale. Both turbulence and turbulence intensity appear to be considerably stronger in the deep coral reef groove than any normal channelized or open ocean conditions would suggest.

Concluding Remarks

Results of physical process studies on a narrow fore-reef shelf are summarized in Fig. 7 and Table 1. Wave- and current-dominated parts of the shelf are defined in Fig. 7, where a common measure of their force across the reef profile is plotted. Representative current speeds, wave characteristics, and bathymetry from field data were used in the force, F, calculations. The common quadratic stress law, $F = 1/2\ \rho A C_d U^2$, was used, where ρ is the density of seawater, A is an exposed cross-sectional area (taken as 1 cm^2 on a vertical plane), C_d is the drag coefficient [taken as 1.95 (11)], and U is velocity ($cm\ s^{-1}$). A representative current speed of 50 $cm\ s^{-1}$ (includes both wind and tidal currents) was decreased linearly across the shelf following measured velocities at the shallow shelf current meter station and the fringing reef crest. Wave force calculations were made for typical trade wind generated waves (T = 6 s, H = 75 cm) by estimating maximum orbital speeds from linear wave theory.

It is interesting to note (Fig. 7) that current-induced forces at the shelf edge are approximately equal to wave-induced forces at a depth of ≈3 meters near the fringing reef crest. Crossing of the wave and current profiles (Fig. 7) delineates a position that separates the shallow wave-dominated portion of the shelf from the deeper current-dominated zones. Sediments have accumulated in abundance at this site and appear to be relatively stable, forming a mid-shelf sediment reservoir. Also, at this position on the shelf the coral community changes from a shallow, wave-resistant Acropora palmata dominated assemblage to a deeper group characterized by the intricately branched Acropora cervicornis (Table 1). Obviously, the manner in which the force is applied will help determine the response characteristics in the coral community. Periodic oscillatory perturbations by waves, for example, may result in quite different growth form responses from those produced by more steady, long-term current oscillations. These detailed interactions are, however, beyond the scope of this paper. Less detailed form-process relationships are summarized in Table 1.

In summary, the following statements can be made as a result of the physical process study of Grand Cayman's fore-reef shelf:

(1) A feedback relationship exists on the fore-reef shelf such that reef morphology and composition are somewhat dependent on the combinations, intensities, and spatial-temporal variations of physical processes while at the same time the rates of these processes are distinctly influenced by reef morphology and its associated bottom roughness.

(2) An interaction between deepwater waves and shelf morphology results in a 20% decrease in wave height over an ≈0.4-km width of shelf. This attenuation rate is about 10 times that expected for a sandy shelf.

(3) High-velocity (>50 $cm\ s^{-1}$), rather unidirectional currents that have a diurnal tidal frequency were found to dominate the deep fore-reef shelf. Shallow shelf currents were found to be weak and directionally variable. A current speed attenuation of 60-70% from the shelf edge to the shallow fore-reef shelf is attributed to lateral and vertical frictional attenuation associated with the unusual bottom roughness.

(4) A dye experiment conducted at the peak of the tidal current cycle in a deep shelf-edge groove illustrated that on-shelf flow is directed up-groove. Remarkably high levels of turbulence (turbulence intensity ≈23 $cm\ s^{-1}$, diffusion coefficient ≈2.4×10^3 $cm^2\ s^{-1}$) characterize this channelized flow.

(5) Calculations illustrate the greater relative importance of current forces over wave forces on the deep fore-reef shelf. Current force on the

Table 1

Major Form-Process Relationships

	Wave Dominated		Current Dominated	
Parameters	Near-Reef Crest	Shallow Terrace Margin	Deep Terrace	Shelf-Edge Reef
Zonation	Acropora palmata Millepora alcicornis	Acropora palmata Agaricia	Acropora cervicornis Agaricia	Montastrea Agaricia
Growth Forms	Thickly branched Bladed Encrusting	Branched Bladed	Delicately branched Massive	Massive Platelike
Coral Cover	Moderate	Moderate	Abundant	Abundant
Bottom Roughness	<2 meters	<5 meters	<4 meters	<30 meters
Shelf Morphology	Limestone pavement, low-relief spurs and grooves	Moderate-relief spurs and grooves	Moderate-low-relief spurs and grooves	High-relief spurs and grooves
Sediment	Sparse	Thin veneer in grooves	Extensive impounded sediment plains	Off-shelf mass movement down grooves
Waves	Breaking, high turbulence, high wave force	Moderate wave forces, 20% height reduction from shelf edge	Moderate-low wave force, small-scale turbulence	Low wave force, small-scale turbulence
Currents	Weak, multidirectional flow	Multidirectional flow, 60-70% speed reduction from shelf	Moderate on-shelf rectilinear tidal currents	Strong on-shelf rectilinear tidal currents (>50 cm s^{-1})

reef at the shelf edge is approximately equivalent to wave forces on the shallow shelf at a depth of ≈5 meters.

(6) Position of the boundary between wave-dominated and current-dominated zones on the fore-reef shelf, as defined by the crossing of wave and current force curves, corresponds to the position on the shelf where the coral community undergoes a distinct compositional change. The wave-dominated zone is characterized by thickly branched, bladed, and encrusting growth forms and is dominated by the wave-adaptable coral Acropora palmata. Delicately branched, massive, and platelike growth forms are common in the current-dominated zone. Acropora cervicornis and Montastrea represent this coral community. This latter zone, which is subject to minimal wave forces yet experiences considerable current force and associated high levels of turbulence, displays the most thriving coral communities on the fore-reef shelf.

Acknowledgments

This research was performed under a contract with Geography Programs, Office of Naval Research, Arlington, Virginia 22217. Technical assistance in the field and laboratory was provided by Norwood Rector, Rodney Fredericks, and Manuel Hernandez-Avila. Ms. Gerry Dunn is acknowledged for preparation of illustrations.

References Cited

(1) Roberts, H. H., Murray, S. P., and Suhayda, J. N., 1975, Physical processes in a fringing reef system. J. Marine Res., 23, pp. 233-260.

(2) Roberts, H. H., 1974, Variability of reefs with regard to changes in wave power around an island. Proc., Second Inter. Coral Reef Symp., Great Barrier Reef Committee, Brisbane, Australia, p. 497-512.

(3) Long, R. B., 1973, Scattering of surface waves by an irregular bottom. J. Geophys. Res. 78, p. 7861-7870.

(4) Kajiura, K., 1963, On the partial reflection of water waves passing over a bottom of variable depth. Inter. Union Geodesy and Geophys. Monograph 24, Proc. Tsunami Meetings 1961, 10th Pacific Sci. Congr., Honolulu, Hawaii, p. 206-230.

(5) Munk, W. H., and Sargent, M. S., 1954, Adjustment of Bikini Atoll to ocean waves. U.S. Geol. Survey Prof. Paper 260-C, p. 275-280.

(6) Taylor, G. I., 1921, Diffusion by continuous movements. Proc. London Math. Soc. 20, pp. 196-212.

(7) Roberts, H. H., Murray, S. P., and Suhayda, J. N., in press, Evidence for strong currents and turbulence in a deep coral reef groove. Limnology and Oceanography.

(8) Murray, S. P., 1972, Turbulent diffusion of oil in the ocean. Limnology and Oceanography, 17, p. 651-660.

(9) Murray, S. P., 1971, Turbulence in hurricane-generated coastal currents. Proc. Coastal Engr. Conf. (12th), Am. Soc. Civil Engr., pp. 2051-2068.

(10) Okubo, A., 1961, Oceanic diffusion diagrams. Deep-Sea Res. 18, p. 789-802.

(11) Rouse, H., 1961, Fluid mechanics for hydraulic engineers. Dover, New York, p. 228.

Unclassified

Security Classification

DOCUMENT CONTROL DATA - R & D

(Security classification of title, body of abstract and indexing annotation must be entered when the overall report is classified)

1. ORIGINATING ACTIVITY (Corporate author)	2a. REPORT SECURITY CLASSIFICATION
Coastal Studies Institute Louisiana State University Baton Rouge, Louisiana 70803	Unclassified
	2b. GROUP Unclassified

3. REPORT TITLE

PHYSICAL PROCESSES IN A FORE-REEF SHELF ENVIRONMENT

4. DESCRIPTIVE NOTES (Type of report and inclusive dates)

5. AUTHOR(S) (First name, middle initial, last name)

Harry H. Roberts, Stephen P. Murray, and Joseph N. Suhayda

6. REPORT DATE	7a. TOTAL NO. OF PAGES	7b. NO. OF REFS
December 1977	9	11

8a. CONTRACT OR GRANT NO.	9a. ORIGINATOR'S REPORT NUMBER(S)
N00014-75-C-0192 b. PROJECT NO. NR 388 002 c.	Technical Report No. 240
d.	9b. OTHER REPORT NO(S) (Any other numbers that may be assigned this report) A043 694

10. DISTRIBUTION STATEMENT

Approved for public release; distribution unlimited.

11. SUPPLEMENTARY NOTES	12. SPONSORING MILITARY ACTIVITY
Reprint from Proceedings, Third International Coral Reef Symposium, Miami, Florida, May 1977, pp. 507-515.	Geography Programs Office of Naval Research Arlington, Virginia 22217

13. ABSTRACT

Wave and current measurements were made across a rough-bottomed fore-reef shelf along the south coast of Grand Cayman Island. Wave heights attenuated 20% and current speeds 30% from the shelf margin (∿22-meter depth) to a depth of approximately 8 meters, a distance of ≈0.4 km. Strong, rectilinear tidal currents (≈50 cm s^{-1}) dominated the deep shelf margin, but weak, directionally variable currents were characteristic of the shallow shelf. Attenuation of wave heights and current speeds across the shelf is attributed to frictional effects resulting from strong interactions with the unique boundary conditions of the extremely rough bottom. (U)

A dye experiment illustrated that strong (≈35 cm s^{-1}) on-shelf flow is directed up the deep coral reef grooves at the shelf margin. High levels of turbulence (turbulence intensity ≈ 23 cm s^{-1}, diffusion coefficient ≈ 2.4 x 10^3 s^{-1}) characterize this process. (U)

Wave force-dominated versus current force-dominated portions of the fore-reef shelf were defined from *in situ* measurements. Variations in organic communities, growth forms, and reef structure are consistent with these zones. (U)

DD FORM 1 NOV 68 1473 (PAGE 1)

S/N 0101-807-6811

Unclassified

Security Classification

A-31408

14 KEY WORDS	LINK A		LINK B		LINK C	
	ROLE	WT	ROLE	WT	ROLE	WT
Wavesand currents						
Fore-reef shelf						
Grand Cayman Island						
Bottom roughness						
Turbulence						
Tidal current						
Wave-dominated zone						
Current-dominated zone						

Coastal Studies Institute
Center for Wetland Resources
Louisiana State University
Baton Rouge, Louisiana 70803

Technical Report No. 241

NEARSHORE CURRENT FIELDS AROUND CORAL ISLANDS: CONTROL ON SEDIMENT ACCUMULATION AND REEF GROWTH

Stephen P. Murray, Harry H. Roberts, Dennis M. Conlon,
and Geoffrey M. Rudder

December 1977

Reprint from
Third International Coral Reef
Symposium, Miami,
Florida, May 1977, pp. 53-59.

Office of Naval Research
N00014-75-C-0192
Project No. NR 388 002

Proceedings, Third International Coral Reef Symposium
Rosenstiel School of Marine and Atmospheric Science
University of Miami
Miami, Florida 33149, U.S.A.
May 1977

NEARSHORE CURRENT FIELDS AROUND CORAL ISLANDS: CONTROL ON SEDIMENT ACCUMULATION AND REEF GROWTH

Stephen P. Murray and Harry H. Roberts
Coastal Studies Institute
Louisiana State University
Baton Rouge, Louisiana 70803

Dennis M. Conlon
Geography Programs
Office of Naval Research
Arlington, Virginia 22217

Geoffrey M. Rudder
Caribbean Meteorological Institute
Husbands, St. James, Barbados

ABSTRACT

Observations of drogues drifting with the current, combined with current meter data from Barbados and Grand Cayman Islands, indicate that zones of high current speed (jets or rips, 50-80 cm/sec) and zones of weak, disorganized flow (stagnation zones, 2-10 cm/sec) are systematically located around these islands. Theoretical models of the flow around islands predict the existence, strength, and location of these current zones with reasonable accuracy. Net circulations around the islands as observed by several other investigators play an important role in the location and number of jets or stagnation zones around a specific island. Extensive volumes of sediment accumulate to the lee of high-speed current zones. These sediments appear to be deposited as the carrying capacity of the current rapidly diminishes as it leaves the jet zone. Subsequent reworking of the sediment along the shore is produced by wave and current action. This process of accumulation and shifting of sediments on the lee sides of islands restricts substrate areas suitable for coral colonization and subsequent reef growth. Therefore, interplay between "around-the-island" circulations and sediment transport appears to be significant in producing sites favorable for sediment accumulation but unfavorable for reef growth.

KEY WORDS: Currents, Circulation, Sediments, Transport, Islands, Reef, Coral, Theory, Siltation, Shoaling

NEARSHORE CURRENT FIELDS AROUND CORAL ISLANDS: CONTROL ON SEDIMENT ACCUMULATION AND REEF GROWTH

Stephen P. Murray and Harry H. Roberts
Coastal Studies Institute, Louisiana State University
Baton Rouge, Louisiana 70803

Dennis M. Conlon
Geography Programs, Office of Naval Research
Arlington, Virginia 22217

Geoffrey M. Rudder
Caribbean Meteorological Institute
Husbands, St. James, Barbados

Introduction

The large-scale current flow around oceanic islands has attracted considerable attention in recent years from physical oceanographers primarily interested in the effect of an island on the interior of the surrounding ocean. Hogg (1), for example, explained the vertical displacement (~100 m) of isopycnals observed around the periphery of the Bermuda platform with a theoretical model of steady, frictionless, stratified flow past a circular island. Observations of stagnation points, or zones of very low speed, on the northern and southern flanks of the bank were consistent with the theory. In a similar study of the flow past an equatorial island Hendry and Wunsch (2) reported that the frictionless equations of flow past a cylindrical obstacle described deformations in the density field observed around Jarvis Island (160° 01' W, 0° 23' S). In these cases only a few current measurements were obtained, and they were restricted to distances of more than an island diameter away from the coast and water depths greater than 400 m. Direct measurements of currents were made, however, by Knox (3) about 10 km off Addu Atoll, another isolated island in the equatorial Pacific. Knox reported westerly speeds of 20-30 cm/sec in the surface layer and easterly speeds of 75-100 cm/sec below 70 m. His data showed that the flow does tend to stagnate upstream of the atoll and that current speeds are increased along the atoll flanks, as expected from theory. None of these studies was designed to provide understanding of the dynamics of the currents affecting the coasts and shelves of the islands themselves; rather, they were intended to determine the perturbations introduced into the main flow by the island, which acts as an obstacle.

In contrast, the purpose of this paper is to present data and theoretical deductions concerned with currents within a few kilometres of the coastline. Both observations and theory show that zones of intense currents (jets or rips) and zones of weak currents (stagnation zones) are systematically distributed around the shores of islands and that prisms of sediment tend to accumulate in response to the deceleration of high-speed currents, providing substrate unfavorable for reef growth.

Observations

Our program to assess the role of currents on the shelves of steep-sided islands began in 1972 on the southwestern coast of Grand Cayman, in the Caribbean. By instrumenting in detail one particular transect across the shelf, much was learned (4) about the variability in time of the mean drift current along the shelf and the unexpectedly strong tidal current signal at the shelf edge. It subsequently became apparent that large and systematic along-the-shore gradients in current activity might exert considerable influence on the location and nature of coastal and shelf sediment accumulation forms and reef growth.

Observations of currents moving in space entail the tracking of drifters or drogues with a drag collector such as a parachute or biplane set at a prescribed depth below the sea surface. To locate the surface marker we have used various electromagnetic techniques, such as (a) visually locating drifting drogues with a ship and then locating the position with respect to the island by ship radar, (b) tracking the drogues from shore by radar [in this method an active target (transponder) is attached to the drogue pole which

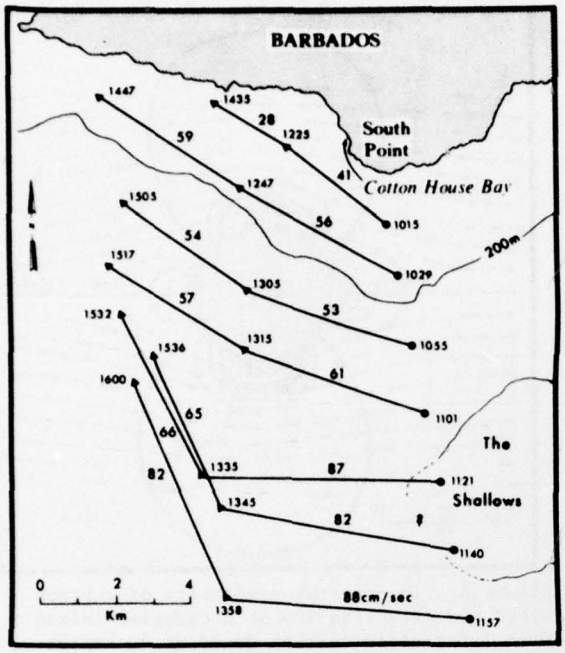

Figure 1. Current tracks from drogues off the south coast of Barbados July 25, 1973.

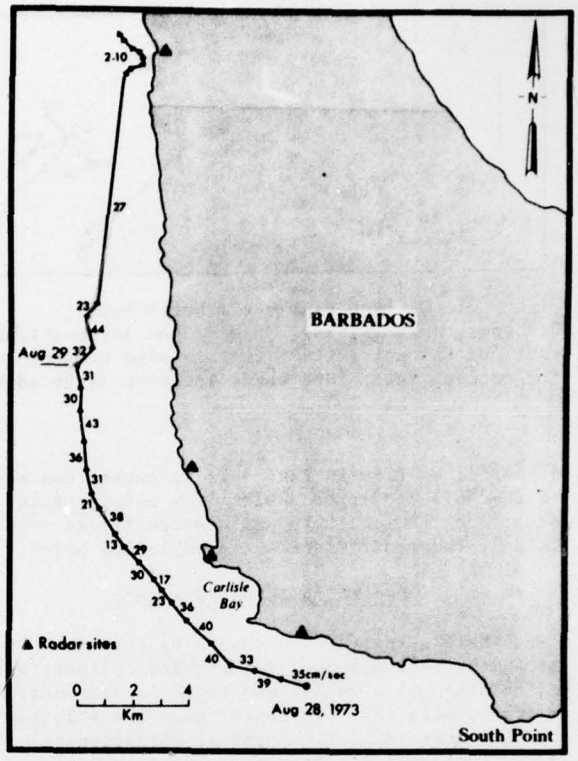

Figure 2. A current track from a drogue equipped with an x band radar transponder, August 28, 1974. A portable radar ashore is used to locate the drogue.

replies to the radar signal at a frequency different from that transmitted to avoid sea clutter, and (c) tracking the drogues by attaching an over-the-horizon type transmitter to the pole and triangulating from the shore by two portable direction-finding units (5).

Such techniques have been employed repeatedly on Barbados, Grand Cayman, and several other islands to determine the strength and characteristics of currents along the shelf. Figure 1 shows a field of drogues moving with the current at the 9-m depth level off the southwestern coast of Barbados. Although Warsh et al. (6) reported that current speeds in the open waters 25 km east of Barbados have a mean of 20 cm/sec and rarely exceed 25 cm/sec, these drogues show quite high speeds of 40-80 cm/sec. Currents just off South Point are in the range of 40-60 cm/sec and are capable of moving grains 1-2 mm in diameter on the bottom. The decrease in speed toward the island suggests the presence of a frictional boundary layer of about 5-km thickness along the coast. The sharp turn toward the island of the outer three drogues is perhaps related to a flow readjustment after they have traversed The Shallows, a 10-km-long bank whose western edge is seen in Fig. 1. From South Point the currents generally flow northward all along the western coast of Barbados. For example, Fig. 2 shows a drogue track of about 26 km along the western coast. Speeds gradually decrease along the northward track from about 40 cm/sec at the onset to 2-10 cm/sec at the end of the track, where the drogue is likely trapped in the frictional boundary layer. A track that is similar but farther offshore was shown in Murray et al. (5). Our observations on Barbados and on Grand Cayman show that reversing tidal currents became increasingly important in the immediate vicinity of the coast (within a few hundred metres). It appears that the long-term drift decays rapidly across the shelf while the tidal current is correspondingly amplified. Observation by Peck (7) clearly showed the dominance of the tidal current over the mean drift inside Carlisle Bay (Fig. 2).

At the northern end of Barbados the current structure was studied by both in situ current meters and drogue techniques. A current meter located about 800 m off Harrison Point consistently showed a weak, extremely disorganized flow in which the tidal currents (clearly seen in the records from other locations around the island) could not easily be identified. Figure 3 shows five drogue tracks around North Point obtained only 18 hours after the data seen in Fig. 1. All other data suggest that the same current patterns were in force around the island on July 26 as on July 25. This weak, oscillating,

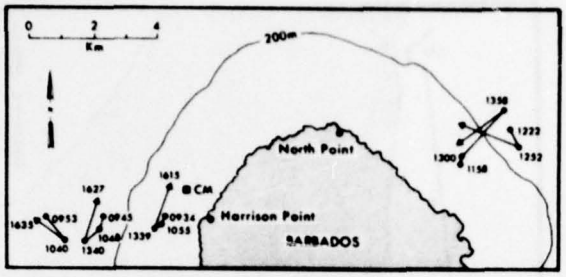

Figure 3. Current tracks off North Point, Barbados, July 26, 1973 showing the intermittent confused current pattern that is also present in the current meter data whose location is noted by CM.

disorganized flow in Fig. 3 is in marked contrast to the well-developed, swift flow persistently seen along the southern and western flanks of the island. These differences are explained below.

Theoretical Considerations

The flow patterns produced by current streaming past a submerged circular cylinder with no friction is a well-known topic in elementary hydrodynamics (8). White (9) gave the solution for the more realistic physical situation of current streaming past a circular island that pierces the water's surface on a rotating earth. The solution for the stream function Ψ is given in terms of an infinite series of modified Bessel functions of the first and second kind as shown in White's equation 17. This solution allows calculation of the radial U_r and tangential U_T components of the current velocity by differentiating Ψ with respect to θ and r; i.e.,

$$U_r = 1/r \frac{\partial \Psi}{\partial \theta} , \quad U_T = - \frac{\partial \Psi}{\partial r} .$$

Thus we calculate the direction of the streamlines from the stream function and the absolute current speed from

$$V = (U_r^2 + U_T^2)^{1/2} .$$

To apply the theory two parameters must be set. First, one must specify the far-field current speed U_o, i.e., the upstream current speed beyond the influence of the island. Warsh et al. (6) provide a good estimate of 20 cm/sec, which we will use for computational purposes. Secondly, the value of the stream function on the island boundary must be set. A value of $\Psi = 0$ on the boundary implies symmetry across the flow axis, which hydrodynamically means there is no net circulation around the island. Figure 4 shows the flow predicted for this case with $U_o = 20$ cm/sec. Stagnation zones (weak currents) form on

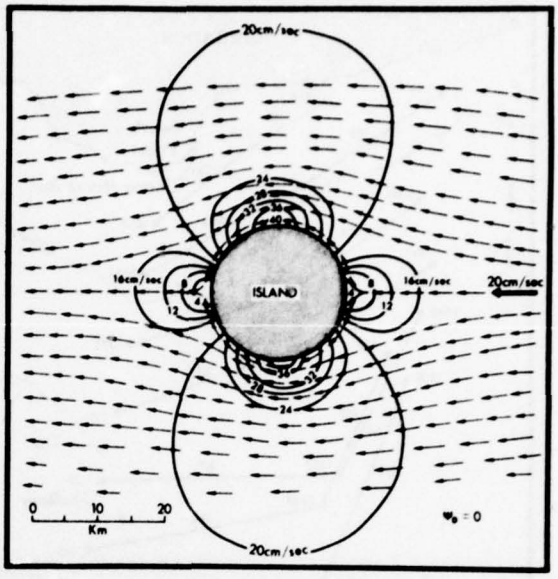

Figure 4. Theoretical prediction of current speed and direction around a circular island with a far field current speed of 20 cm/sec.

the nose of the island and directly behind it, whereas zones of very strong currents (jets or rips) form on the flanks. It is recalled that this general pattern of stagnation zones and accelerated currents was observed by Hendry and Wunsch (2) off Jarvis Island and Knox (3) off Addu Atoll, and it agrees with our current meter observations on Grand Cayman (4). The departure of the flow directly behind the island and the current jet at the top (northern) end of island in this model do not agree, however, with our observations around Barbados. These observations (Fig. 1, 2, 3) show northerly flow all along the back side of the island and departure at the northern end in or near a zone of weak, confused currents.

There are, however, a number of studies in the literature that definitely indicate the presence of clockwise net circulations around islands. Patzert (10) shows this phenomenon to be common in the Hawaiian Islands. One example, in Fig. 5 (replotted from his data), shows a strong clockwise flow around Kauai. The net clockwise speed of 30 cm/sec for 15 days on the southern coast is particularly striking. The geophysical mechanisms that produce these net clockwise circulations remain unclear.

A net circulation around an island such as observed by Patzert (10) and others can be produced in White's (9) theoretical model by setting Ψ unequal to zero on the boundary. Figure 6 is the solution predicted by the theory with $\Psi_o = 0.5 \times 10^8$ cm^2/sec for an island diameter of 20 km and a far-field speed of 20 cm/sec; the current

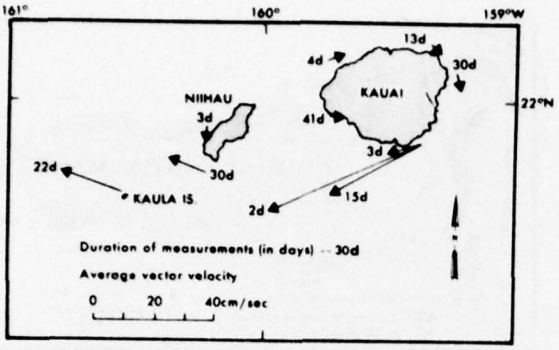

Figure 5. Net clockwise circulation around the island of Kauai observed by Patzert (10) from current meter data.

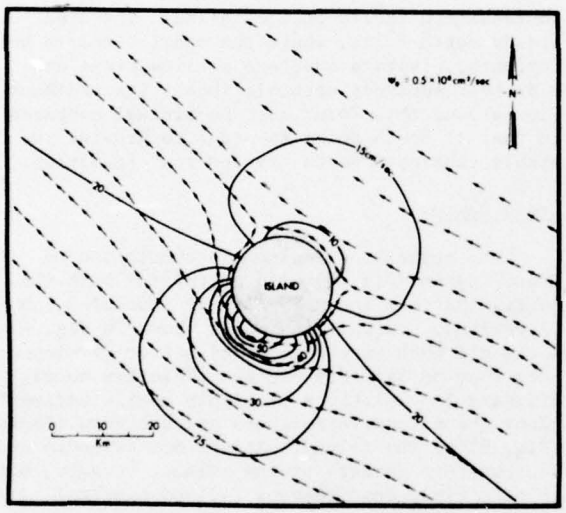

Figure 6. Theoretical prediction of current speed and direction around a circular island exhibiting a net clockwise ciculation. The far field current speed is 20 cm/sec from the southeast.

approaches the island from the east-southeast, as is the usual case off Barbados. This value of Ψ_o is simply a best fit to the data selection. Notice that (a) the two stagnation zones have migrated northward and coalesced to form a zone of weak currents off the northern end of the circular island, (b) the flow is all northerly along the back of the island (western coast), and (c) there is a belt of extremely high speeds concentrated at the southwestern corner. These three features are essentially in agreement with the flow patterns depicted by our numerous drogue experiments off Barbados. Also note that our observations indicate that the superimposed oscillatory tidal current is on the order of 10 cm/sec. Thus drogues at the northern end of the island should be weakly oscillated back and forth

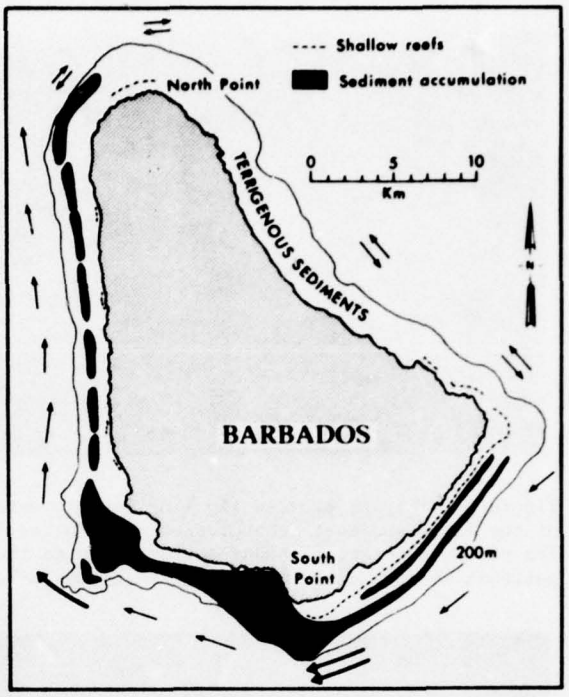

Figure 7. Distribution of accumulations of sediment and shallow reef growth around Barbados and generalized current pattern.

by the tide in a mean drift that which only occasionally can overpower the tidal currents and push the drogues northwesterly. This is apparently the situation depicted in Fig. 3.

Patterns of Sediment Accumulation

Barbados

The extensive areas of sediment accumulation that occur on the southwestern shelf of Barbados (Fig. 7) appear to be well correlated with the distribution of currents summarized in the model (Fig.6). These sediments are dominantly skeletal carbonates derived from both shallow- and intermediate-depth coral-algal reefs growing along the southeastern-facing facet of the island. At South Point, in particular, a broad apron of these sediments has spread across the shelf and over the shelf margin. A large-scale depositional feature ~24 m in vertical dimension has developed at the shallow-shelf abrupt break in slope (Fig. 8). Reconnaissance dives demonstrated that the feature resulted from draping of Recent carbonate sediments over the shelf edge into an adjacent basin. No remnants of the original shelf platform were visible through the Recent sediment cover. Extensive siltation problems along the adjacent shoreline near Cotton House Bay (Fig. 1) illustrate that these sediments are being swept not

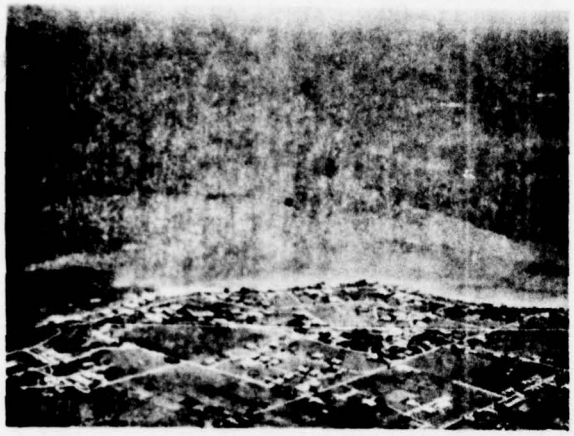

Figure 8. (A) Aerial view (looking roughly west) of the large sediment accumulation area in the lee of South Point, Barbados (asterisk notes the position where underwater picture 8 (B) was taken.

Figure 8. (B) Divers sitting on the seaward face of the large sediment accumulation form which has a vertical dimension of ~24 m.

only across the shelf into deeper water but also along shore to the northwest.

This immense prism of sediment observed to be accumulating near South Point appears to be carried into the area by the strong currents predicted by the model. The rapid deceleration of current speed and loss of sediment-carrying capacity away from the Point contribute toward the piling up of sediment at this location. As expected, and as shown on Fig. 7, the occurrence of reefs on the unstable bottoms of these sediment-rich areas is minimal. Other areas of abundant sediment shown in this figure are in the form of mid-shelf bands caught between old, submerged reef ridges (11) along the western and

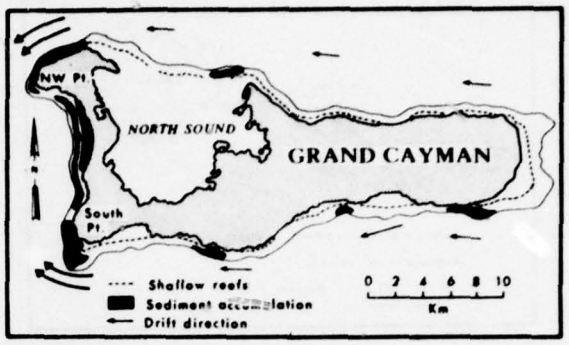

Figure 9. Distribution of accumulations of sediment and shallow reef growth around Grand Cayman and generalized current pattern.

southeastern facets of the island. The area around North Point, where the model predicts weak currents, displays numerous shallow reefs and mid-shelf sediment accumulations. The sediment flux around this Point must be minimal compared to that at South Point in order to provide the stable substrate necessary for reef formation.

Grand Cayman

The pattern of sediment accumulation on Grand Cayman (Fig. 9) also correlates with the current pattern but more closely resembles the flow-without-circulation model shown in Fig. 4. Reefs are much more common and better developed here than on Barbados because there are no significant accumulations of highly mobile sediment along the extensive northern and southern flanks (Fig. 9) of the island. At the northwestern and southwestern corners of the island, however, both in situ field measurements (4) and nautical charts indicate the presence of intense current rips much like those depicted in Fig. 4. The rapid deceleration of the current in the lee of these points leads to deposition and accumulation of large amounts of sediment on the shelf (Fig. 9). As on Barbados, reef growth is poor at these locations inasmuch as this process excludes reef development on many hard shelf substrates because they are drowned in sediment. On both islands long carbonate beaches form on the lee sides and reefs are confined to small patch reef varieties as well as discontinuous deep shelf margin reefs.

Summary

Current meter and drogue observations, theoretical analysis of the flow around islands, and air photo and diver inspection of bottom conditions lead to the following conclusions relating the strength and location of currents to the degree of sediment accumulation and reef growth.

1. Observations of drogues drifting with the current, combined with current meter data, have delineated zones of high current speed (jets or

rips, 50-80 cm/sec) along the shores of both Barbados and Grand Cayman Islands. Zones of weak, intermittent, and disorganized flow (stagnation zones, 2-10 cm/sec) are also systemically located around these islands.

2. Theoretical models of the flow around islands predict the existence and correct locations of these jets and stagnation zones. Grand Cayman appears to be a type with two jets on its flanks and two stagnation zones (nose and tail), predicted by a model with no net circulation, around the island. Barbados, on the other hand, represents a type with a finite net circulation around its circumference. In this latter case an intense jet forms on the southwestern flank and a single large stagnation zone occupies the northern end.

3. Extensive areas of sediment accumulation occur to the lee of these high-speed current zones. As the carrying capacity of currents in the accelerated flow zone decreases toward the island lee, sediments are deposited and then gradually worked onshore and along shore by wave action as well as other currents.

4. The accumulation and shifting of sediments on the lee sides of islands restrict suitable substrate areas for coral colonization and subsequent reef growth. Where shallow reefs appear, they are generally patch-like in design and not extensive. Deep shelf reefs generally occur at the shelf margin and have frequent breaks in the reef trend to allow mass movement of sediment off the shelf.

5. The interplay between "around-the-island" circulation and sediment transport appears to play a significant role in producing favored sites of sediment accumulation, thereby restricting substrate areas where reefs can develop. These processes are of primary importance in the exclusion of well-formed reefs on the lee sides of islands.

Acknowledgments

Special thanks are due to the Caribbean Meteorological Institute, the Barbados Deep Water Harbour authority, and the crew of the tug Barbados, without whose enthusiastic cooperation this project could not have been undertaken. Norwood Rector and Rod Fredericks provided outstanding technical support under difficult circumstances. Support for this research was provided by the Geography Programs, Office of Naval Research, Arlington, Virginia 22217. Mrs. G. Dunn provided the excellent cartographic work.

References Cited

(1) Hogg, N. G., 1972, Steady flow past an island with application to Bermuda. Geophys. Fluid Dyn. 4, p. 55-81.

(2) Hendry, R. and Wunsch, C., 1973, High Reynolds number flow past an equatorial island. J. Fluid Mech. 58, p. 97-114.

(3) Knox, R. A. , 1974, Reconnaissance of the Indian Ocean equatorial undercurrent near Addu Atoll. Deep Sea Res. 21, p. 123-129.

(4) Roberts, H. H., Murray, S. P., and Suhayda, J. N., 1975, Physical processes in a fringing reef system. J. Mar. Res. 33, p. 233-260.

(5) Murray, S. P., Roberts, H. H., Wiseman, W. J., Tornatore, H. G., and Whelan, W. T., 1975, An over the horizon radio direction finding system for tracking coastal and shelf currents. Geophys. Res. Letters 2, p. 211-214.

(6) Warsh, K. L., Echternacht, K. L., and M. Garstang, 1971, Structure of near surface currents east of Barbados. J. Phys. Oceanography 1, p. 123-129.

(7) Peck, S., 1974, Oceanographic considerations near Carlisle Bay. In Report on the Bridgetown Sewage Study, Ministry of Health and Welfare, Bridgetown, Barbados.

(8) Goldstein, S., 1965, Modern Developments in Fluid Dynamics. Dover, New York, U.S.A., p. 21-26.

(9) White, W. B., 1971, A Rossby Wave due to an island in an eastward current. J. Phys. Oceanography 1, p. 161-168.

(10) Patzert, W. C. and Wyrtki, K., 1974, Anticyclonic flow around the Hawaiian Islands indicated by current meter data. J. Phys. Oceanography 4, p. 673-676.

(11) Macintyre, I. G., 1967, Submerged coral reefs, west coast of Barbados, West Indies. Canadian J. Earth Sci. 4, p. 461-474.

Unclassified
Security Classification

DOCUMENT CONTROL DATA - R & D

(Security classification of title, body of abstract and indexing annotation must be entered when the overall report is classified)

1. ORIGINATING ACTIVITY (Corporate author)	2a. REPORT SECURITY CLASSIFICATION
Coastal Studies Institute Louisiana State University Baton Rouge, Louisiana 70803	Unclassified
	2b. GROUP Unclassified

3. REPORT TITLE

NEARSHORE CURRENT FIELDS AROUND CORAL ISLANDS: CONTROL ON SEDIMENT ACCUMULATION AND REEF GROWTH

4. DESCRIPTIVE NOTES (Type of report and inclusive dates)

5. AUTHOR(S) (First name, middle initial, last name)

Stephen P. Murray, Harry H. Roberts, Dennis M. Conlon, and Geoffrey M. Rudder

6. REPORT DATE	7a. TOTAL NO. OF PAGES	7b. NO. OF REFS
December 1977	7	11

8a. CONTRACT OR GRANT NO.	9a. ORIGINATOR'S REPORT NUMBER(S)
Contract N00014-75-C-0192 b. PROJECT NO. NR 388 002 c.	Technical Report No. 241
d.	9b. OTHER REPORT NO(S) (Any other numbers that may be assigned this report) A043 719

10. DISTRIBUTION STATEMENT

Approved for public release; distribution unlimited.

11. SUPPLEMENTARY NOTES	12. SPONSORING MILITARY ACTIVITY
Reprint from Proceedings, Third International Coral Reef Symposium, Miami, Florida, May 1977, pp. 53-59.	Geography Programs Office of Naval Research Arlington, Virginia 22217

13. ABSTRACT

Observations of drogues drifting with the current, combined with current meter data from Barbados and Grand Cayman Islands, indicate that zones of high current speed (jets or rips, 50-80 cm/sec) and zones of weak, disorganized flow (stagnation zones, 2-10 cm/sec) are systematically located around these islands. Theoretical models of the flow around islands predict the existence, strength, and location of these current zones with reasonable accuracy. Net circulations around the islands as observed by several other investigators play an important role in the location and number of jets or stagnation zones around a specific island. Extensive volumes of sediment accumulate to the lee of high-speed current zones. These sediments appear to be deposited as the carrying capacity of the current rapidly diminishes as it leaves the jet zone. Subsequent reworking of the sediment along the shore is produced by wave and current action. This process of accumulation and shifting of sediments on the lee sides of islands restricts substrate areas suitable for coral colonization and subsequent reef growth. Therefore, interplay between "around-the-island" circulations and sediment transport appears to be significant in producing sites favorable for sediment accumulation but unfavorable for reef growth. (U)

14 KEY WORDS	LINK A		LINK B		LINK C	
	ROLE	WT	ROLE	WT	ROLE	WT
Currents						
Circulation						
Sediments						
Transport						
Islands						
Reef						
Coral						
Theory						
Siltation						
Shoaling						

Coastal Studies Institute
Center for Wetland Resources
Louisiana State University
Baton Rouge, Louisiana 70803

Technical Report No. 242

HURRICANE-GENERATED WAVES AND COASTAL BOULDER RAMPART FORMATION

M. L. Hernandez-Avila, H. H. Roberts, and L. J. Rouse, Jr.

December 1977

Reprint from: Proceedings,
3rd International Coral Reef
Symp., University of Miami,
Miami, Florida, pp. 71-78.

Office of Naval Research
Contract N00014-75-C-0192
Project No. NR 388 002

Proceedings, Third International Coral Reef Symposium
Rosenstiel School of Marine and Atmospheric Science
University of Miami
Miami, Florida 33149, U.S.A.
May 1977

HURRICANE-GENERATED WAVES AND COASTAL BOULDER RAMPART FORMATION

M. L. Hernandez-Avila
Department of Marine Sciences
University of Puerto Rico
Mayaguez, Puerto Rico 00708

and

Harry H. Roberts and Lawrence J. Rouse
Coastal Studies Institute
Louisiana State University
Baton Rouge, Louisiana 70803

ABSTRACT

Coral boulder ramparts along the south coast of Grand Cayman Island have no source area near the shoreline. Coral communities acting as a source of rampart rubble are found 0.3 km from shore and at a depth of 10-12 m. Theoretical calculations of wave-induced forces from wave refraction analyses of hurricane-generated waves indicate that the probable hurricane dynamic force spectrum is sufficient to break and transport coral rubble from depths of up to 12 m. In situ breaking force tests accomplished in Puerto Rico on Acropora palmata coral colonies support the theoretical calculations.

KEY WORDS: Coral, Boulder Ramparts, Wave Forces, Grand Cayman Island, Puerto Rico, Wave Refraction, Breaking Force

HURRICANE-GENERATED WAVES AND COASTAL BOULDER RAMPART FORMATION

M. L. Hernandez-Avila
Department of Marine Sciences, University of Puerto Rico
Mayaguez, Puerto Rico 00708

Harry H. Roberts and Lawrence J. Rouse
Coastal Studies Institute, Louisiana State University
Baton Rouge, Louisiana 70803

Introduction

Descriptive reports documenting the geomorphic and structural changes induced by extreme storm conditions on island coasts, atolls, and coral cays have been published (1), (2), (3), (4), (5), (6), (7), (8), (and others). One common observation has been the occurrence of linear coral rubble accumulations or ridges parallel to the coast; the coral constituents of these structures, usually called boulder ramparts, range in size from pebble to boulder. Formation of these topographic features, commonly found along high-energy coastal sectors, is generally attributed to wave-induced forces and storm-surge effects.

The objective of this paper is to calculate theoretically the magnitude of hurricane wave-induced forces instrumental in destruction of stony corals, which constitute the source of rubble for ridge formation on island coasts. Calculated wave-induced forces that result in the initial breakup of coral fragments are compared to actual mechanical breaking forces measured in situ.

The analytical procedure consisted of (a) a case study of a boulder rampart and its governing physical characteristics at a specific location on Grand Cayman Island, British West Indies, (b) theoretical determination of hurricane-generated swell characteristics, (c) calculation of wave-induced forces employing the resultant orbital velocities of the swells after refraction has taken place, and (d) a comparison of calculated wave force magnitudes with preliminary observations of actual mechanical forces that break Acropora palmata coral colonies.

Grand Cayman Boulder Rampart

Rigby and Roberts (8) described boulder ramparts on the coasts of Grand Cayman Island (Fig. 1) as being composed of hurricane-tossed coral fragments that reach 0.6 to 1.0 m in diameter in areas of coarsest accumulations. Rampart heights reach a maximum of 4.5 m above sea level. A study area near Spots Bay (sector 3 of Fig. 2) was chosen as the site for analyses of hurricane wave-induced forces. Constituents of the boulder rampart present in this sector have a mean width of 20 cm, a vertical thickness of 10 cm, and a maximum length of about 58 cm. For the purpose of analysis, a mean length of 30 cm was chosen. A. palmata fragments are the major constituent of the boulder ramparts (Fig. 3).

Two major observations relevant to this analysis are (a) the source of A. palmata fragments is found at an approximate distance of 0.3 km from the shoreline at depths ranging from 8 to 10 m (Fig. 4) and (b) the rampart's constituent fragments are relatively unabraided, a fact that suggests that transit time from growth areas was minimal.

Hurricane-Generated Wave Characteristics

The yearly mean shore wave power distribution for six sectors along the coast of Grand Cayman Island is shown in Fig. 2. A similar analysis employing the same bathymetric data (9) was used as input to a wave refraction-wave power computer program (10) for an analysis of hurricane waves. Four hurricane conditions were assumed to be generating swells at fetches located in the southeastern Caribbean Sea. It was determined from wave hindcasting analyses, employing accepted methods (11), (12) and corroborating the results with historical data, that swells reaching the study area from these storm centers would have the characteristics shown in Table 1. These values were employed in the wave refraction-wave power computer program to determine their variations at a depth of 12 m over the A. palmata reef section, which was the probable source for the boulder rampart constituents. Results of the wave refraction

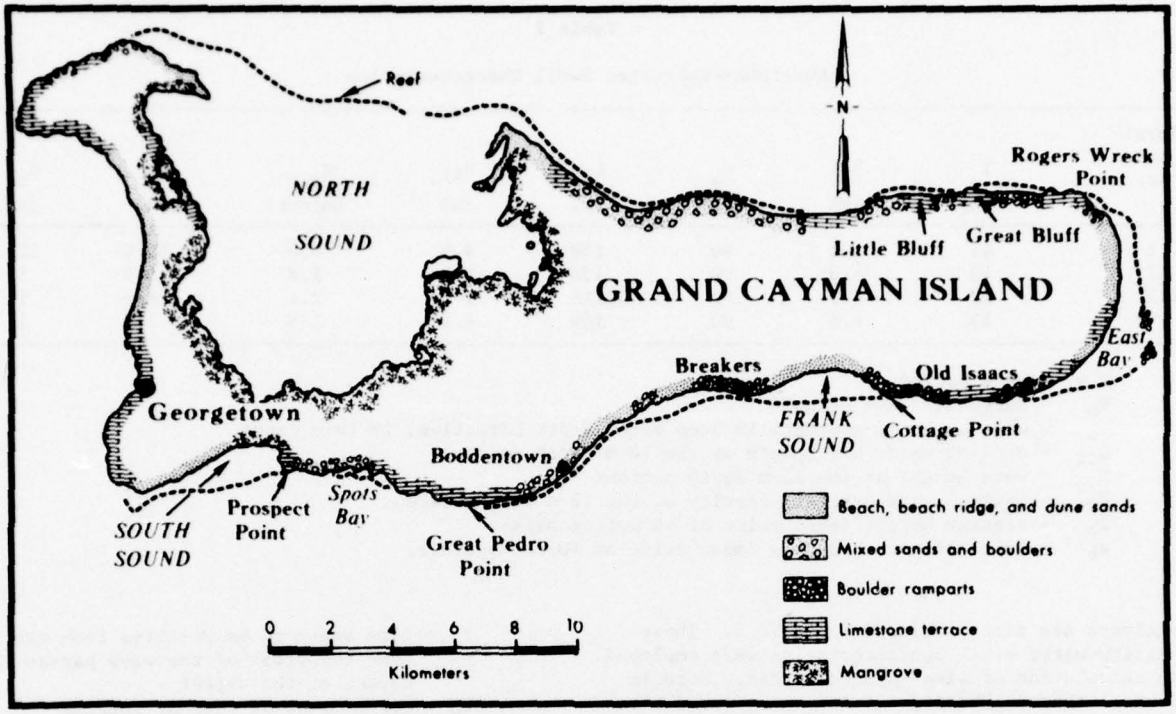

Figure 1. Grand Cayman Island boulder rampart distribution [after Rigby and Roberts (8)].

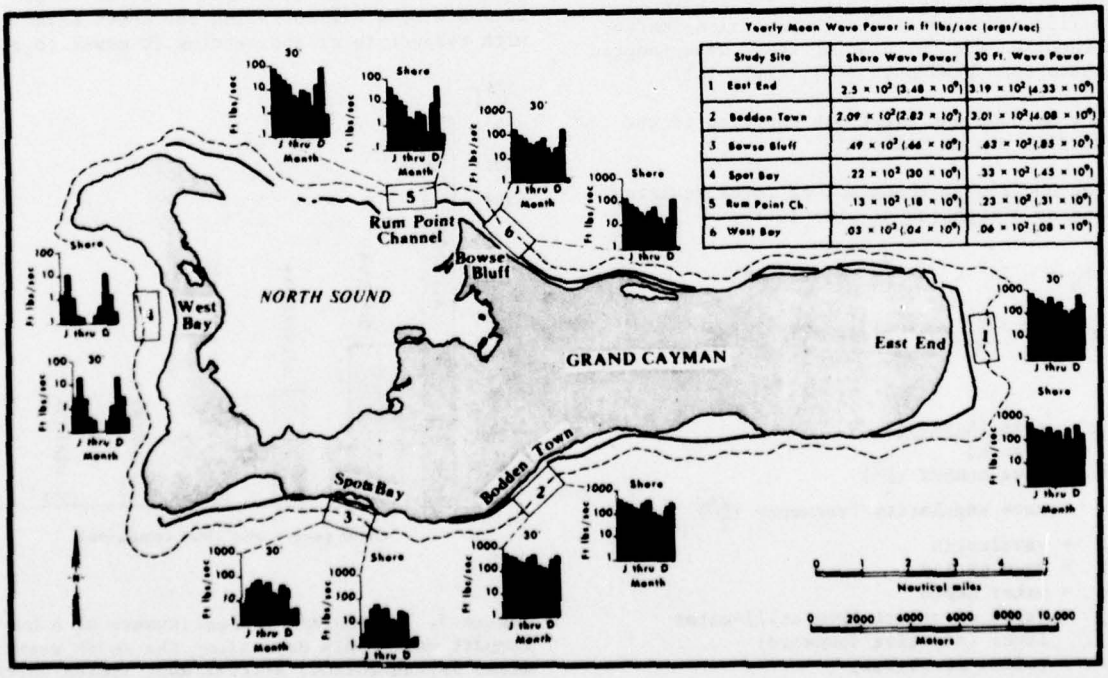

Figure 2. Case study location (sector 3) and wave power distribution [after Roberts (9)].

Table 1

Hurricane-Generated Swell Characteristics

Hurricane No.	T (sec)	H_o (m)	α_o (°)	L_{12} (m)	H_{12} (m)	U_{max} (m/sec)	H_b (m)	d_b (m)
I	15	9.1	90	158	9.8	4.0	10.0	12.2
II	13	4.3	90	135	4.3	1.8	8.8	1.5
III	12	6.1	90	124	6.1	2.4	8.8	1.5
IV	13	4.6	90	109	4.6	1.8	7.0	1.5

T = = wave period
H_o = deepwater wave height
α_o = wave angle of approach in deep water (east direction, in this case)
L_{12} = shallow-water wavelength at the 12-m depth contour
H_{12} = wave height at the 12-m depth contour
U_{max} = maximum wave orbital velocity at the 12-m depth contour
H_b = breaker height (mean value of 40 orthogonals)
d_b = depth of wave breaking (mean value of 40 orthogonals)

analyses are also tabulated in Table 1. These shallow-water swell characteristics were employed in calculation of wave-induced forces. Note in Table 1 that in Hurricane I the waves would break on the A. palmata reef flat.

Wave-Induced Force Calculations

Forces exerted by waves on submerged objects have been studied theoretically (linear wave theory) (13; and many others). Several summaries of the theories for calculating these wave-induced forces have been presented (14), (15), (16).

The methods and equations employed in the analyses (15) are as follows:

The horizontal component of force equation expressed as a function of time is:

$$F_h = -2\pi^2 C_M \rho V \frac{H}{T^2} (W) \sin \sigma t$$

$$+ \frac{1}{2} C_D \rho A \pi^2 \frac{H^2}{T^2} (W)^2 \cdot |\cos \sigma t| \cos \sigma t$$

where

$W = \frac{\cosh [k(y+d)]}{\sinh kd}$
k = wave number $(\frac{2\pi}{T})$
σ = wave angularity frequency $(\frac{2\pi}{T})$
L = wavelength
T = wave period
d = water depth
y = depth of object from still-water level (negative downward)
V = volume of object
A = area of object
ρ = density of water (1031 kg/m^3)
H = wave height
t = time measured as positive from the time the crest of the wave passes the center of the object
C_M = coefficient of mass or inertia
C_D = drag coefficient

The phase angle (15), B_{hf}, at which the maximum horizontal component of force occurs can be found by differentiating the above equation with respect to σt and setting it equal to zero:

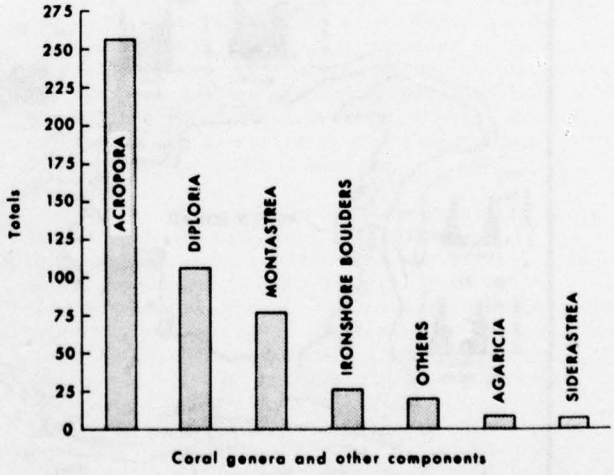

Figure 3. Histogram of constituents of a boulder rampart near Spots Bay, along the south coast of Grand Cayman Island, British West Indies [after Rigby and Roberts (8)]. Data were generated from 500 counts on a grid randomly placed over the outcrop.

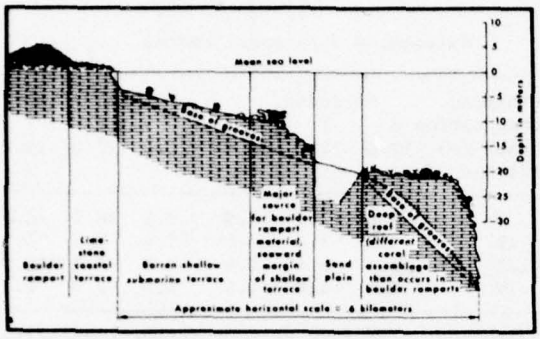

Figure 4. Schematic profile of the fore-reef shelf, adjacent to the boulder rampart study area [after Rigby and Roberts (8)].

$$\frac{\partial F_h}{\partial \sigma t} = -2\pi^2 C \rho V \frac{H}{T^2} (W) \cos \sigma t$$

$$- C_D \rho A \pi^2 \frac{H^2}{T^2} (W)^2 \cdot |\cos \sigma t| \sin \sigma t = 0 .$$

The solution to this equation is either

$$\sin B_{hf} = \pm \frac{2 C_M V}{C_D A H} \cdot \frac{\sinh kd}{\cosh k(y+d)} ,$$

where B_{hf} is in the second and fourth temporal quadrants of the wave form, or

$$\cos B_{hf} = 0$$

when

$$\frac{2 C_M V \sinh kd}{C_D A H \cosh k(y+d)} > 1 .$$

The equation to determine the vertical component of force is

$$F_v = -2\pi^2 \rho C_M V \frac{H}{T^2} \left[\frac{\sinh k(y+d)}{\sinh kd}\right] \cos \sigma t$$

$$- \frac{1}{2} \rho C_D A \frac{\pi^2 H^2}{T^2} \left\{\frac{\sinh k(y+d)}{\sinh kd}\right\}^2 \cdot |\sin \sigma t| \sin \sigma t$$

The phase angle, B_{vf}, at which the maximum vertical component of force occurs is either

$$\cos B_{vf} = \frac{2 C_M V}{C_D A H} \cdot \frac{\sinh kd}{\sinh k(y+d)}$$

or

$$\sin B_{vf} = 0 ,$$

when

$$\frac{2 C_M V}{C_D A H} \cdot \frac{\sinh kd}{\sinh k(y+d)} > 1 .$$

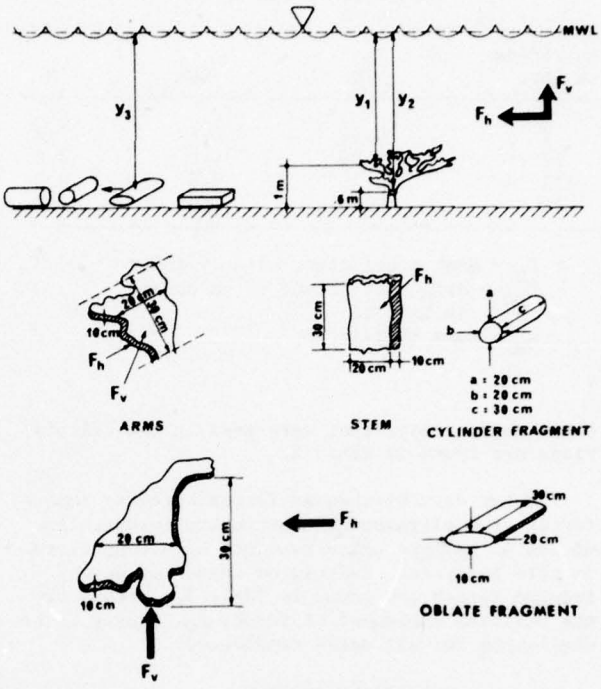

Figure 5. Conceptual model employed in the analysis and calculations of wave-induced forces on an oblate and a cylindrical coral fragment at the bottom and suspended above the bottom.

Analysis of wave-induced forces was made for cylinders and oblate cylindroids because A. palmata structural units and fragments approximate these shapes and forms. Figure 5 shows the conceptual models for boulder-sized fragments at the bottom and for the structural units in situ. The calculations that follow are made for coral fragments of the dimensions indicated in this figure.

The great difficulty in calculating (or choosing) values for the coefficient of drag and inertia according to geometrical characteristics of the objects has been explicitly shown by many investigators (13), (15), (14), (17), (18), (16). The coefficients of drag for cylindrical fragments were obtained from a curve published by Wiegel (15). The coefficient of drag for oblate fragments was chosen from a middle value for a cylinder because no published values for this shape could be found. The coefficient of mass for both shapes was the theoretical value for cylinders (15). A change in the coefficient of mass from 2.0 to 1.6 produced no significant difference in the calculated forces. The values of

Table 2

Values of C_D and C_M

Hurricane Number	C_D	C_{DO}	C_M
I	0.34	0.6	2.0
II	0.80	0.6	2.0
III	0.32	0.6	2.0
IV	0.70	0.6	2.0

C_D = drag coefficient of a cylinder
C_{DO} = drag coefficient of an oblate cylindroid
C_M = mass coefficient

these coefficients that were used in the calculations are found in Table 2.

Water current-induced forces, breaker impact forces, and alignment and structural properties of the A. palmata units have not been considered in this analysis. Calculated values of wave-induced forces are shown in Table 3. Values of the vertical component of force, F_V, proved to be negligible for all cases considered.

Field Experiment

A graduated industrial spring balance was used to estimate the force that breaks the branches and stems of A. palmata structural units in situ (Fig. 6). Maximum range of the balance was 68 kg. An effort was always made to apply the force on the visually estimated center of gravity. The turnbuckle was rotated until breaking took place. A plastic band moving with the balance force indicator remained in place at the measured force limit after breaking occurred.

Tests for the breaking threshold were also performed in the laboratory by holding the stem of a broken structural unit with a vise and applying the force on an extended branch. Force was applied in the direction of dominant wave advance as estimated from field observations.

The experiment was conducted on the reef flat off Cayo Turrumote at a depth of ∿10 m. Cayo Turrumote (Fig. 7) lies ∿4.0 km southeast of La Parguera, Puerto Rico. It is 500 m long and an average of 24 m wide on its exposed parts. This reef is concave to the south-southeast, trending east-west, and a wave-built rampart on the windward (east) end reaches an average height of 1.5 m above mean tide level and is about 50 m long. The rampart slopes on an angle of 44° on its seaward side and 23° toward the lagoon (Fig. 8). Boulder-sized coral rubble on the rampart is 80% A. palmata fragments; it ranges from 3.5 cm to huge boulders that reach

Table 3

Calculated Horizontal Forces

Fragment Orientation	Cylinder X	Cylinder Y	Cylinder Z	Oblate X	Oblate Y	Oblate Z
Depth (m)	12.0	12.0	11.4	12.0	12.0	11.0
Hurricane						
I	8.6*	17.9	17.9	8.5	16.2	32.5
II	3.5	7.6	7.6	1.4	2.8	5.9
III	1.6	5.4	5.4	2.8	5.4	11.5
IV	1.9	4.6	4.6	0.9	2.0	4.1

Orientation: X = long axis of fragment parallel to bottom and to wave orthogonals
Y = long axis of fragments parallel to bottom and perpendicular to wave orthogonals
Z = long axis of fragments perpendicular to bottom - large cross section of oblate fragment perpendicular to wave orthogonals

*Measurements in kilograms

lengths of up to 2.5 m. The source of A. palmata fragments starts at a depth of 1.5 m, 10 m from the boulder rampart shoreline. This reef surface extends around the cay to a depth of ∿20 m. In 1962 the reef was found to be nowhere wider than 20 m and nowhere longer than 300 m (19). After Hurricane Edith (September 1963) the effects on the coral reefs of La Parguera shelf were surveyed (20), and a large change in Cayo Turrumote was detected. Three years after Hurricane Betsy (September 1965) the cay was surveyed by Hernandez (unpublished report); length, width, and height of the ramparts and the entire cay had increased markedly to the dimensions cited above. Lateral and lagoonward migration of the ramparts had taken place between the surveys.

Ten A. palmata colonies were tested in situ for mechanical breakage of their stems and branches. Their stem diameters varied from 5 to 15 cm and ranged in height from 0.5 to 1.5 m. The thicker and stronger colonies were found close to shore, at 3 m depth. Test results showed that these colonies always broke at the stem where boring by organisms had taken place. The range of breakage was found to be from 23 to 35 kg force for a mean diameter of 13 cm. Two of the broken colonies were taken to the laboratory, where further tests were conducted. Both colonies broke again at the stem with a force of 40 kg, although the force was applied to one of the thicker branches. Degree of boring was found to be the controlling factor. When a healthy stem was tested, it resisted forces as high as 50 kg.

Outer parts of colony branches, in the

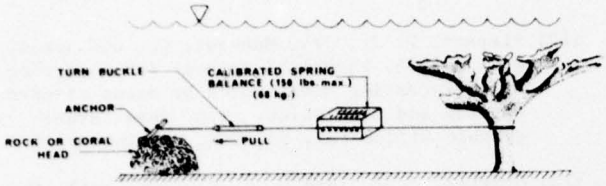

Figure 6. Illustration of method used in measurement of mechanical breaking forces in the in situ experiment.

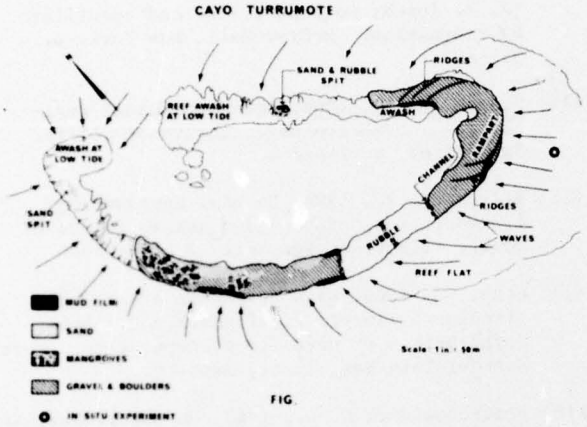

Figure 7. Location of in situ experiment and description of Cayo Turrumote.

small units tested at depths of 10 m, broke at pulls of 6 to 40 kg whenever the colony stem withstood the same range of force. Thicker (3 cm) branches of healthy coral colonies withstood forces greater than the industrial balance's scale (68 kg). Most of the broken parts in these tests had a mean length of 40 cm, varying in width from about 10 to 30 cm. The range in dimensions of A. palmata colonies is so varied that preliminary tests performed in this experiment should be greatly increased for statistical tests suitability.

Conclusions

Theoretical calculations indicate that the spectrum of forces generated by hurricane swells as a function of depth (12 m), object dimensions, and wave refraction are greater than mechanical forces necessary to break coral colonies tested in situ and in the laboratory. Forces were calculated on both cylindrical and oblate objects that had average characteristic dimensions similar to those of coral fragments comprising subaerial boulder ramparts at the field site, south coast of Grand Cayman Island. Magnitudes of forces for Hurricane I on these objects, oriented with the long axis perpendicular (Z) to the bottom, fell within the general range of forces necessary for breaking A. palmata stems as measured in the field. Forces generated by waves

Figure 8. Cayo Turrumote boulder rampart seen from the lagoon.

from the other three hurricanes were significantly smaller than field-measured breaking values. However, with the exception of forces generated by Hurricane IV, calculated values for cylindrical and oblate fragments in the Z orientation were comparable to the range of forces necessary to break colony branches as measured in field tests. Calculated forces are considered minimal values because of the selection of a drag coefficient. The rough-surfaced coral fragments would certainly have a higher drag coefficient than the smooth-surfaced objects used in the theoretical calculations.

Using a porosity of 0.5 (21) and a specific gravity for aragonite (2.93 g/cm^3), the weight of the cylindrical object in seawater is approximately 9 kg and of the oblate fragment is ≈4.5 kg. Horizontal forces on these objects exerted by waves of Hurricane I at a depth of 12 m exceed the object weights and probably would result in shoreward transport. The coefficient of friction for this setting is unknown, but considering the forces involved it is reasonable to assume that shoreward displacement of particles would occur.

Laboratory as well as field experiments indicate that breaking strength of A. palmata colonies depends considerably on the degree of skeletal weakening caused by boring organisms.

Comparisons of wave forces generated during hurricanes with field measurements of A. palmata breaking forces indicate that coral colonies at a depth of 12 m could be the source for boulder ramparts along the adjacent shoreline. The average-sized particles in these coral rubble accumulations could be transported onshore by hurricane waves generated in this theoretical study.

Acknowledgments

The research reported in this paper was supported both by the Geography Programs, Office of

Naval Research, Arlington, Virginia 22217, under contract with Coastal Studies Institute, Louisiana State University, and the Department of Marine Sciences, University of Puerto Rico, Mayaguez, Puerto Rico.

Appreciation is extended to Ms. Gerry Dunn and Mrs. M. L. Hernandez for preparing illustrations.

References Cited

(1) Verstappen, H. T., 1954, The influence of climatic changes on the formation of coral islands. Amer. J. Sci. 3, p. 428-435.

(2) McKee, E. D., 1959, Storm sediments on a Pacific atoll. J. Sediment. Petrol. 29, p. 354-364.

(3) Wiens, H. J., 1962, Atoll environment and ecology. Yale Univ. Press, New Haven, Conn., p. 45-136.

(4) Verneer, D. E., 1963, Effects of Hurricane Hattie, 1961, on the cays of British Honduras. Zeit. Geomorph. 7, p. 332-354.

(5) Stoddart, D. R., 1963, Effects of Hurricane Hattie on the British Honduras reefs and cays, October 30-31, 1961. Atoll Res. Bull. 95, p. 1-142.

(6) Stoddart, D. R., 1965, Re-survey of hurricane effects on the British Honduras reefs and cays. Nature 207, p. 589-592.

(7) Perkins, R. D., and Enos, P., 1968, Hurricane Betsy in the Florida-Bahama area--geologic effects and comparison with Hurricane Donna. J. Geol. 76, p. 710-717.

(8) Rigby, J. K., and Roberts, H. H., 1976, Grand Cayman Island: geology, sediments, and marine communities. Brigham Young Univ. Geol. Studies, Spec. Pub. 4, p. 17-26, Provo, Utah.

(9) Roberts, H. H., 1974, Variability of reefs with regard to changes in wave power around an island. Proc., Second Inter. Coral Reef Symp., Great Barrier Reef Committee, Brisbane, p. 497-512.

(10) Coleman, J. M., and Wright, L. D., 1971, Analysis of major river systems and their deltas: procedures and rationale, with two examples. Coastal Studies Inst., Louisiana State Univ., Baton Rouge, Tech. Rept. 95, p. 1-125.

(11) Sverdrup, H. U., and Munk, W. H., 1947, Wind, sea, and swell: theory of relations for forecasting. U.S. Naval Hydrographic Office Pub. No. 601, Washington, D.C.

(12) Pierson, W. J., Jr., Neumann, G., and James, R. W., 1955, Practical methods for observing and forecasting ocean waves by means of wave spectra and statistics. U.S. Naval Hydrographic Office Pub. No. 603, Washington, D.C.

(13) O'Brien, M. P., and W. R. Morison, 1952, The forces exerted by waves on objects. Trans. Amer. Geophys. Union, 33, p. 32-38.

(14) Dean, R. G., and Harleman, D. R. F., 1966, Interaction of structures and waves. In (A. T. Ippen, ed.) Estuarine and coastline hydrodynamics. McGraw-Hall, New York, p. 341-403.

(15) Wiegel, R. L., 1964, Oceanographical engineering. Prentice-Hall, Englewood Cliffs, New Jersey, p. 248-268.

(16) Silvester, R., 1974, Coastal engineering, 1, generation, propagation and influence of waves. Elsevier, New York, p. 143-214.

(17) Goda, Y., 1964, Wave forces on a vertical circular cylinder: experiments and a proposed method of wave force computation. Port Harbour Tech Res. Inst., Rept. 8.

(18) Bretschneider, C. L., 1965, On the probability distribution of wave force and an introduction to the correlation drag coefficient and the correlation inertial coefficient. Proc. Santa Barbara Conf. on Coastal Engr., 1965, p. 183-217.

(19) Almy, C. C., and Carrión-Torres, C., 1963, Shallow-water stony corals of Puerto Rico. Caribbean J. Sci. 3, p. 133-162.

(20) Glynn, P. W., Almodovar, L. R., and Gonzales, J. G., 1964, Effects of Hurricane Edith on marine life in La Parguera, Puerto Rico Caribbean J. Sci. 4, p. 335-345.

(21) Pingitore, N. E., Jr., 1970, Diagenesis and porosity modification in Acropora palmata, Pleistocene of Barbados, West Indies. J. Sediment. Petrol. 40, p. 712-722.

Unclassified
Security Classification

DOCUMENT CONTROL DATA - R & D

(Security classification of title, body of abstract and indexing annotation must be entered when the overall report is classified)

1. ORIGINATING ACTIVITY (Corporate author)	2a. REPORT SECURITY CLASSIFICATION
Coastal Studies Institute Louisiana State University Baton Rouge, Louisiana 70803	Unclassified
	2b. GROUP Unclassified

3. REPORT TITLE

HURRICANE-GENERATED WAVES AND COASTAL BOULDER RAMPART FORMATION

4. DESCRIPTIVE NOTES (Type of report and inclusive dates)

5. AUTHOR(S) (First name, middle initial, last name)

M. L. Hernandez-Avila and Harry H. Roberts and Lawrence J. Rouse

6. REPORT DATE	7a. TOTAL NO. OF PAGES	7b. NO. OF REFS
December 1977	8	21

8a. CONTRACT OR GRANT NO.	9a. ORIGINATOR'S REPORT NUMBER(S)
N00014-75-C-0192 b. PROJECT NO. NR 388 002 c. d.	Technical Report No. 242
	9b. OTHER REPORT NO(S) (Any other numbers that may be assigned this report) A044 167

10. DISTRIBUTION STATEMENT

Approved for public release; distribution unlimited.

11. SUPPLEMENTARY NOTES	12. SPONSORING MILITARY ACTIVITY
Reprint from: Proceedings, Third International Coral Reef Symp., University of Miami, Miami, Florida, May 1977, p. 71-78.	Geography Programs Office of Naval Research Arlington, Virginia 22217

13. ABSTRACT

Coral boulder ramparts along the south coast of Grand Cayman Island have no source area near the shoreline. Coral communities acting as a source of rampart rubble are found 0.3 km from shore and at a depth of 10-12 m. Theoretical calculations of wave-induced forces from wave refraction analyses of hurricane-generated waves indicate that the probable hurricane dynamic force spectrum is sufficient to break and transport coral rubble from depths of up to 12 m. In situ breaking force tests accomplished in Puerto Rico on Acropora palmata coral colonies support the theoretical calculations.

DD FORM 1 NOV 68 1473 (PAGE 1)

S/N 0101-807-6811

Unclassified
Security Classification

A-31408

14. KEY WORDS	LINK A		LINK B		LINK C	
	ROLE	WT	ROLE	WT	ROLE	WT
hurricanes						
hurricane waves						
coastal boulder ramparts						

Coastal Studies Institute
Center for Wetland Resources
Louisiana State University
Baton Rouge, Louisiana 70803

Technical Report No. 243

CONTINGENCY PLANNING FOR THE IMPACT OF OIL SPILLS IN DIFFERENT COASTAL ENVIRONMENTS OF CANADA

Edward H. Owens

December 1977

Reprint from
1977 Oil Spill Conference
Proceedings, New Orleans, La.,
March 8-10, 1977, pp. 115-122

Office of Naval Research
N00014-75-C-0192
Project No. NR 388 002

CONTINGENCY PLANNING FOR THE IMPACT OF OIL SPILLS IN DIFFERENT COASTAL ENVIRONMENTS OF CANADA

Edward H. Owens
Coastal Studies Institute
Louisiana State University
Baton Rouge, Louisiana 70803

ABSTRACT

Planning for a cleanup operation of the shore zone requires consideration of the physical nature of the coast (including the sediment types), wave energy levels, and tidal range. Beaches exist in a dynamic state and are continuously changing in response to littoral processes. In addition to these temporal variations, there is frequently considerable variability of shoreline types and process characteristics within a small region. In eastern Canada, contingency planning must cover rocky shorelines, sand beaches, and muddy coasts. There also is a wide range of littoral process environments, from the exposed Atlantic coast to the sheltered Bay of Fundy, which has tidal ranges on the order of 10 to 15 meters. Three examples from eastern Canada illustrate the variability of shorelines and processes in the context of cleanup planning.

INTRODUCTION

During the 10 years since the first large-scale cleanup program, which followed contamination of the coasts of England and France by the spill of crude oil from the tanker *Torrey Canyon*, a large number of major spills have occurred throughout the world. Despite the experience that has been gained, there is considerable room for improvement in contingency planning. This discussion will focus on one method by which improvements could be made, that is, by reconnaissance surveys of environments in areas where there is a high risk of coastal oil spills.

The major factors that determine the effects of a large spill on a coast are the volume of oil in the spill, the type of oil involved, the climatic and meteorological conditions at the time of the spill, the characteristics of the littoral energy environment (waves and tides), and the geological character of the coastal environment. Although much is known about the behavior of different types of oil under different conditions, because of the number of variables involved the first three factors are basically unpredictable. The last two factors can be predetermined from field work or from reconnaissance surveys. They can be used as the basis for local and regional contingency plans by providing estimates of how and where the oil will be deposited, the persistence of the oil, the suitability of cleanup techniques to a particular location, and the availability and cost of those techniques.

Three examples from very different coastal environments in eastern Canada will be used to illustrate the importance of understanding the variability of littoral processes and of geological parameters in planning cleanup programs:

1. the south coast of Chedabucto Bay is essentially a rocky coast on which there are a few pocket beaches of pebble-cobble sediments. In this instance, contingency plans need only allow for two types of shoreline in a single littoral energy environment.
2. the sandy beaches of the Madgalen Islands represent only one shoreline type but have two distinct littoral energy environments, so that two plans are necessary even though the shoreline type is uniform.
3. in marked contrast to these relatively simple coastal environments, the Bay of Fundy has a large number of shoreline types and littoral energy conditions that vary considerably. The contingency plan for that area must include specific cleanup responses to accommodate each environment.

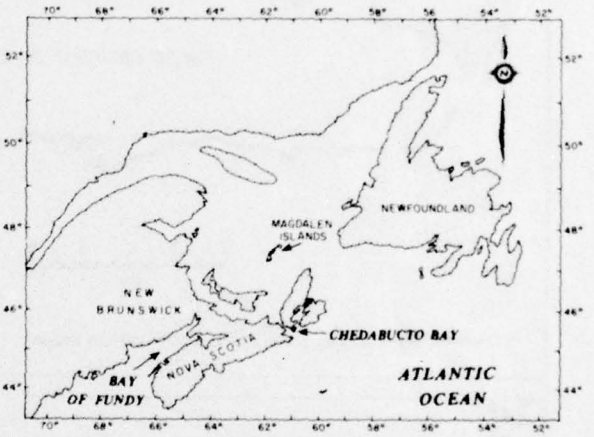

Figure 1. Location of the three areas of study in eastern Canada

Chedabucto Bay, south shore

The south shore of Chedabucto Bay (Figure 1) is typical of much of the exposed rocky shorelines of the Atlantic coast of Nova Scotia. The process environment is one of high wave energy conditions and a tidal range on the order of 1.5 meters. This is a storm-wave environment,[2] and the physical processes are relatively uniform along this straight section of coast, although there is a small decrease in energy levels to the west as the coast becomes more sheltered from the Atlantic. The variability of coastal environments is related primarily to the two major shoreline types that are present in this section.

This straight shoreline is a fault-line coast that is characterized by low, resistant cliffs and intertidal rock platforms. The uniform character is interrupted by small bays that have been formed by wave erosion along secondary faults or other lines of weakness. The rocky coast is largely devoid of sediment; the only deposits occur within the bays and form pocket beaches of pebble-cobble material. Very little material is supplied to the coast, so that the rate of sediment accumulation is very slow.[5]

The deposition and fate of oil on exposed rocky coasts is very different

from that on the beaches of the small bays. Oil coats the surface of the rocks and the intertidal algae and collects in supratidal rock pools if contamination occurs during periods of high water levels (spring tides or storms). The trapping of oil in the supratidal rock pools is particularly important because oil is stored there until released by a subsequent high water level. Recontamination of adjacent shorelines that may already have been cleaned (naturally or by a cleanup operation) may occur. Removal of oil from rock surfaces or rock pools is usually a slow and difficult operation requiring manual techniques in different terrain. However, in this high-energy environment, natural self-cleaning is rapid and usually effective.

Figure 2 shows those sections of shoreline that were contaminated following the spill of Bunker C oil from the tanker *Arrow* in 1970. The upper diagram indicates all locations where oil was observed in the shore zone between March and June 1970. The lower diagram shows the actual distribution by the end of June 1970. On high-energy, exposed rocky coasts, wave action abrades and disperses the oil. In addition to this mechanical action, weathering processes, such as chemical oxidation and microbial attack, are accelerated, and the shoreline is cleaned naturally within a few months.

By contrast, virtually all types of oil deposited on the pocket beaches would permeate the pebble-cobble sediments, making it necessary to remove a sediment-oil mixture using a tracked vehicle or a front-end loader. Graders could not be used on this type of beach. At one site on this coast (Indian Cove, in Fox Bay) studied following the *Arrow* spill, the beach was contaminated near the high-water level to depths up to 20 cm.[3, 6] The beach was recontaminated on several occasions by oil released from adjacent rock pools during high spring tides.

Removal of sediment from this pocket beach led to lowering of the surface by as much as two meters. Because no sediment was available to naturally replace what was lost, waves washed over the beach crest, and within 12 months the beach crest had retreated between 10 and 20 m. Sediment removal must be avoided in this type of environment unless the beach material is replaced by equal amounts of similar-sized sediment. In the example from Indian Cove, more damage resulted from the removal of sediment during cleanup than had occurred originally from the contamination. The persistence time of oil in these small bays is high because they are set back from the main trend of the exposed coast and, therefore, are sheltered from wave activity.

On cobble beaches, oil that is deposited on the upper beach during storms is unaffected by normal wave action. Inasmuch as the oil is not subject to abrasion, it will degrade very slowly. Subsequent storm waves may erode the beach and deposit cobbles on the upper beach, thus burying the oil layer (Figure 3). The beach may appear clean on the surface, but substantial amounts of oil may merely have been covered (Figure 4).

Summary. Exposed rock coast: natural cleaning is rapid except above the limit of wave activity; cleanup operations would require manual removal of oil from pools to prevent redistribution. Pocket beaches: sheltered from waves; therefore, oil persists longer and natural cleaning is less effective; oil would permeate pebble-cobble sediments; if cleanup is necessary it would require removal of oil-sediment layer up to 60 cm deep and replacement by material of similar size; graders could not be used; tracked vehicle would be required for mechanical cleanup.

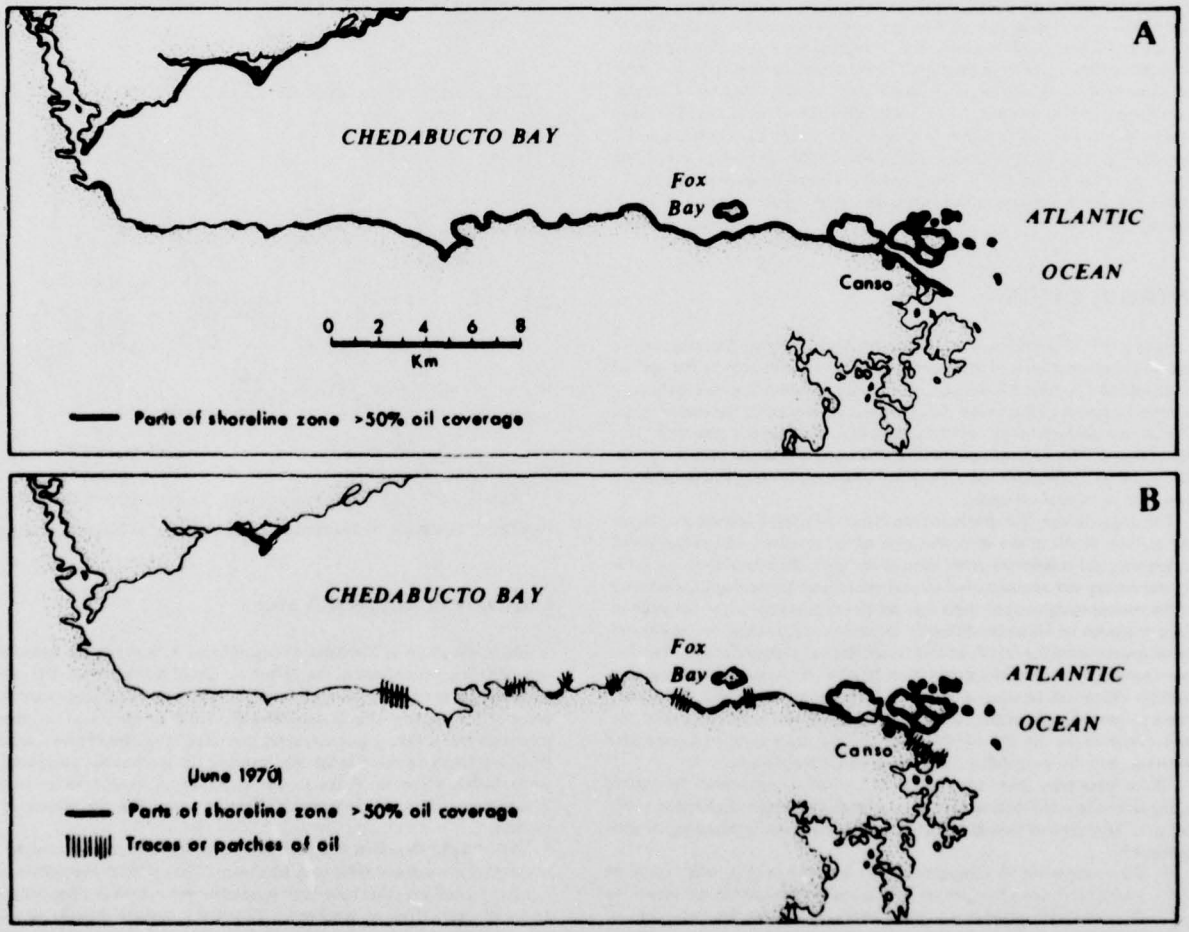

Figure 2. Distribution of oil residues on the south shore of Chedabucto Bay; (A) a compilation of all locations where oil was observed between March and June 1970; (B) oil residues in the shore zone in June 1970, from ground and aerial observations (adapted from Owens and Rashid[3])

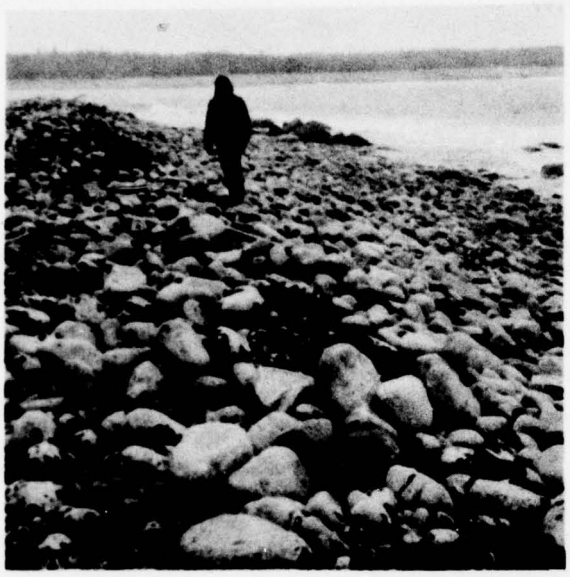

Figure 3. Cobble beach, Chedabucto Bay: this beach was severely contaminated during the spring of 1970; the photograph, taken in the spring of 1973, shows that the oil deposited above the high water mark had undergone little abrasion during the three-year period, but that it was being buried by material thrown up onto the top of the beach by the action of storm waves

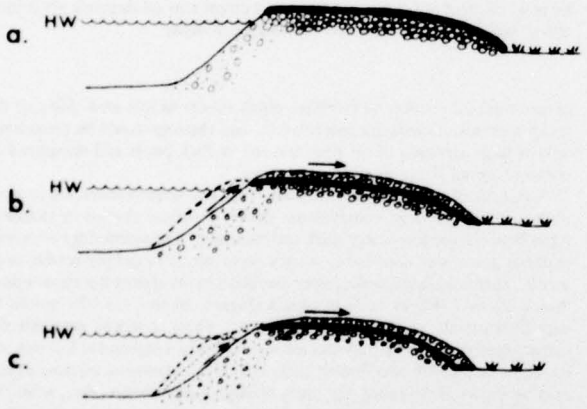

Figure 4. Effects of storm-wave action on oil residues deposited on a cobble beach; in (a) oil is deposited above the high water mark (HW), (b) a subsequent storm will erode the intertidal beach and waves will push the cobbles onto the upper beach to cover the oil deposit; (c) a second storm will continue this process, gradually exposing more of the buried oil-sediment layer

Magdalen Islands

The Magdalen Islands, located in the central Gulf of St. Lawrence (Figure 1), consist of a series of barrier beaches that connect small bedrock outcrops (Figure 5). Because the tidal range is less than one meter, wave energy is concentrated in a narrow vertical band. The wave climate is dominated by locally-generated wind waves. Wave energy levels are higher on the west coast in all seasons owing to the prevailing onshore winds on that coast.[4] The characteristic feature of the west coast process environment is the seasonal variation in energy levels due to the higher frequency of storms in winter months. Wave energy levels also are higher in winter than in summer months on the east coast, but the seasonal variations in wave height are overshadowed by the effects of storm waves, which produce large, short-term variability throughout the year.

Both coasts have long, straight sand beaches; therefore, in terms of shoreline types and sediment characteristics, the west- and east-facing barriers are similar. The differences that have been reported[4] result from the contrast in the littoral energy environments. The effects of a major spill in the vicinity of the Magdalen Islands would be very different on the west than on the east coast, making it necessary to have two response plans available. Oil would be deposited in the same manner and at the same locations on the beach in these two environments. Owing to the small grain size of the sediments, the oil will not penetrate the beach unless it is fresh crude or a very light grade petroleum.

Mechanical cleanup with graders would not be easy on the western barriers as the beach is too narrow (20 to 30 m) and beach gradients are frequently too steep, particularly during winter months. It is likely, therefore, that tracked vehicles, front-end loaders, or even manual techniques would be necessary on this coast. Graders most probably could be used on the wider, flatter eastern barriers.

One problem on the east coast would occur if the oil were deposited during storm-wave conditions. The eroded beach would recover very rapidly inasmuch as accretion has been observed within two or three days following a storm.[7] Unless oil were removed quickly from these east coast beaches, it would be buried by sand bars that migrate onto the beach during the post-storm recovery phase (Figure 6). Cleanup would then involve excavation of the beach to remove the oil (Figure 7). The persistence time of oil on the two beaches would also be very different. With higher wave energy levels on the west coast, the mechanical and chemical breakdown of oil in the littoral environment would be more rapid.

The most important aspect of the sand beaches of eastern Canada and many parts of the east coast of the U.S. is that the beaches are very mobile as a result of storm wave activity and post-storm accretion. The constant movement of sediments would lead to burial of oil in some locations, whereas in others it would be eroded. If cleanup is necessary it should, therefore, be carried out as soon as possible after the oil reaches the beach.

Summary. Oil would affect both beaches in a similar manner, but different cleanup techniques would be required. On the west coast, the beach generally is narrow and steep so that graders could probably not be used; tracked vehicles or manual techniques would be required. Because of high wave energy levels, dispersal and chemical degradation would be relatively rapid. On the east coast, graders probably could be used. If the beach is contaminated during storm conditions, oil residues would probably be buried within two or three days. Because wave energy levels are lower than on west coast, residues persist longer.

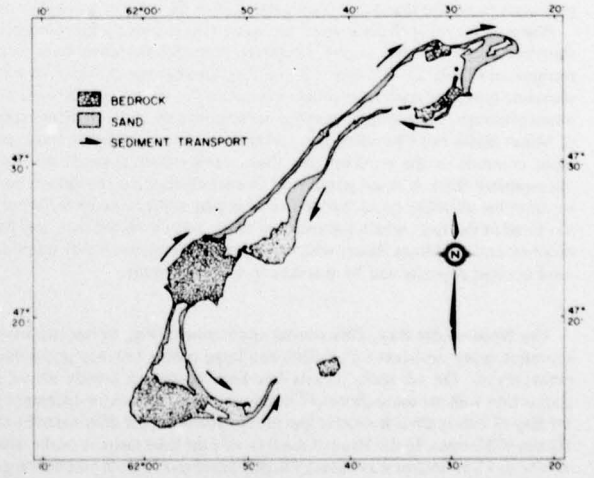

Figure 5. The Magdalen Islands, Quebec; distribution of barrier beaches and directions of sediment transport

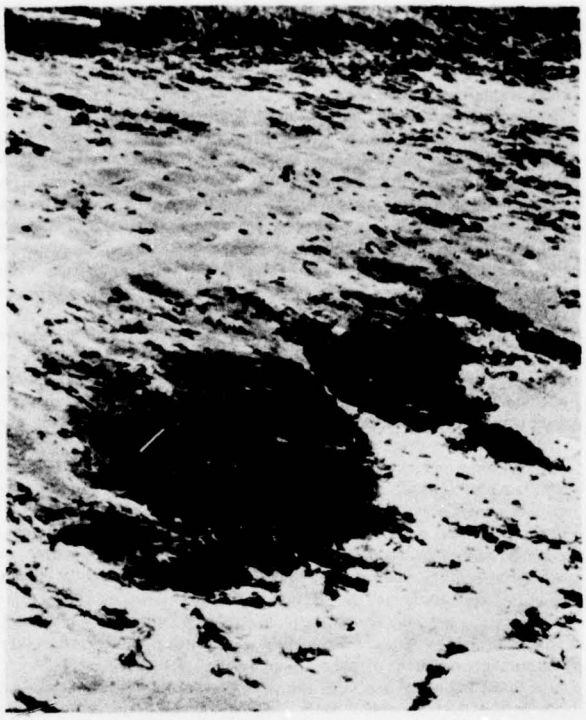

Figure 6. Sand beach, Chedabucto Bay: the beach was covered by a thick deposit of oil on the upper parts of the intertidal zone; this photograph, taken a month after the oil had been laid down, shows that most of the oil was buried by sand with only the outer portion of the oil-sediment layer exposed (see Figure 7f)

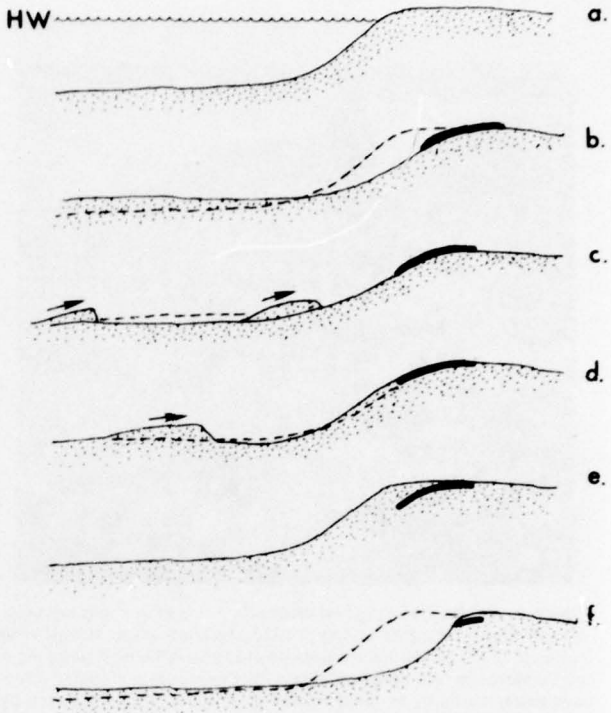

Figure 7. Effects of storm-wave action on oil residues deposited on a sandy beach: (a) the pre-storm beach; (b) oil is deposited on the upper beach after a storm has eroded the intertidal beach; (c) post-storm recovery commences and sand migrates back into the intertidal beach; (d) and (e) the sand then will cover the oil deposit; (f) a later storm will expose the buried oil-sediment layer

Bay of Fundy

Planning response tactics at the local level takes into account variations in shoreline types and process characteristics. Preparation of contingency plans at the regional level involves a much wider range of responses in order to include all the local aspects. In the Bay of Fundy, which has a coastline of approximately 1,400 km, six major coastal environments have been identified (Figure 8, Table 1). Each of the coastal environments either has distinctive physical parameters (geology or geomorphology) or distinctive processes (waves or tides) that distinguish it from the other coasts of Fundy.

Planning for oil spill cleanup of the coast also requires a knowledge of shoreline types. In this region 12 major types of shoreline have been recognized (Table 2). Oil deposition and persistence are different in each shoreline type, and each type could occur in any of the six coastal environments although, for example, marshes occur primarily in the sheltered areas of Minas Basin and Chignecto Bay, whereas sheltered, resistant coasts are more common in the northwestern shore environment (particularly Passamaquoddy Bay). It is not possible to discuss each of the coastal environments or the shoreline types, and so two examples will be considered briefly: the Head of the Bay, which has resistant cliffs, large embayments, and bay beaches; and the Minas Basin, which is characterized primarily by intertidal sand or mud deposits and by marshes in sheltered areas.

The Head of the Bay. This coastal environment (Fig. 9) has two major shoreline types: resistant rocky cliffs and large cobble beaches in the three embayments. Oil on rocky coasts has been discussed briefly above in connection with the south shore of Chedabucto Bay. One major difference in the Bay of Fundy environment is that littoral processes are dominated by the effects of the tides. In the Head of the Bay area the tidal range is on the order of nine to 12 m, so that wave energy is dissipated over a wide vertical range. Also, this is a sheltered wave environment, and levels of wave energy initially are lower than on the exposed Atlantic coast. Mechanical abrasion of intertidal oil residues is therefore much slower in this area. Most of the rocky sections of coast are inaccessible, and cleanup would be considered only if large amounts of oil were trapped in rock pools and threatened to contaminate adjacent marshes or beaches.

An idealized cross section across one of the bay-head beaches that occur in each of the three large embayments shows a distinct change in sediment types between the low-water mark and the marsh. The storm ridge of cobble material gives way seaward to a very steep beach of pebble-cobble sediments. This is replaced in the lower foreshore by an almost flat mud deposit that is up to 1,000 m wide in places (Figure 10 and 11). Oil would be deposited mainly on the coarse sediments, where it would penetrate the surface material. As the mud flats are wet even when exposed at low tide, oil on the surface would be refloated by the flood tide. However, oil that collects in depressions or permeates the mud, through burrow holes, etc., would be rapidly covered by a mud veneer after only one or two tidal cycles. Once buried, this oil would persist because of lack of mechanical abrasion and anaerobic conditions that prevent oxidation and microbial degradation.

Amounts of oil on the central and upper sections of the beaches would probably be very large in these three embayments. Wind-driven surface currents are primarily from the west-southwest and are generated by the prevailing and dominant westerly winds along the axis of the bay. The embayments face the west or southwest and are bounded by rocky headlands. Any slicks that entered the three embayments would be trapped, and the oil most likely would be deposited on the bay-head beaches. These bay-head beaches would present a problem for a cleanup program because oil almost certainly would be trapped in rock pools on the rocky coasts adjacent to the beaches, and the problem of recontamination would be very real. Access to these rocky headlands is difficult and often dangerous owing to the rapid speed with which the flooding tide rises. Removal of contaminated sediments from the beaches would lead to an unstable condition inasmuch as the input of sediment to replace that which would be removed would be very slow. Replacement of the material would be necessary to avoid initiating any erosion.

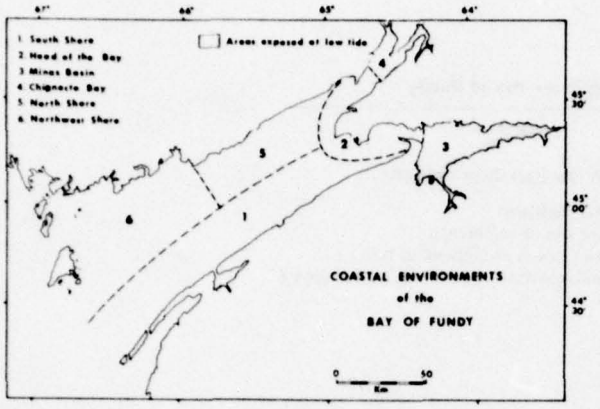

Figure 8. Subdivisions of the Bay of Fundy shoreline into six coastal environments

It is clear that in this instance many factors must be considered before a cleanup operation could be initiated. It is also important that each of the points discussed briefly above is predictable, so that a practicable contingency plan for this environment can be prepared in advance.

Minas Basin. The characteristics of the shoreline of the Minas Basin are extremely varied, ranging from sandstone cliffs to marshes and from wide intertidal sand flats to rock platforms. Two of the most common combinations of shoreline types are mud flats or sand flats backed by either unresistant till cliffs or marshes (Figure 12). The tidal range is greater than 10 m; a maximum of 16 m has been recorded in places during spring tides. This large tidal range, coupled with low coastal zone gradients, gives a wide intertidal zone that is exposed at low tides (Figure 8). Where present, the intertidal deposits are either sand or mud and rest on a wave-cut till and/or bedrock platform.

The mud flats rarely are completely dry at low tide and frequently have a thin film of water on the surface of the sediments. Oil deposited on the surface would be refloated by rising tide and carried elsewhere. As noted above, any oil that is buried would be protected from mechanical, chemical, and microbial degradation and will, therefore, persist for a long time unless subsequently exposed by changes in bottom morphology.

Table 1. Characteristics of the coastal environments of the Bay of Fundy

Subdivision	Geological character	Backshore relief	Beach character	Fetch and wave exposure	Mean tidal range	Sediment availability
1. South Shore	resistant basalt dyke parallels coast	low rocky coast or cliffs up to 30 m	absent or narrow cobble beach at high water mark, with wide intertidal platform	sheltered (50 km)	6 to 10 m	very sparse
2. Head of the Bay	resistant rocks; basalts or granites	cliffed coast, up to 200 m	absent or large pocket beaches of peb/cob on beachface and mud overlying coarse sediments in intertidal zone	exposed (50-100 km)	10 m	sparse, but locally abundant
3. Minas Basin	sandstone and shales, or unconsolidated glacial deposits	cliffs, up to 30 m	wide intertidal mud or sand flats on rock platform, peb/cob beach at hwm; marshes in sheltered areas	very sheltered (<50 km)	>10 m	abundant
4. Chignecto Bay	sandstones and shales	cliffs, up to 20 m	wide intertidal mud flats on rock platform, peb/cob beach at hwm; extensive marshes in sheltered areas	very sheltered (<50 km)	>10 m	abundant
5. North Shore	resistant rocks, sedimentary rocks and intrusives, thin till cover	cliffs (west, 5 to 60 m; east, >100 m)	absent or coarse-grained pocket beaches	sheltered (<50 km	6 to 10 m	very sparse
6. Northwest Shore	resistant rocks, thin till cover	low rocky coast or cliffs, 5 to 30 m	absent or coarse-grained and narrow	outer coast exposed, rest sheltered (<50 km)	6 m	sparse

Table 2. Shoreline types in the Bay of Fundy

I. Rock or cliff shorelines

1. Exposed, resistant coast with low backshore or cliffs
   - with no beach or intertidal platform
   - with wave-cut platform devoid of sediments
   - with wave-cut platform and beach at high-water line
   - with wave-cut platform and intertidal sediments (see 9, below)
2. Sheltered, resistant coasts
3. Exposed, unresistant cliffs
4. Sheltered, unresistant cliffs

II. Shorelines with beaches

5. Cobble or mixed-sediment beaches
   - beach at base of cliff
   - beach with overwash
   - beach with inlet and/or lagoon
6. Sand beaches
7. Pocket beaches
   - on rocky coasts
   - in a large embayment
8. Beaches in sheltered environments

III. Shorelines with intertidal sediments

9. *Coarse sediments on a wave-cut platform*
10. Intertidal mud
11. Intertidal sand

IV. Shorelines with vegetation

12. Marshes

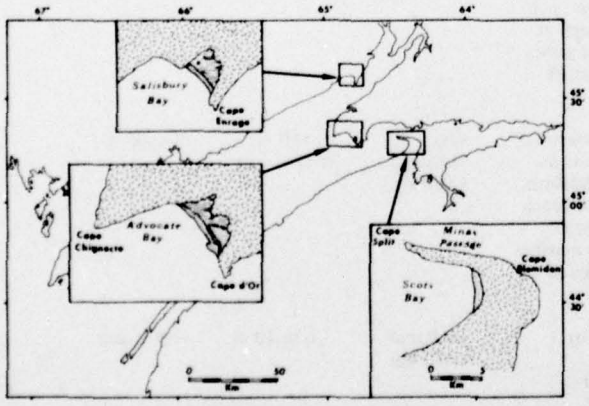

Figure 9. The Head of the Bay: this subdivision is characterized by three large embayments that are exposed to the southwest; each has a large pebble-cobble beach that is backed by marshes and fronted by mud flats (Figure 11)

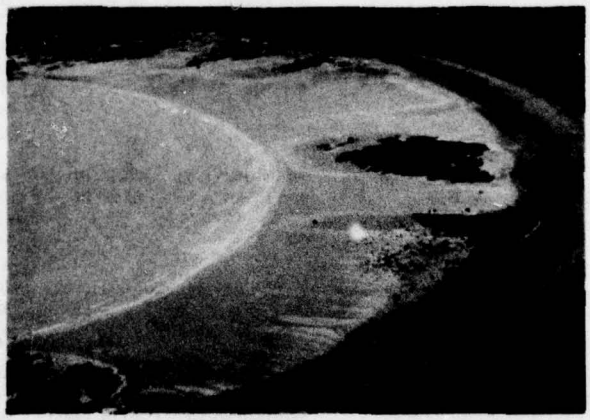

Figure 10. A pocket beach on the north shore of the Bay of Fundy: although this beach is much smaller than those in the large embayments, it has the same sequence of cobble ridge-pebble/cobble intertidal beach-mud flats; the tidal range at this site is 7.5 m; the photograph was taken at low tide

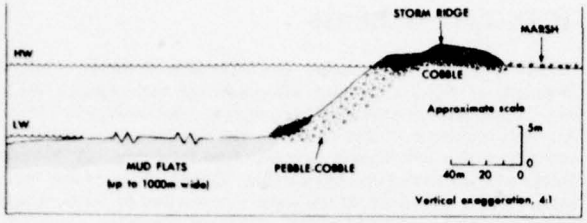

Figure 11. Idealized profile across the intertidal zone on one of the large embayment beaches in the Head of the Bay subdivision.

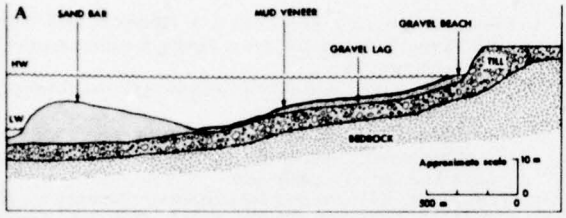

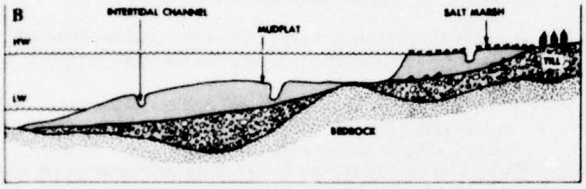

Figure 12. Idealized profiles across two of the major shoreline types that occur in the Minas Basin: (A) intertidal sand flats with a gravel beach at the highwater mark and an unresistant till cliff; (B) intertidal mud flats that give way to salt marshes above the high water mark (adapted from Dalrymple *et al.*,[1] Swift *et al.*[8])

Oil deposited on dry mud flats or sand flats would be subject to mechanical abrasion and burial. The sand deposits are in a state of constant motion, primarily in association with the strong tidal currents, which reach velocities up to 2 m/sec.[1] Although wave action is minimal inasmuch as this is a very sheltered environment, the high level of tidal energy generates rapid sediment transport. Sand grains are moved individually along the surface and mechanical abrasion results. Sand waves up to 2 m thick can be formed that migrate as a body across the sand flats (Figures 13 and 14). The migration of these sand waves or of mud deposits would lead to temporary burial of oil deposited in the intertidal zone. Cleanup on the mud flats would be almost impossible owing to the great difficulty of access for walking across mud flats is often very slow and exhausting. The sand flats can be traversed easily on foot, but operations would be complicated by the speed at which the rising tide crosses the wide flats, which often is faster than a person can run.

Where the intertidal deposits have a pebble-cobble beach and a till cliff in the upper foreshore (Figure 12, top), any oil deposited on the beach would only slowly be abraded. Wave energy levels are low in this environment, and the waves are active on the beach only for brief periods at the flood of the tide. Mechanical abrasion, however, may be less important in this environment than weathering. The small surface area and low adsorptive capacity of pebble-sized material would expose more oil to chemical oxidation and to photochemical and microbial weathering than would be the case on smaller sized sediments.

The till cliffs are composed largely of easily erodable unconsolidated clays, sands, and cobble. The beach acts as a buffer to protect the base of the cliff from erosion, so that removal of contaminated material from the beach could reduce the level of protection and could initiate a period of cliff erosion. If replacement of sediment is not possible, natural cleaning could be hastened by pushing the contaminated sediments down the beach toward the water line and allwing the rising tide to transport the material back up the beach. This technique would not lead to complete removal of the oil but would at least speed up the process of mechanical abrasion.

Figure 13. Sand waves in the intertidal zone of the Minas Basin: the distance between the crests of the waves is approximately 5 m, and the height of the sand waves is about 1 m; the sand waves are migrating from left to right in this photograph

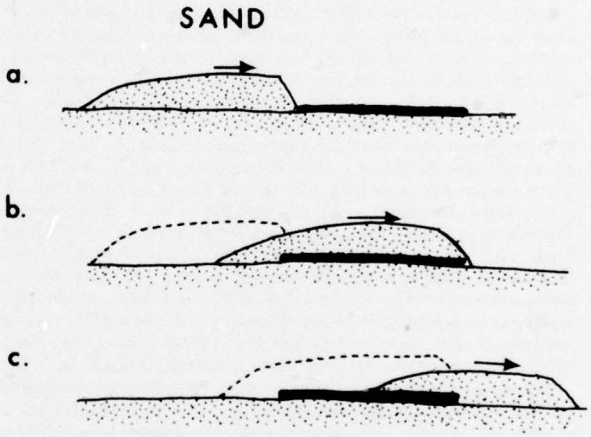

Figure 14. Sand wave migrating across an intertidal oil deposit (see Photo 13)

If the intertidal deposits are backed by marshes, oil would be deposited on the marsh surface only during periods of spring tides or high water levels that result from storm surges. The level of the marsh is above the mean high water mark, and oil would otherwise be confined to the tidal creeks. During slack tides wind-driven slicks would be carried to the east by the prevailing and dominant westerly winds. They would be carried toward the marshes because these occur primarily at the eastern ends of Minas Basin and Chignecto Bay (Figure 8). Unless carried out of the marsh areas by the ebb tides, the oil would be trapped there. In terms of preventive measures, the marsh areas should receive high priority inasmuch as cleanup is very difficult in this type of environment and they are very sensitive ecological systems in terms of both fauna and flora.

Summary. The Bay of Fundy includes a complex suite of shoreline types within six major coastal environments. At the Head of the Bay, the large embayments would act as traps for wind- or current-driven slicks moving from west to east. On mud flats in the lower foreshore, buried oil would not be subjected to mechanical, chemical, or microbial degradation. Manual cleanup before burial would be the only effective technique for oil removal. Oil should be removed from adjacent rock shores to prevent reoiling of cleaned sections. Removal of oiled sediments from cobble-pebble beaches would require replacement of the material.

In the Minas Basin area, sediments constantly are being redistributed in the intertidal zone, so that burial of oil is very probable. No practical or

effective way to clean the intertidal zone is known. If material is removed from the base of unconsolidated cliffs, it should be replaced to protect cliff from erosion. Marshes would be better protected than cleaned.

CONCLUSIONS

Many aspects of a spill, such as the type and volume of oil, will be unknown until the event occurs. Nor can the meteorological and oceanographic conditions be predicted accurately. Other aspects of spill behavior can be studied, though, as part of preparing contingency plans. Prediction of the movement of oil using modeling techniques is a valuable tool in defining probable areas where a slick would impact on the coast.[9] Knowledge of the shoreline types, the beach sediment types, and the temporal variations in shoreline morphology are critical elements in predicting or estimating the distribution and persistence of an oil slick that reaches the coast. This information can be obtained either from existing data sources or from field studies and can be related to potential spill situations.

Beach dynamics, including spatial and temporal variations of the beach, are relatively well understood, particularly for sand coasts. Although the exact forcing functions and sediment pathways may be open to question, beach responses on sand and pebble-cobble coasts can be defined for given environmental conditions. Muddy coasts are less well known at present, primarily because of the difficulties of field study in this type of environment. The coastal geologist is in a position to provide contingency plans on specific sections of coast that will be valuable in determining the impact of oil on the shore, and to assess the effects of various cleanup techniques in terms of beach stability and sediment replenishment. The latter point is of great importance inasmuch as application of unsuitable techniques may lead to more damage than would have been caused by the oil alone. This is particularly important in areas of limited sediment supply to the beach and where a beach acts as protection for unconsolidated backshore cliffs.

It is well known that the type of oil and the nature of the sediments are important in predicting such factors as the depth to which oil will penetrate a beach. Many other parameters must be considered also in order to estimate the effects of a spill on different sections of coast. Longshore currents, tidal range, and levels of wave energy will affect the nature of the contamination as much as the type of oil or the size of the sediments. These parameters vary considerably along shore even on very short sections of coast, thus making the development of effective local contingency plans more difficult.

The examples from eastern Canada illustrate the variety of conditions that can face a cleanup manager. The development of local contingency plans[10] requires not only the organization of prepared personnel with defined responsibilities but also an adequate knowledge of the site conditions. Reconnaissance studies of high-risk coasts can provide this information which then can be presented in a format suitable for use by field personnel.

ACKNOWLEDGMENTS

Field studies in eastern Canada were undertaken as part of a series of investigations of coastal processes and morphology at the Atlantic Geoscience Center, Bedford Institute of Oceanography, Dartmouth, Nova Scotia. A reconnaissance of the Bay of Fundy coast was carried out as part of a contingency plan development program of the Environmental Protection Service, Department of the Environment, Halifax, Nova Scotia. Salary support during preparation of this paper was provided by the Geography Programs, Office of Naval Research, Arlington, Virginia.

REFERENCES

1. Dalrymple, R. W., R. J. Knight, and G. V. Middleton, 1975. Intertidal sand bars in Cobequid Bay (Bay of Fundy). *Estuarine Research*. L. E. Cronin (ed.) v2
2. Davies, J. L., 1972. *Geographical Variation in Coastal Development*. Oliver and Boyd, Edinburg
3. Owens, E. H., and M. A. Rashid, 1976. Coastal environments and oil spill residues in Chedabucto Bay, Nova Scotia. *Canadian Journal of Earth Sciences*. v13, pp908–928
4. Owens, E. H., 1977. Process and morphology characteristics of two barrier beaches in the Magdalen Islands, Gulf of St. Lawrence, Canada. *Proceedings of 15th International Conference on Coastal Engineering*. American Society of Civil Engineers, New York. (in press)
5. Owens, E. H., 1971. A Reconnaissance of the Coastline of Chedabucto Bay. Dept. of Environment, Marine Science Paper 4, Ottawa, Ontario
6. Owens, E. H., 1971. The Restoration of Beaches Contaminated by Oil in Chedabucto Bay, Nova Scotia. Manuscript Report Series No. 19, Marine Sciences Branch, Ottawa, Ontario
7. Owens, E. H., and D. H. Frobel, 1977. Ridge and runnel systems in the Magdalen Islands, Quebec. *Journal of Sedimentary Petrology*. v47, (in press)
8. Swift, D. J. P., B. R. Pelletier, A. K. Lyall, and J. A. Miller, 1973. Quaternary sedimentation in the Bay of Fundy. *Earth Science Symposium on Offshore Eastern Canada*. Paper 71-23, P. J. Hood (ed.). Geology Canada, Ottawa, Ontario
9. Williams, G. N., R. Hann, and W. P. James, 1975. Predicting the fate of oil in the marine environment. *Proceedings of Joint Conference on Prevention and Control of Oil Spills*. American Petroleum Institute, Washington, D.C.
10. Yates, R. A., 1975. The making of a local contingency plan. *Proceedings of Joint Conference on Prevention and Control of Oil Spills*. Washington, D.C.: American Petroleum Institute, Washington, D.C.

Unclassified

Security Classification

DOCUMENT CONTROL DATA - R & D

(Security classification of title, body of abstract and indexing annotation must be entered when the overall report is classified)

1. ORIGINATING ACTIVITY (Corporate author)	2a. REPORT SECURITY CLASSIFICATION
Coastal Studies Institute Louisiana State University Baton Rouge, Louisiana 70803	Unclassified
	2b. GROUP Unclassified

3. REPORT TITLE

CONTINGENCY PLANNING FOR THE IMPACT OF OIL SPILLS IN DIFFERENT COASTAL ENVIRONMENTS OF CANADA

4. DESCRIPTIVE NOTES (Type of report and inclusive dates)

5. AUTHOR(S) (First name, middle initial, last name)

Edward H. Owens

6. REPORT DATE	7a. TOTAL NO. OF PAGES	7b. NO. OF REFS
December 1977	8	10

8a. CONTRACT OR GRANT NO.	9a. ORIGINATOR'S REPORT NUMBER(S)
N00014-75-C-0192	
b. PROJECT NO. NR 388 002	Technical Report No. 243
c.	9b. OTHER REPORT NO(S) (Any other numbers that may be assigned this report) A043 713
d.	

10. DISTRIBUTION STATEMENT

Approved for public release; distribution unlimited.

11. SUPPLEMENTARY NOTES	12. SPONSORING MILITARY ACTIVITY
Reprint from 1977 Oil Spill Conference Proceedings, New Orleans, La., March 8-10, 1977, pp. 115-122	Geography Programs Office of Naval Research Arlington, Virginia 22217

13. ABSTRACT

Planning for a cleanup operation of the shore zone requires consideration of the physical nature of the coast (including the sediment types), wave energy levels, and tidal range. Beaches exist in a dynamic state and are continuously changing in response to littoral processes. In addition to these temporal variations, there is frequently considerable variability of shoreline types and process characteristics within a small region. In eastern Canada, contingency planning must cover rocky shorelines, sand beaches, and muddy coasts. There also is a wide range of littoral process environments, from the exposed Atlantic coast to the sheltered Bay of Fundy, which has tidal ranges on the order of 10 to 15 meters. Three examples from eastern Canada illustrate the variability of shorelines and processes in the context of cleanup planning.

DD FORM 1 NOV 68 1473 (PAGE 1)

S/N 0101-807-6811

Unclassified

Security Classification

A-31406

14 KEY WORDS	LINK A		LINK B		LINK C	
	ROLE	WT	ROLE	WT	ROLE	WT
coastal ecology oil spills Canada						

Coastal Studies Institute
Center for Wetland Resources
Louisiana State University
Baton Rouge, Louisiana 70803

Technical Report No. 244

WAVE ACTION AND BOTTOM MOVEMENTS IN FINE SEDIMENTS

by

Michael W. Tubman and Joseph N. Suhayda

December 1977

Reprint from
Proceedings, 15th Coastal Eng.
Conf., Honolulu, Hawaii, July 11-17,
1976, pp. 1168-1183 (Amer. Soc. of
Civil Eng.).

Office of Naval Research
N00014-75-C-0192
Project No. NR 388 002

Reprinted by the American Society of
Civil Engineers from the Proceedings of
the 15th Coastal Engineering Conference,
Honolulu, Hawaii, July 11-17, 1976

CHAPTER 69

WAVE ACTION AND BOTTOM MOVEMENTS IN FINE SEDIMENTS

Michael W. Tubman and Joseph N. Suhayda
Coastal Studies Institute, Louisiana State University
Baton Rouge, Louisiana 70803

Abstract

Mudbanks have been observed to have an extraordinary calming effect on the sea surface. In certain cases this effect is due primarily to the transfer of energy through the sea/mud interface and its frictional dissipation within the bottom sediments. This paper describes an experiment that measured wave characteristics and the resulting sea floor oscillations in an area where the bottom is composed of fine-grained sediments. The energy lost by the waves at the position of the experimental setup is calculated and compared with a direct measurement of the net energy lost by the waves in going from the point of the experiment to a station 3.35 km inshore. Results show that bottom motions in the range of wave-induced bottom pressures from near zero to 2.39×10^3 Pascal have the appearance of forced waves on an elastic half space. The apparent effect of internal viscosity is seen in a phase shift between the crest of the pressure wave and the trough of the mud wave. Measurements show this angle to be 22° (±11°) for the peak spectral component (T = 7.75 seconds). The energy lost to the bottom by the waves at the field site was found to be at least an order of magnitude greater than that resulting from the processes of percolation or that caused by normal frictional effects. This newly observed mechanism for the dissipation of wave energy is particularly important for waves in intermediate-depth water and could be a prime factor in determining design wave heights in muddy coastal areas.

Introduction

The extraordinary calming effect that mudbanks exert on surface waves has been recognized for at least two centuries. With the development of the offshore oil industry there also came a recognition that large vertical and horizontal dislocations of the sea floor could occur in areas where the bottom is composed of fine-grained sediments. That these large-scale movements might be linked to wave activity was dramatically suggested in 1969 when two oil platforms were toppled during Hurricane Camille (Sterling and Strohbeck, 1973). The problem of fine-grained sediment mass movements has led to both theoretical and laboratory studies of the interaction of surface-wave-induced bottom pressures and fine-grained sediments. However, direct measurements of wave-induced pressures and resulting bottom movements have not been reported prior to our work.

The results of our work describing the response of bottom sediments to wave pressures were first presented by Suhayda et al. (1976). The analysis

of the field data presented here concentrates on the effect that this interaction has on the loss of wave energy. In the area where our study was conducted (see Fig. 1), the sediment concentration of the water column was not a significant factor contributing to the loss of wave energy. It has been suggested that water column sediment concentration is the key factor in the calming effect of mudbanks (Delft Hydraulics Laboratory, 1962); however, the forcing of a mud wave by wave-induced pressures is also a part of the physical processes wherever fine-grained sediments occur. An understanding of this process is important not only in the Mississippi Delta but also in such coastal areas as the Guianas, the northern coast of China, and southwest India, where extensive areas of fine-grained sediments occur.

Methods

As a cooperative research effort by scientists of the Marine Geology Branch, United States Geological Survey, Corpus Christi, Texas, and the Coastal Studies Institute, Louisiana State University, two field sites were instrumented in East Bay, Louisiana. The primary experimental station and the location of a nearby soil boring are shown in Figure 1.

Results of analysis of the boring (Fig. 2) show the bottom sediments to be very soft, recently deposited material from the Mississippi River. Shear strengths range from 1.57 kilonewtons/meter^2 (kN/m^2) near the water/sediment interface to 2.36 kN/m^2 3 meters into the sediment. These low values of shear strength are common in the Mississippi Delta. The boring log shows no evidence of the crust zone that often occurs in these sediments between -3 and -10 meters. In places where the sharp increase in shear strength that defines a crust zone occurs, it is convenient to model the physical system as a light Newtonian fluid overlying a dense, non-Newtonian fluid with a rigid bottom.

The measurement of bottom movement was complicated by two factors. First, the measurements had to be made away from a platform to ensure that the motion of natural muds would be measured. Secondly, bottom motions under typically encountered wave conditions were thought to be small, and therefore high resolution was needed. Both problems were overcome by burying accelerometers in the mud. Though displacements were around 1 cm, accelerations were such that they could be reliably measured and required no fixed reference.

Three Bruel and Kjoer type 8306 accelerometers were mounted so as to measure the accelerations in three dimensions (Fig. 3). They were placed in a water-proof cylindrical PVC housing measuring 0.215 meter in diameter and 0.635 meter in length and having a submerged weight of 5.5 kg. The housing was pushed into the mud by a diver so that the top of the package was 0.15 meter below the mud line. The electronic cable coming from the top of the package was given 4.5 meters of slack, all of which was buried in the mud, and then fixed to a taut galvanized cable that was laid along the bottom between a nearby well jacket and our main instrumented site, Platform V. Platform V, in 19.2 meters of water, is shown in Figure 4. The cable from the accelerometer was brought along the galvanized cable and up the platform leg to the recorders. The location of the accelerometer was

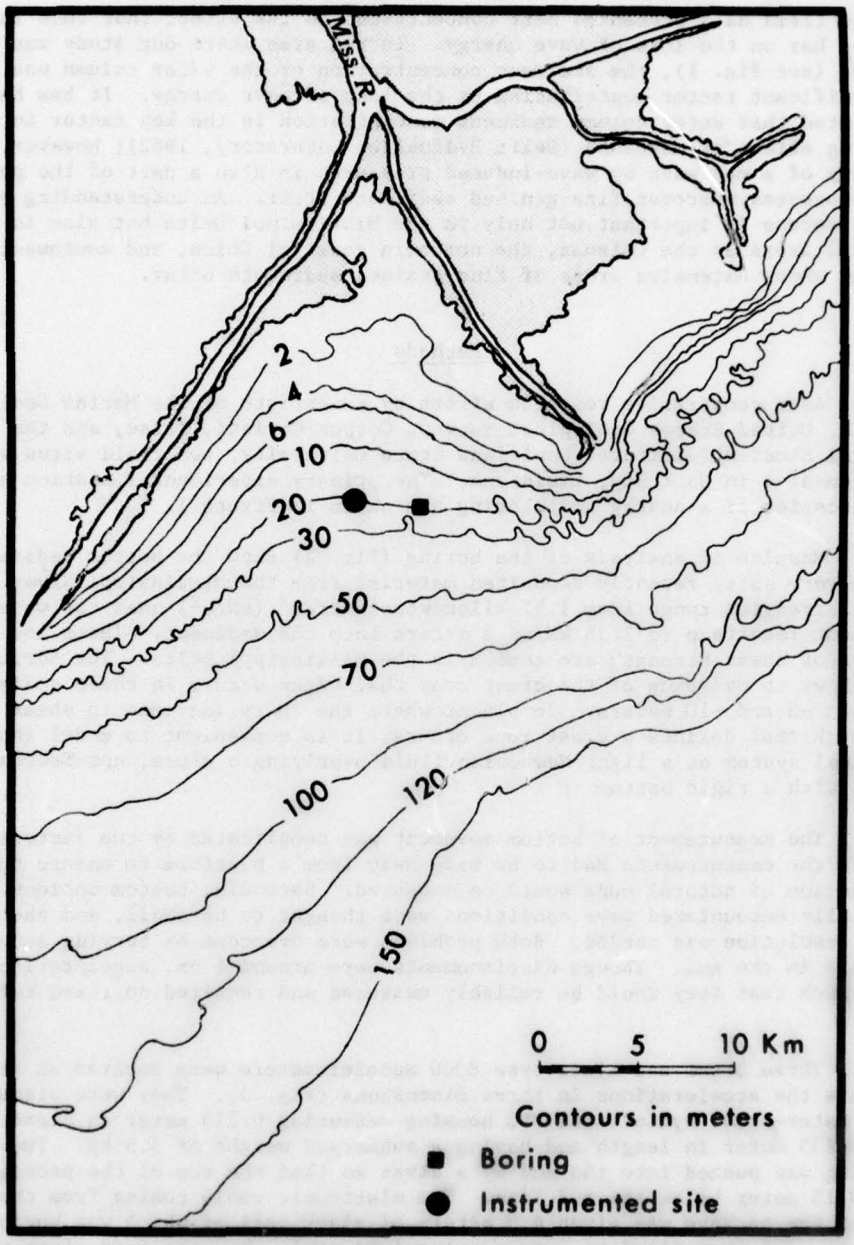

Figure 1. Location of the field site in East Bay, Louisiana.

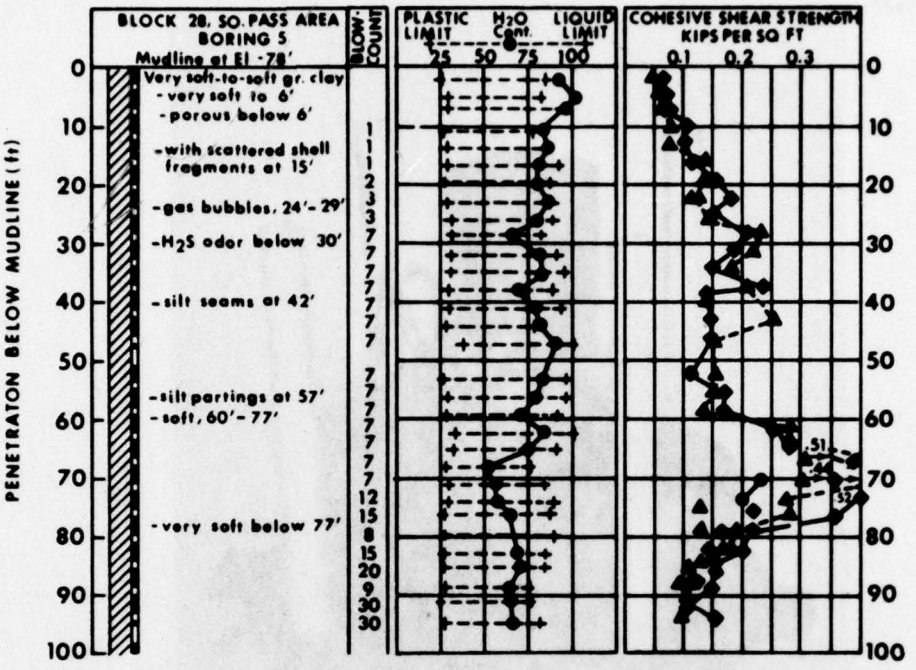

Figure 2. Results of soil boring taken near field site (1 kip/ft^2 = 48 kilonewtons/m^2). For location see Figure 1. (Boring courtesy U.S. Geological Survey, Marine Geology Branch, Corpus Christi.)

directly beneath the catwalk between the two structures so that a pressure cell attached to a weighted cable could be suspended over the package. Figure 5 is a schematic representation of the experiment and the physical system. The location of the pressure sensor was known to be within a radius of 2 meters from the accelerometer. This uncertainty in position could cause an error in the measured phase angle ϕ between the crest of the surface wave and the trough of the mud wave of $\pm 11°$ for a characteristic wave with a period of 7.75 seconds. The importance of such an error will be seen in the calculation of the dissipation of wave energy. Wave properties were measured with a wave staff, a pressure sensor, and a two-axis electromagnetic current meter attached to wire cables that were suspended from the platform and anchored to the bottom through pulleys. A system of winches and pulleys allowed us to adjust the instruments to any depth.

Platform S (see Fig. 10), 3.35 km inshore of Platform V in 5.3 meters of water, was instrumented with an anemometer, a Bendix Q-15 ducted current meter, two pressure sensors, and a wave staff. By running the instruments on Platform S simultaneously with those on Platform V it was possible to compare the net energy lost by the waves while traveling between the two data

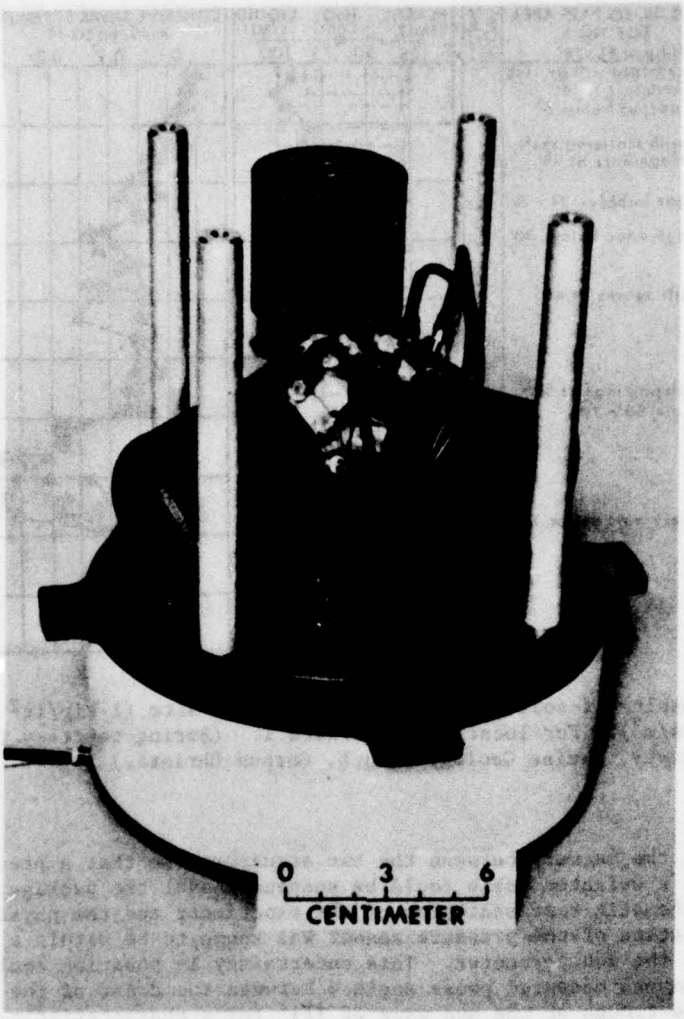

Figure 3. Array of three accelerometers.

stations with a rate of energy loss calculated from the measurements of mud movement at Platform V.

Results

Simultaneous measurements of wave height and wave-induced pressure resulted in the data represented in Figure 6. The term n is a correction

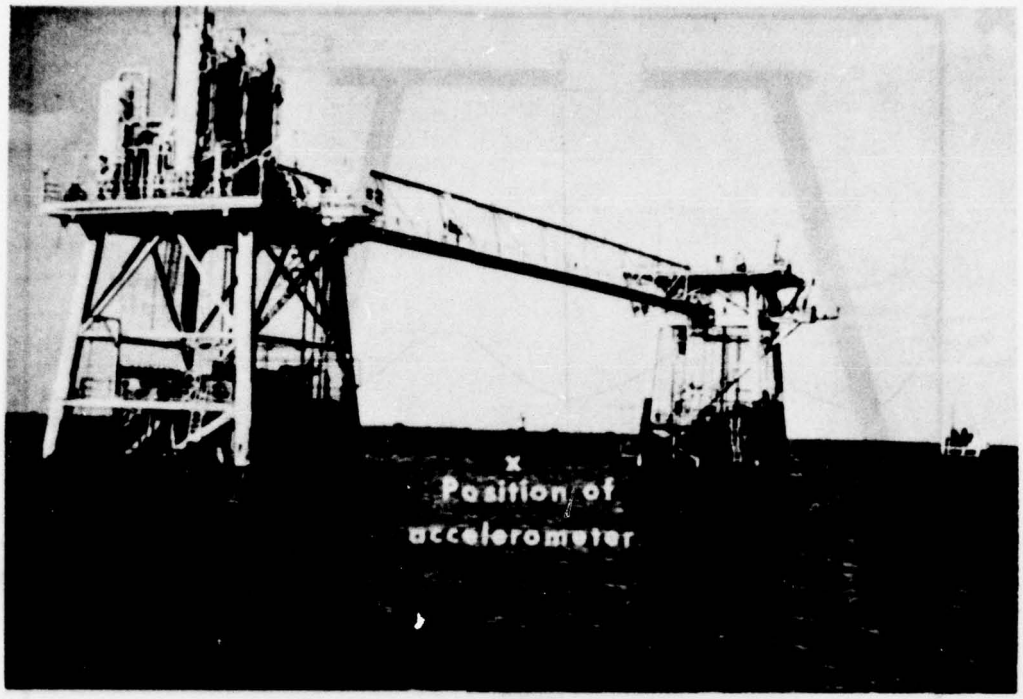

Figure 4. The main instrumented site, Platform V.

factor that matches linear theory with observed pressures and wave heights in the manner shown (where Kp = cosh k (h + Z)/cosh kh). If the observed data were in perfect agreement with linear theory, the data points would fall along the line n equal to 1.00. Further experimentation using two pressure cells placed at different depths in the water column showed that linear theory accurately predicts the change in wave-induced pressures from near the surface to within 0.5 meter of the bottom. The fact that other researchers have obtained similar results (Hom-ma et al., 1966) supported the use of a corrected linear theory for determining surface wave heights from pressure measurements made in the water column above the accelerometer. The actual values of the correction factor n that were used were those values lying along the two least squares fit lines shown in Figure 6.

A sample of the data taken in the study is shown in Figure 7. The accelerations appear sinusoidal in form and have the same general appearance as the wave record.

The shape of the bottom pressure spectrum is similar to that of the spectrum of the vertical acceleration, and the peaks occur at the same

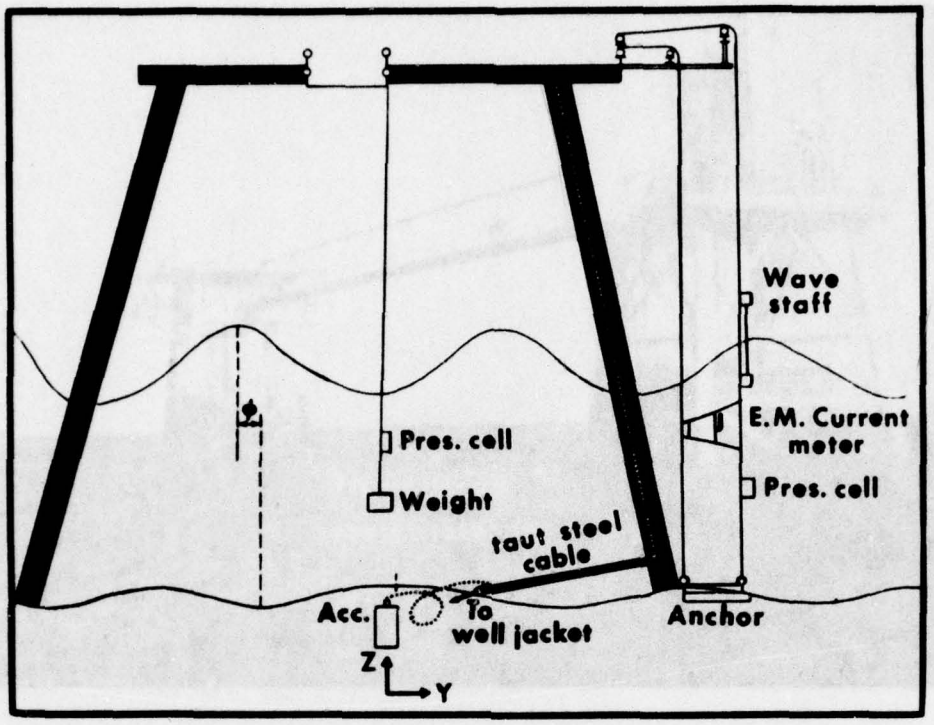

Figure 5. Experimental setup at Platform V.

frequency (Fig. 8). The low-frequency spectral components visible in the acceleration spectrum are believed to be electronic drift. (The phase angle between the crest of the mud wave and the crest of the pressure wave was 202° for the peak spectral component.) Horizontal mud motions are approximately 90° out of phase with the vertical motions, and a backward horizontal movement occurs at the crest of the bottom wave. Similar motion occurs for forced waves on an elastic half space. The ratio of vertical displacement to horizontal displacement over several sets of data averaged about 2.0.

A plot of the amplitude of the pressure wave at the bottom versus the amplitude of the mud wave (Fig. 9) reveals a roughly linear relationship for the range of pressures from near zero to 2.39×10^3 Pascal.

The average energy transmitted through the sea/sediment interface per unit and time over one wave cycle is (Gade, 1958)

$$Dm = -\frac{1}{T}\int_{o}^{T} P\,\frac{dh}{dt}\,dt \qquad (1)$$

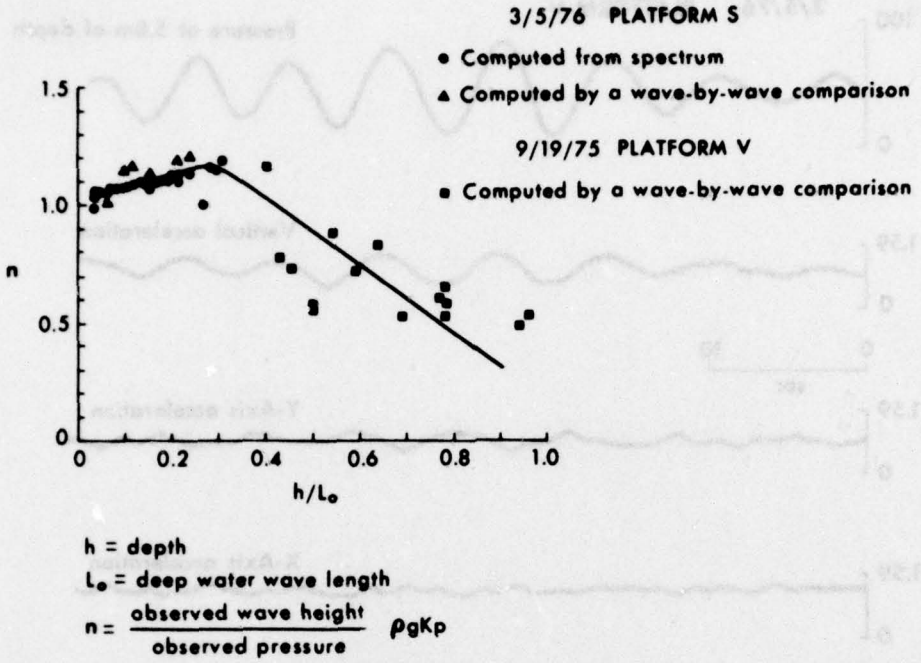

Figure 6. Comparison of observed wave height and observed wave pressure with small-amplitude wave theory.

where T = wave period
P = wave-induced bottom pressure
dh = an infinitesimal increase in the height of the interface

The general characteristics of the data show that the following functions will accurately describe the motions:

$$P = Pa + A \cos (kx - \sigma t)$$

$$h = ho + MA \cos (kx - \sigma t + \psi)$$

where Pa = steady-state bottom pressure
A = amplitude of the wave-induced bottom pressure
h_o = depth of mud over which motion occurs
M = proportionality constant between the amplitudes of the mud wave and the pressure wave
ψ = phase angle between the crest of the bottom pressure wave and the crest of the mud wave

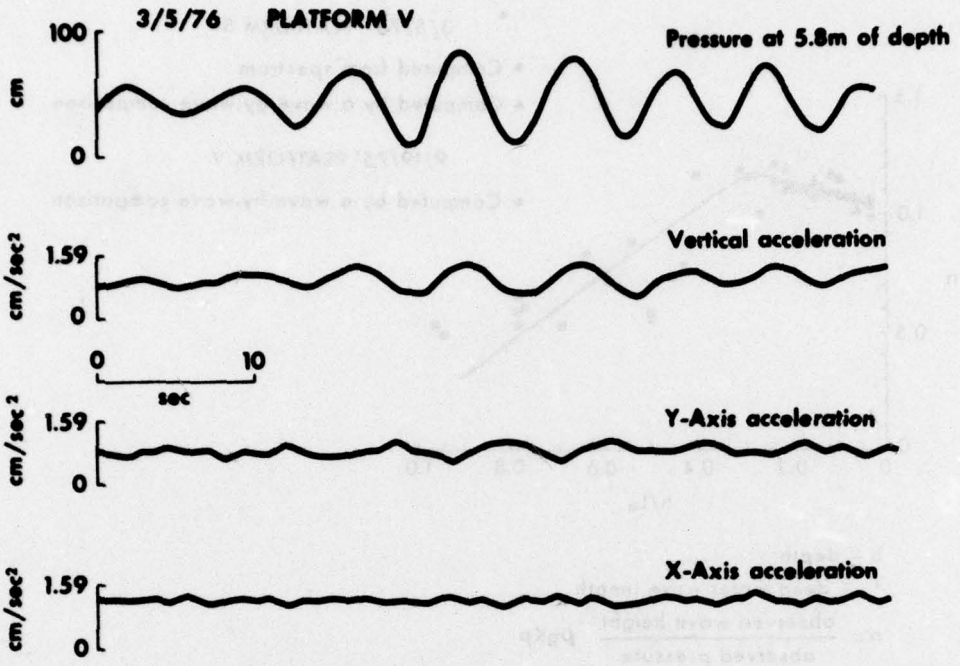

Figure 7. Sample of the data taken during the study.

After substituting equations (2) and (3) into (1) and integrating, and then using linear theory to put bottom pressures in terms of surface wave height, the equation for the rate of energy loss to the bottom is obtained:

$$Dm = \frac{\pi \rho g M H^2 \sin \phi}{4T \cosh^2 kh} \qquad (4)$$

where $\phi = 180° - \psi$.

For purposes of comparison with other theories for the dissipation of wave energy, the pressure correction factor for linear theory is not incorporated into the equation. At most this can change the energy loss rate by 20 percent. From equation (4) it can be seen that the dissipation of wave energy by the soft bottom involves only two important factors, determined by the physics of the sediment movement: (1) the relationship between the pressure force on the sediment and the resultant vertical displacement, given by M, and (2) the phase angle between the crest of the pressure wave and the trough of the mud wave, given by ϕ.

The results of the two-station experiment allowed us to estimate the energy lost from the waves. Conditions during the two-station experiment

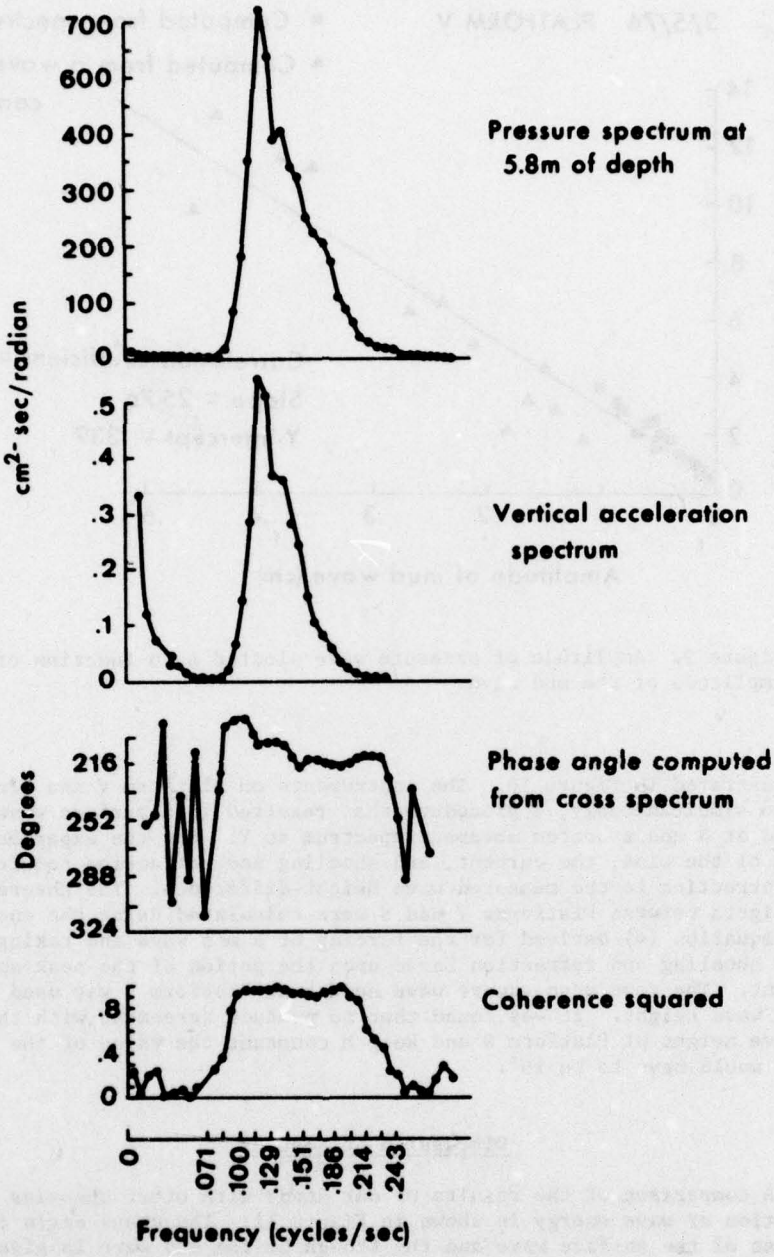

Figure 8. Results of spectral analysis of data.

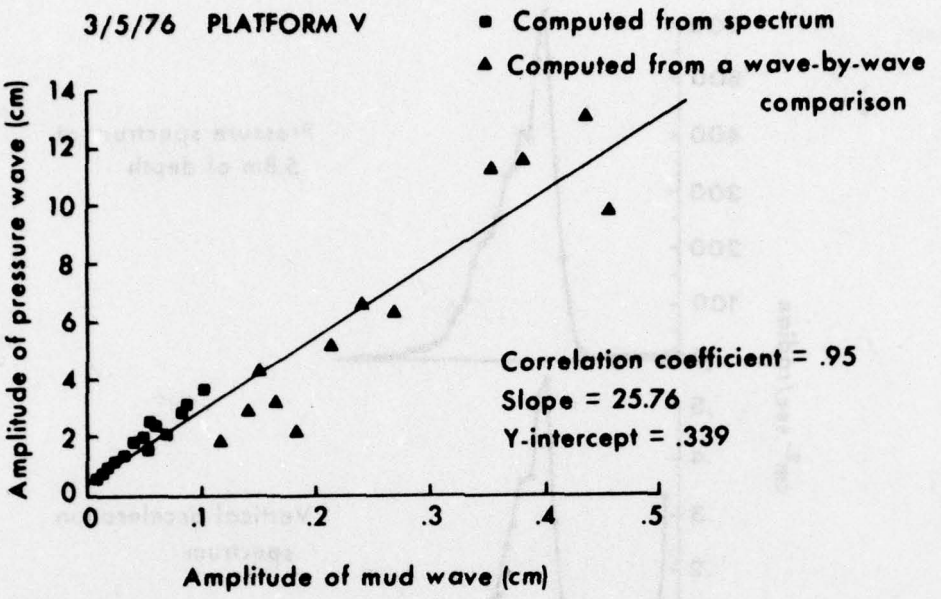

Figure 9. Amplitude of pressure wave plotted as a function of the amplitude of the mud wave.

are illustrated in Figure 10. The instruments on platform V and Platform S were run simultaneously, a procedure that resulted in a surface wave spectrum at V and at S and a bottom movement spectrum at V. For the experiment the effects of the wind, the current, and shoaling and refraction required a small correction to the measured wave height difference. The theoretical wave heights between Platforms V and S were calculated using the energy dissipation equation (4) derived for the forcing of a mud wave and taking into account shoaling and refraction based upon the period of the peak spectral component. The root mean square wave height at Platform V was used for the initial wave height. It was found that to produce agreement with the measured wave height at Platform S and keep M constant the value of the phase angle ϕ would have to be 10°.

Discussion of Results

A comparison of the results of our study with other theories for the dissipation of wave energy is shown in Figure 11. The phase angle ϕ between the crest of the surface wave and the trough of the mud wave is given two values: 22° is the angle that was actually measured at V, and 10° is the angle that results in the correct average dissipation of wave energy between Platforms V and S, assuming that M is constant. Note that the use of the smaller angle does not significantly reduce the magnitude of the dissipation

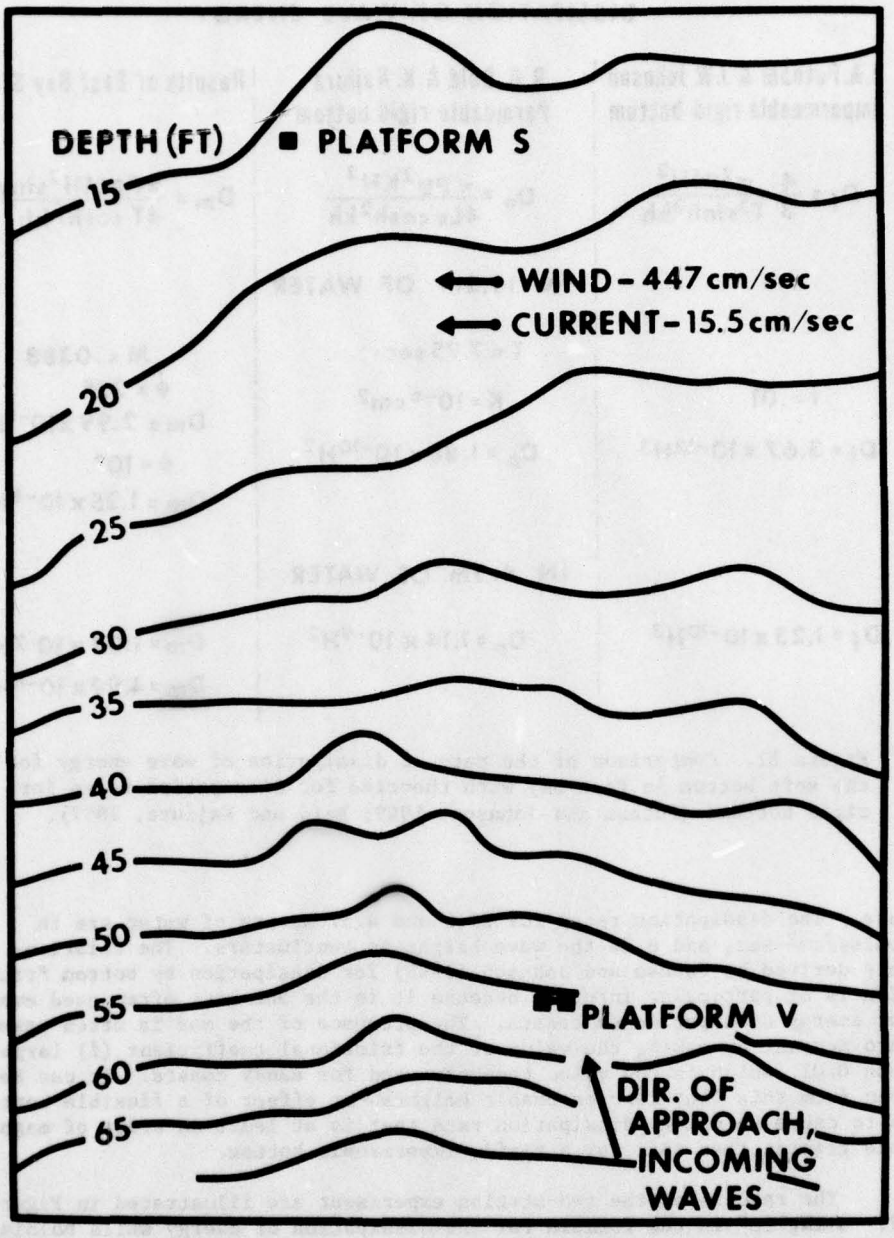

Figure 10. Conditions during two-station experiment.

DISSIPATION OF WAVE ENERGY

J.A. Putnam & J.W. Johnson Impermeable rigid bottom	R.O. Reid & K. Kajiura Permeable rigid bottom	Results of East Bay Study
$D_f = \frac{4}{3}\frac{\pi^2 \rho f H^3}{T^3 \sinh^3 kh}$	$D_p = \frac{\pi \rho g^2 K H^2}{4Lv \cosh^2 kh}$	$D_m = \frac{\pi \rho g M H^2 \sin\phi}{4T \cosh^2 kh}$
	IN 19.2m OF WATER	
	$T = 7.75$ sec	$M = .0388$
$f = .01$	$K = 10^{-6}$ cm^2	$\phi = 22°$
$D_f = 3.67 \times 10^{-12} H^3$	$D_p = 1.86 \times 10^{-10} H^2$	$D_m = 2.99 \times 10^{-8} H^2$
		$\phi = 10°$
		$D_m = 1.25 \times 10^{-8} H^2$
	IN 4.5m OF WATER	
$D_f = 1.23 \times 10^{-10} H^3$	$D_p = 1.14 \times 10^{-9} H^2$	$D_m = 1.07 \times 10^{-7} H^2$
		$D_m = 4.99 \times 10^{-8} H^2$

Figure 11. Comparison of the rate of dissipation of wave energy for the soft bottom in East Bay with theories for dissipation rates for rigid bottoms (Putnam and Johnson, 1949; Reid and Kajiura, 1957).

rate. The dissipation rates for 19.2 and 4.57 meters of water are in joules/cm^2-sec, and H is the wave height in centimeters. The relationship derived by Putnam and Johnson (1949) for dissipation by bottom friction is of particular interest because it is the one most often used even for energy dissipation on coasts. The presence of the mud is often taken into account by making the value of the frictional coefficient (f) larger than 0.01, which is the value commonly used for sandy coasts. It can be seen from this that for reasonable heights the effect of a flexible bottom is to cause an energy dissipation rate that is at least an order of magnitude greater than that for a rigid, impermeable bottom.

The results of the two-station experiment are illustrated in Figure 12. Using 10° in the formula for the dissipation of energy while holding M constant in order to make the total dissipation agree with theory is somewhat an arbitrary choice. It is entirely possible that the properties of the sediments change between V and S and cause changes in M as well as ϕ, but it should be remembered that because of the uncertainty in the

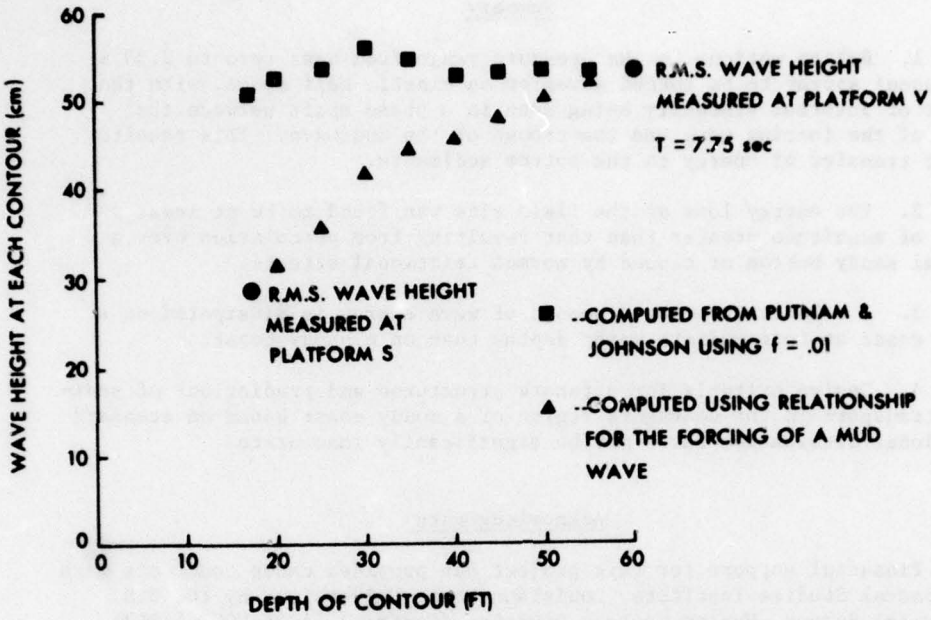

Figure 12. Comparison of the dissipation of wave energy for East Bay and that predicted using the theory of Putnam and Johnson (1949) with the measured wave height change.

position of the pressure sensor relative to the accelerometer it is possible that 10° was the true and constant phase angle.

Figure 12 also illustrates another important point concerning the dissipation of wave energy on muddy coasts. The predicted wave heights between Platforms V and S are shown in the figure as they would be predicted by Putnam and Johnson (1949). Certainly order-of-magnitude higher dissipation rates on sandy coasts can occur when well-formed ripples and the proper velocities are present (Tunstall, 1973), but even in such cases the contrasting trend, made more extreme by using Putnam and Johnson's theory, is present. By comparing the two curves in Figure 12 it can be seen that for bottom friction the dissipation of wave energy occurs mainly in shallow water, whereas for a flexible bottom a relatively greater amount of wave energy is dissipated in intermediate-depth water. Nearshore wave energy for muddy coasts can therefore be expected to be greatly reduced from that present on the outer shelf. Such coasts, in comparison to sandy coasts, tend to protect their shoreline by the dissipation of wave energy in the bottom sediments.

Summary

1. Bottom motions in the pressure range from near zero to 2.39 x 10^3 Pascal appear to be forced waves on an elastic half space, with the effect of internal viscosity being seen in a phase shift between the crest of the forcing wave and the trough of the mud wave. This results in the transfer of energy to the bottom sediments.

2. The energy loss at the field site was found to be at least an order of magnitude greater than that resulting from percolation over a typical sandy bottom or caused by normal frictional effects.

3. A relatively greater amount of wave energy is dissipated on a muddy coast at intermediate water depths than on a sandy coast.

4. Design criteria for offshore structures and predictions of sediment transport in the nearshore region of a muddy coast based on standard frictional dissipation rates may be significantly inaccurate.

Acknowledgments

Financial support for this project was provided under contracts with the Coastal Studies Institute, Louisiana State University, by the U.S. Geological Survey, Marine Geology Division (Contract 14-08-0001-14963) and the Geography Programs, Office of Naval Research. We thank Shell Oil Company for cooperation during the project.

References

Delft Hydraulics Laboratory, 1962, Demerara coastal investigation. The Netherlands, 240 pp.

Gade, H. G., 1958, Effects of a non-rigid, impermeable bottom on plane surface waves in shallow water. J. Mar. Res., 16:61-82.

Hom-ma, M., K. Horikawa, and S. Komori, 1966, Response characteristics of an underwater wave gauge. Proc., 10th Internat. Conf. on Coastal Engr., Tokyo, Japan,

Putnam, J. A., and J. W. Johnson, 1949, The dissipation of wave energy by bottom friction. Trans., Am. Geophys. Union, 30(1):67-74.

Reid, R. O., and K. Kajiura, 1957, On the damping of gravity waves over a permeable sea bed. Trans. Am. Geophys. Union, 38(5):662-666.

Sterling, G. H., and E. E. Strohbeck, 1973, The failure of the South Pass 70 "B" platform in Hurricane Camille. Fifth Offshore Technology Conf., Houston, Texas, Preprint 1898.

Suhayda, J. N., T. Whelan, III, J. M. Coleman, J. S. Booth, and L. E. Garrison, 1976, Marine sediment instability, interaction of hydrodynamic forces and bottom sediments. Eighth Offshore Technology Conf., Houston, Texas, Preprint 2426.

Tunstall, E. B., 1973, Experimental study of vortices generated by oscillatory flow over rippled surfaces. Ph.D. dissertation, Univ. of California at San Diego.

Unclassified
Security Classification

DOCUMENT CONTROL DATA - R & D

(Security classification of title, body of abstract and indexing annotation must be entered when the overall report is classified)

1. ORIGINATING ACTIVITY (Corporate author)	2a. REPORT SECURITY CLASSIFICATION
Coastal Studies Institute Louisiana State University Baton Rouge, Louisiana 70803	Unclassified
	2b. GROUP Unclassified

3. REPORT TITLE

WAVE ACTION AND BOTTOM MOVEMENTS IN FINE SEDIMENTS

4. DESCRIPTIVE NOTES (Type of report and inclusive dates)

5. AUTHOR(S) (First name, middle initial, last name)

Michael W. Tubman and Joseph N. Suhayda

6. REPORT DATE	7a. TOTAL NO. OF PAGES	7b. NO. OF REFS
December 1977	16	8

8a. CONTRACT OR GRANT NO.	9a. ORIGINATOR'S REPORT NUMBER(S)
N00014-75-C-0192	
b. PROJECT NO. Project NR 388 002	Technical Report No. 244
c.	9b. OTHER REPORT NO(S) (Any other numbers that may be assigned this report)
d.	A043 696

10. DISTRIBUTION STATEMENT

Approved for public release; distribution unlimited.

11. SUPPLEMENTARY NOTES	12. SPONSORING MILITARY ACTIVITY
Reprint from: Proceedings, 15th Coastal Engineering Conf., Honolulu, Hawaii, July 11-17, 1976 (Amer. Soc. of Civil Eng.) pp. 1168 - 1183.	Geography Programs Office of Naval Research Arlington, Virginia 22217

13. ABSTRACT

Mudbanks have been observed to have an extraordinary calming effect on the sea surface. In certain cases this effect is due primarily to the transfer of energy through the sea/mud interface and its frictional dissipation within the bottom sediments. This paper describes an experiment that measured wave characteristics and the resulting sea floor oscillations in an area where the bottom is composed of fine-grained sediments. The energy lost by the waves at the position of the experimental setup is calculated and compared with a direct measurement of the net energy lost by the waves in going from the point of the experiment to a station 3.35 km inshore. Results show that bottom motions in the range of wave-induced bottom pressures from near zero to 2.39 x 10^3 Pascal have the appearance of forced waves on an elastic half space. The apparent effect of internal viscosity is seen in a phase shift between the crest of the pressure wave and the trough of the mud wave. Measurements show this angle to be 22° (± 11°) for the peak spectral component (T = 7.75 seconds). The energy lost to the bottom by the waves at the field site was found to be at least an order of magnitude greater than that resulting from the processes of percolation or that caused by normal frictional effects. This newly observed mechanism for the dissipation of wave energy is particularly important for waves in intermediate-depth water and could be a prime factor in determining design wave heights in muddy coastal areas.

14. KEY WORDS	LINK A		LINK B		LINK C	
	ROLE	WT	ROLE	WT	ROLE	WT
mudbanks						
wave measurements						
sedimentation						
bottom pressure						
seafloor oscillations						

Coastal Studies Institute
Center for Wetland Resources
Louisiana State University
Baton Rouge, Louisiana 70803

Technical Report No. 245

PROCESS AND MORPHOLOGY CHARACTERISTICS OF TWO BARRIER BEACHES IN THE MAGDALEN ISLANDS, GULF OF ST. LAWRENCE, CANADA

by

E. H. Owens

December 1977

Reprint from: Proceedings, 15th Coastal Eng. Conf., Honolulu, Hawaii, July 11-17, 1976, pp. 1975-1991 (Amer. Soc. of Civil Engr.).

Office of Naval Research
N00014-75-C-0192
Project No. NR 388 002

Reprinted by the American Society of
Civil Engineers from the Proceedings of
the 15th Coastal Engineering Conference,
Honolulu, Hawaii, July 11-17, 1976

CHAPTER 115

PROCESS AND MORPHOLOGY CHARACTERISTICS OF TWO BARRIER BEACHES IN THE MAGDALEN ISLANDS, GULF OF ST. LAWRENCE, CANADA

by

E. H. Owens

Coastal Studies Institute, Louisiana State University,
Baton Rouge, Louisiana 70803

ABSTRACT

Detailed field investigations of barrier beach morphology and processes at adjacent sites in the Magdalen Islands, Gulf of St. Lawrence, show that the two beaches are in distinctly different morphodynamic environments. The differences are expressed in terms of wave energy levels, sediment dispersal patterns, and nearshore, littoral, and dune geomorphology. The exposed west-facing coast has a steeper offshore gradient, is a zone of sediment bypassing, and has a complex sequence of three nearshore bars. Wave energy levels are lower on the sheltered east coast, and this is a zone of sediment redistribution and deposition with a single, linear nearshore bar. The different morphological characteristics of the two barriers are attributed to the spatial variation in energy levels and to the differences in offshore gradients on the two coasts. Computed wave energy values, derived from data monitored during two study periods (August and November, 1974), indicate that the mean wave energy levels were greater on the west coast as compared to the east coast by factors of 2.25 in summer and 2.95 in winter. This is due primarily to the dominance of winds out of the westerly quadrant throughout the year.

INTRODUCTION

The Magdalen Islands consist of a series of barrier beaches that are oriented northeast-southwest to connect small bedrock outcrops on the shallow central shelf of the southern Gulf of St. Lawrence (Owens, 1975) (Figure 1). This is a microtidal environment (mean tidal range less than 1.0 m) and, as the Gulf is an enclosed sea, the wave climate is dominated by locally-generated wind waves. Winds are dominantly from between southwest and northwest throughout the year, with a higher frequency of storm winds in winter months (Table 1). Limiting factors for wave action on the beach are maximum fetch distances on the order of 300 km and the presence of sea or beach-fast ice for periods up to four months each winter. Littoral processes are dominated by wind waves associated with the west to east passage of low-pressure systems across Atlantic Canada (Table 2). On the west coast of the Magdalen Islands the shoreline is exposed to the dominant and prevailing winds out of the northwest. Maximum wave and breaker height values on the west beach occur at times of maximum wind velocities, independent of wind direction. On the east-facing coast wave characteristics are closely associated with the onshore wind component (Owens, 1977).

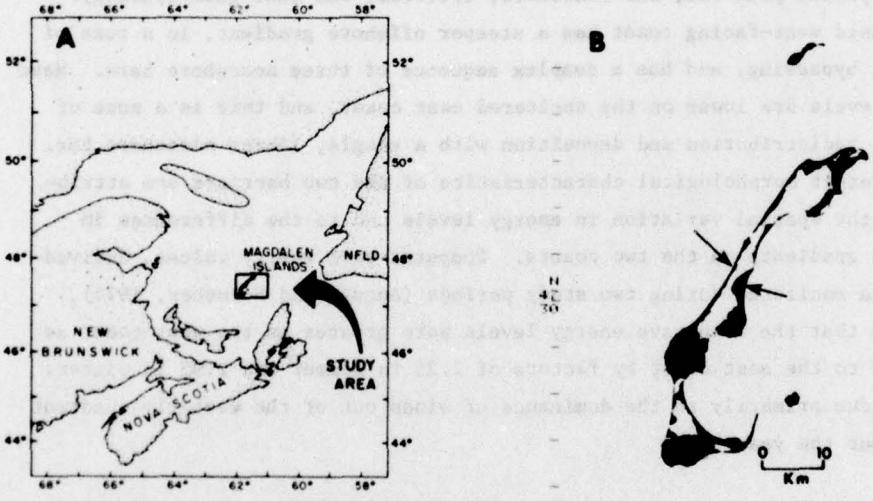

Figure 1. Magdalen Islands study area: A. Location. B. Study sites on the central tombolo.

Table 1. Wind Data, Magdalen Islands (1933-1972)

	Mean Wind Velocity (km/h)	Mean Direction	Mean Hours/Month with Given Wind Velocities		
			88-101 km/h	102-120 km/h	>120 km/h
Jan.	47.2	NW	13.4	2.0	0.1
Feb.	41.4	NW	7.2	1.8	0.4
March	40.6	NW	6.2	0.4	0.4
April	36.2	NW	1.8	0.3	--
May	35.2	NW	0.4	--	--
June	33.3	NW	0.2	--	--
July	30.6	SW	--	--	--
Aug.	30.4	SW	0.7	--	--
Sept.	35.7	NW	1.7	0.4	--
Oct.	41.0	NW	5.0	0.7	--
Nov.	41.7	NW	6.5	1.4	0.7
Dec.	45.7	NW	9.0	2.2	0.2

Table 2. Storm Duration and Frequency, Magdalen Islands

A. Number of Storms with Winds >90 km/h and >115 km/h by Quadrant Over a 40-Year Period

	>90 km/h	Duration >3 hours	Duration >6 hours	>115 km/h	Duration >3 hours
NW-NNE	256	68	37	15	3
NE-ESE	62	12	3	--	--
SE-SSW	124	15	5	2	--
SW-WNW	120	15	9	8	1

B. Annual Frequency of Storm by Quadrant

NW-NNE	6.4/yr	1.7/yr	0.9/yr	2 in 5 yr	1 in 13 yr
NE-ESE	1.5/yr	1 in 3 yr	1 in 13 yr	--	--
SE-SSW	3.1/yr	2 in 5 yr	1 in 8 yr	1 in 20 yr	--
SW-WNW	3.0/yr	2 in 5 yr	1 in 4 yr	1 in 5 yr	1 in 40 yr

Mean and maximum wave height values are greater on the west coast in all seasons due to the prevailing onshore winds. A distinct difference in wave energy levels exists between the two study sites (Figure 2). Comparison of computed wave energy values (Table 3), derived from time-series data monitored during two study periods (August and November, 1974), shows that the mean values are greater on the west coast by factors of 2.25 and 2.95 for the summer and winter phases of the study. The same comparison for the computed longshore sediment transport rates (Table 4) shows that the combined hourly rates are greater on the west coast by 2.7 and 2.0 for the summer and winter study periods. The estimated annual gross volume of longshore sediment transport is approximately four times greater on the west-facing barrier.

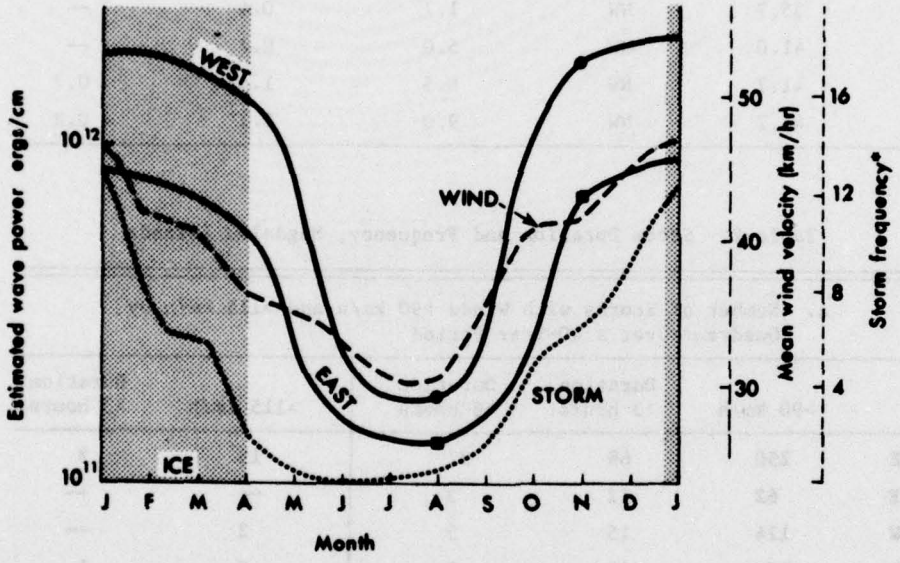

Figure 2. Seasonal variations in (1) estimated wave energy on the east and west barriers, (2) mean monthly wind velocity, and (3) storm frequency. The period of sea-ice cover or beach-fast ice is indicated by the shaded area. Wave energy values are extrapolated. Storm frequency (*) is the number of periods in each month when wind velocities exceed 55 km/h, based on data over a 40-year period.

Table 3. Computed Wave Energy Values (ergs/cm)

		Mean	Minimum	Maximum
Summer	West	2.52×10^{11}	2.12×10^{9}	1.65×10^{13}
	East	1.12×10^{11}	2.12×10^{9}	1.10×10^{13}
Winter	West	2.51×10^{12}	1.68×10^{11}	7.38×10^{13}
	East	8.51×10^{11}	3.04×10^{10}	5.89×10^{13}

Table 4. Summary of Computed Longshore Sediment Transport Rates

		West Coast	East Coast
Average Hourly Rate (m^3/h)	Summer	149 to N	53 to N
		95 to S	39 to S
	Winter	631 to N	265 to N
		519 to S	315 to S
Net Daily Rate (m^3/day)	Summer	428 to N	201 to N
	Winter	1,261 to N	962 to S
Estimated Annual (m^3/yr)	Gross	2,059,030	550,943
	Net	233,931 to N	104,112 to S

Owens (1977) has shown that in addition to this spatial variation there is also a distinct temporal variation in energy levels between the two sites that is reflected in littoral zone morphology. On the west coast there is a seasonal variation in wave energy levels that produces a "summer-winter" beach cycle. On the sheltered east coast variations in energy levels due to the passage of low-pressure systems across the region are more important than the seasonal variations. This produces beach cycles of erosion during storms and deposition during the post-storm recovery period (Table 5).

Table 5. Characteristic Differences between the Coastal Environments of the East and West Barriers--Magdalen Islands

	West	East
Wave energy	a. High energy environment	a. Moderate energy environment
	b. Marked seasonal variation in wave energy levels	b. Large short-term variations due to storm-wave activity
Littoral zone morphology	a. "Summer-winter" beach cycle	a. Storm/post-storm beach cycle
	b. Relatively stable morphology in plan and profile	b. Large short-term variations in morphology
Offshore Slope	0°10'	0°05'
Nearshore Slope	0°33'	0°53'

OFFSHORE ZONE

On the shallow shelf adjacent to the west coast of the Magdalen Islands, sediment is being transported landward by present-day processes (Owens, 1975). This is an area of coarse and medium sands (Table 6) and is a non-depositional sedimentary environment, with local reworking and the formation of lag deposits (Loring and Nota, 1973). Sediment that is transported toward the Islands is moved rapidly alongshore in shallow water toward and around the extremities of the barriers. The shelf adjacent to the east coast is sheltered from waves out of the west and is a depositional area of fine-grained sediments (Table 7) (Loring and Nota, 1973).

The nature of the sedimentary environments on the Magdalen Shelf is controlled in part by differences in the wave climate to the west and to the east of the islands that result from the dominance of wind-generated waves out of the west. In the zone of sediment reworking and transportation on the shelf to the west of the Islands the sandstone bedrock is overlain by a thin, discontinuous layer of sand and gravel. In the depositional area to the east of the Islands the bedrock is buried by a continuous cover of well-sorted

Table 6. Sedimentary Environments--Magdalen Islands

	West	East
Offshore	Coarse/medium sands	Fine sands
Nearshore (<5 m)	Medium sand (1.31ϕ)	Medium sand (1.81ϕ)
Beach	Medium sand (1.67ϕ)	Medium sand (1.87ϕ)
Dunes	Medium sand (1.67ϕ)	Medium/fine sand (1.95ϕ)

Table 7. Energy-Morphology Characteristics--Magdalen Islands

		West	East
Sediment dispersal	Offshore	Toward east	Zone of deposition
	Nearshore	Rapid longshore movement	Zone at redistribution and deposition
Subaqueous profile		Relatively steep (1:300)	Relatively flat (1:625)
Frictional attenuation of waves		Low	High
Amount of energy reaching shoreline		High	Low

sands (Loring and Nota, 1973). The gradients of the subaqueous slope off the west- and east-facing barriers are therefore partially controlled by the sediment dispersal pattern that results from the local wave climate.

Wright and Coleman (1972) note that nearshore wave power is a function of the subaqueous slope, due to the effects of frictional attenuation, and that as water depth decreases frictional attenuation rates increase. The offshore profiles adjacent to the two barriers are very different (Figure 3), particularly between the 15-m and 40-m depth contours. The broad, shallow shelf off the east coast has an average gradient of 0°05' (1:626) from the shoreline to the 20-m contour, approximately half the gradient of the shelf off the west coast (0°11', 1:312). Wave periods are usually less than

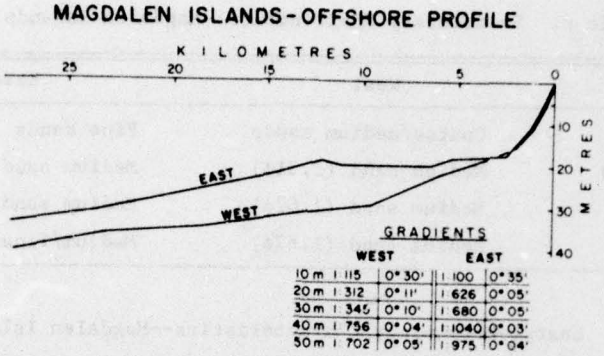

Figure 3. Offshore profiles and gradients--taken on lines perpendicular to the shoreline at the two study sites.

8 seconds in the Gulf, so that although some longer period waves would feel bottom in water depths up to 50 m, the frictional attenuation rates would probably be highest in depths between 30 m and 10 m.

Due to the shallower depths on the east coast the loss of energy by frictional attenuation is much greater than on the west coast. In addition, as the dominant and prevailing winds are out of the west, and locally-generated waves dominate the wave climate, the east coast is a protected environment in which wave heights are lower than on the west-facing barrier (Owens, 1977). The net effect is that (1) more energy is available on the western barriers (Table 3) and (2) a higher proportion of that energy reaches the nearshore zone as compared to the east-facing barrier.

NEARSHORE ZONE

The effects of the difference in the wave energy levels on the two coasts are clearly reflected in the nearshore zones. Surveys on the west study site show a large crescentic bar system that shoals to 5-6 m at 800 m from the beach, a smaller middle crescentic bar, and an intermittent inner bar (Figure 4). Comparison of field surveys in 1974-75 with aerial photographs taken in 1970 indicates that the plan form of the outer bar appears to be constant through time. Small longshore movements of the outer crescentic bar system result in occasional overlapping of the bars in the vicinity

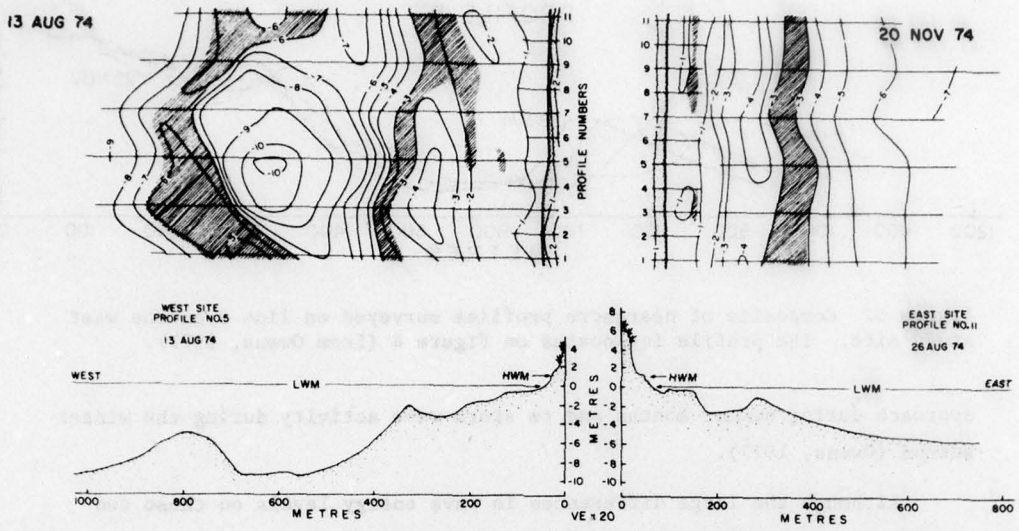

Figure 4. Nearshore profiles and morphology at the west and east coast study sites. The nearshore profiles are spaced at 100-m intervals and shaded areas on the maps indicate the location of subaqueous bars.

of the horns of the crescents. Also, it was found that the apex of the outer bar oscillated perpendicular to the shoreline between 700 and 900 m from the beach (Figure 5). These variations resulted in modification of the crescentic bar form but surveys showed that the basic location and shape of the outer bar did not change over a 9-month period. More variation was observed in the plan form of the two inner bar systems, particularly following periods of storm-generated waves.

By contrast the east-facing barrier is characterized by a single asymmetrical linear nearshore bar that shoals to 1.5-2.5 m at 250 m from the beach (Figure 4). The trough depth on the landward side of the bar varied between 3 and 5 m. Migratory bars were also recorded inshore on the shallow low-tide terrace adjacent to the beach. Although the nearshore bar had a low amplitude rhythmic plan shape following storm-wave activity, the basic linear form of the bar did not change significantly over the 9-month period of the surveys. The plan form of the bars on the low-tide terrace varied considerably, and this has been related to differences in the direction of wave

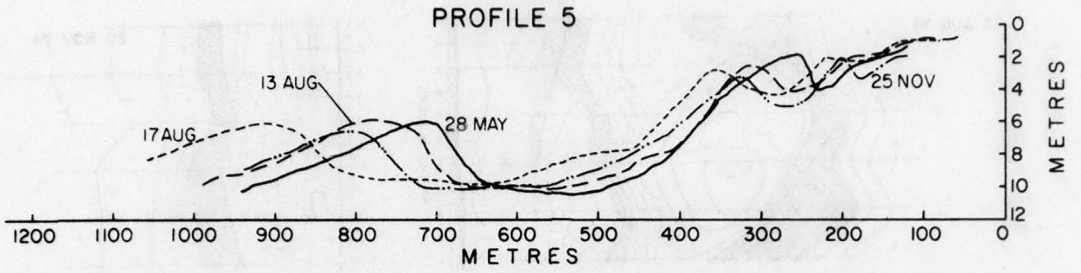

Figure 5. Composite of nearshore profiles surveyed on line 5 on the west study site. The profile is located on Figure 4 (from Owens, 1977).

approach during summer months and to storm-wave activity during the winter season (Owens, 1977).

Although the large differences in wave energy levels on these two barriers clearly affect the character of the nearshore zone, the actual variations in the size and the morphology of the nearshore bar systems could be explained in several ways. If it is assumed that breaking waves control bar formation, then the fact that the bars on the western barrier are farther offshore, in deeper water, and larger than the bar on the east coast would be due simply to higher wave heights on the west coast. But, as the two sets differ so radically in plan form it is difficult to accept that bar formation could result from a simple variation in wave height between the two coasts. On the other hand, it is possible that the variation in the size and spacing of the bars, perpendicular to the shore, could be due to the effects of standing waves generated by the reflection of incident waves from the beach (Bowen and Inman, 1971; Suhayda, 1974). Bowen and Inman suggest that the alongshore plan form of crescentic bars results from the sediment dispersal patterns associated with the formation of edge waves in the surf zone. The absence of a well-defined crescentic bar on the eastern barrier probably results from the consistently oblique wave approach and high breaker angles that generate strong longshore currents, thus preventing the development of rhythmic morphology on the outer bar.

INTERTIDAL ZONE (BEACH)

Sediment size (Table 6) and tidal range are constant between the beaches of the two study sites, so that variability in beach morphology results from differences in wave energy levels or in nearshore topography modifying the incoming incident waves. The beaches of the western barrier are generally narrow (20-30 m) (Photograph 1) with a relatively steep beach-face slope (approximately 1:4) (Figure 6). These beaches are characterized by an overall lowering of beach elevation in winter months, due to increased levels of wave activity during this season. This produces a "summer-winter" beach cycle (Figure 7).

The beaches of the eastern barrier are wider (40-50 m) (Photograph 2) and have a flatter beach-face slope (approximately 1:8) (Figure 6). The dominance of storm-wave activity over seasonal variations in wave energy levels on this coast produces beach cycles that are related to erosion during storms and recovery during post-storm conditions. Although the beach elevation is lower in winter months, as compared to the summer (Figure 7), the short-term variability related to storm-wave activity is more significant (Owens, 1977).

The difference in slope of the beach face at the two sites is a reflection of the different effects of nearshore topography on breaking waves. Waves reaching the beach face on the west coast were predominantly plunging breakers, during both study periods, whereas those on the east coast were predominantly spilling breakers. This difference in breaker type results from the different gradients immediately seaward of the intertidal zone. Water depths and gradients are greater at the west study site (Figure 4) due primarily to the presence of a wide low-tide terrace on the east-facing barrier.

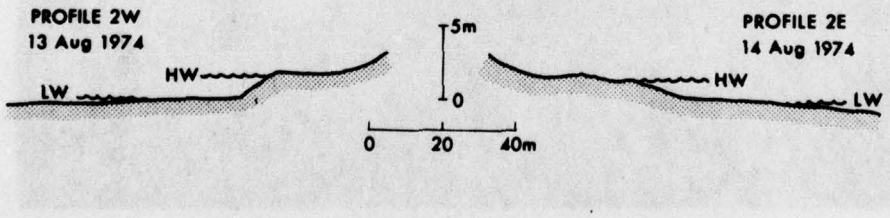

Figure 6. Representative beach profiles for the two study areas.

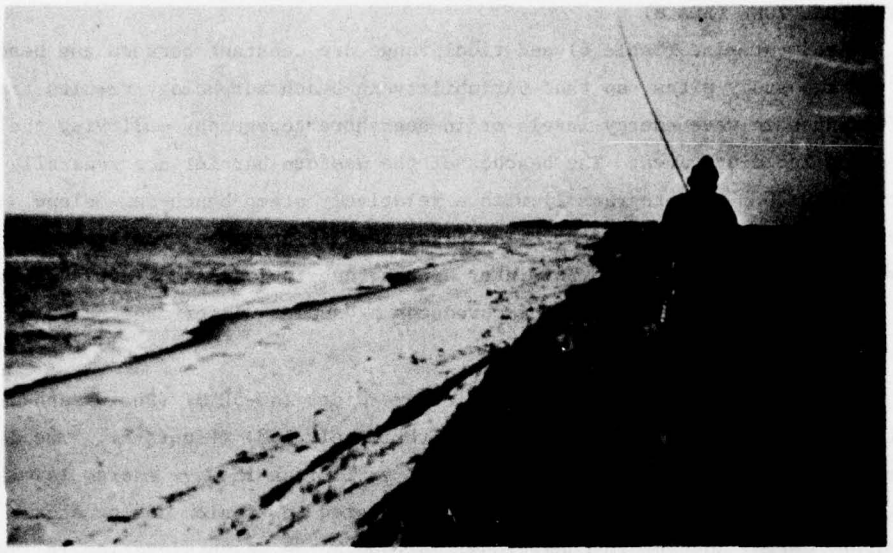

Photograph 1. West study site beach (May 1975).

Photograph 2. East study site beach (August 1974).

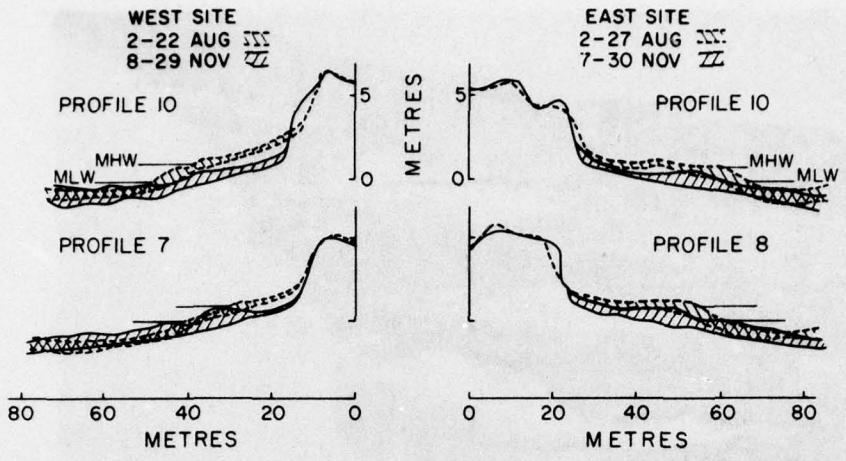

Figure 7. Sweep zone profiles for summer and winter beach profiles at selected locations for the two study sites (after Owens, 1977).

The berm crest was slightly higher on the western beach (Figure 6) as a result of higher wave heights on this coast that lead to a build-up of sand to greater elevations on the berm during high tide periods. Bascom (1954) pointed out that, although storm waves tend to erode the berm, they also create a berm at a greater elevation due to increased wave heights and that they may leave a high, narrow berm that will survive until a larger storm erodes it.

SUBAERIAL ZONE (DUNES)

The dunes on the western barrier are up to 15 m in height, and erosion during major storms produces irregular scarps in the backshore dunes (Photograph 3). During post-storm recovery a new foredune ridge develops adjacent to the beach, leaving an abandoned scarp that is subsequently modified by eolian processes. This pattern of irregular erosion in the backshore, followed by infilling to maintain a regular shoreline, has produced a complex dune topography. The concentration of wave energy at particular locations along the dune barrier is probably a reflection of the effects of the complex nearshore morphology on storm waves.

Photograph 3. Aerial view of dunes at the west study site (August 1974).

The dunes of the east study site are part of a progradational dune-ridge complex (Photograph 4) with a series of parallel ridges that reach 10 m in height adjacent to the beach (Owens and McCann, in preparation). Erosion during storms is relatively constant along this section of barrier, and there is no evidence that the ridges have been breached at any time. This dune-ridge complex is not characteristic of all the east-facing barriers of the Magdalen Islands (Figure 8). Elsewhere dune heights are rarely greater than 5 m and storm-wave erosion causes the development of washover channels that breach the dunes and the development of fan deposits on the lagoonal side of the barrier (Photograph 5).

SUMMARY

The high energy west-facing barriers of the Magdalen Islands are primarily a zone of sediment bypassing. Material that is fed into the nearshore-littoral system is transported rapidly alongshore toward the northeastern and southern extremities. The barriers are relatively stable, with washover deposits occurring only in the updrift sections adjacent to bedrock outcrops

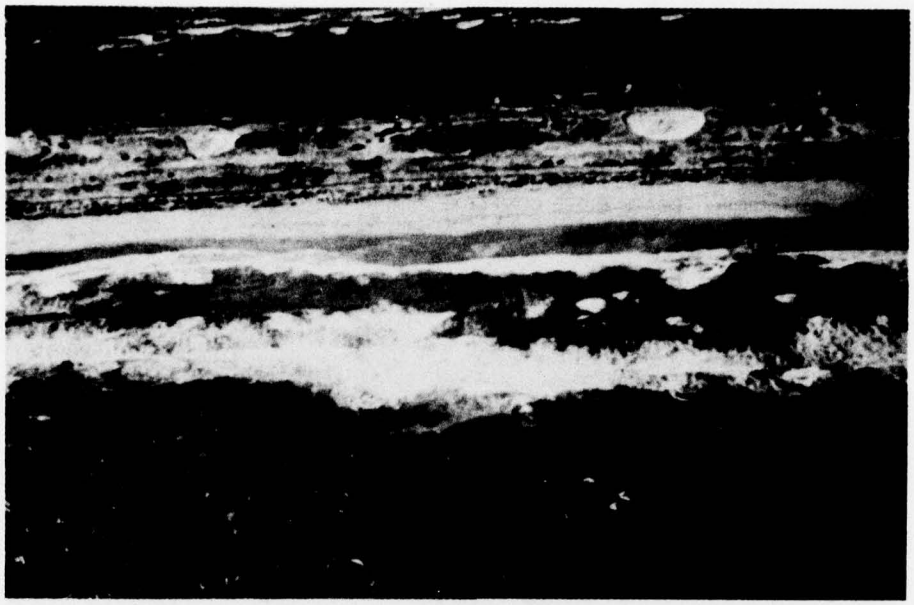

Photograph 4. Aerial view of beach-ridge complex at the east study site (August 1974).

Photograph 5. Washover channels and fan deposits on the east-facing barrier to the north of the east study site (August 1974).

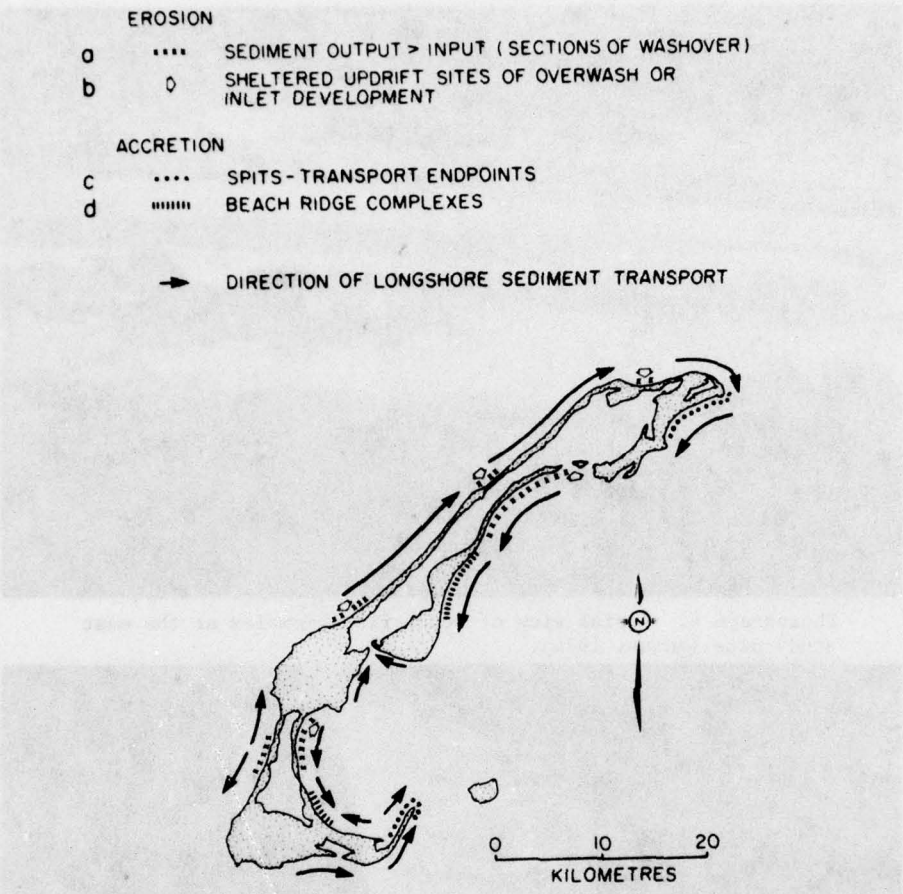

Figure 8. Generalized longshore sediment transport directions and areas of erosion or deposition on the Magdalen Islands barriers.

or, in the case of the southern tombolo, where there is a movement of sediment away from the central section of the barrier (Figure 8). The sheltered, lower energy eastern barriers are both lower and, except for the two beach-ridge complexes, are frequently overwashed. This environment is primarily one of sediment redistribution and deposition, with a net nearshore-littoral transport from northeast to southwest.

These basic mesoscale differences between the two barrier systems are reflected in the morphology and process characteristics of each coast. Spatial variations in offshore, nearshore, beach, and dune morphology can be directly related to the amounts and variability of wave energy levels on the two coasts. The pattern of sediment dispersal in the offshore and nearshore zones is controlled by the dominance of wind-generated waves out of the west (controlling the overall energy levels) and the resulting differences in subaqueous slope gradients (which affect the nearshore wave energy levels).

ACKNOWLEDGMENTS

The research program on the Magdalen Islands was part of a study carried out at the Atlantic Geoscience Centre, Bedford Institute of Oceanography, Dartmouth, Nova Scotia (Geological Survey of Canada Project 740009). Salary support since January 1976 has been provided under a contract with the Geography Programs, Office of Naval Research, Arlington, Virginia 22217. The illustrations were prepared by the Drafting and Illustrations Section of the Bedford Institute and by Mrs. G. Dunn of the Coastal Studies Institute.

REFERENCES

Bascom, W. H., 1954, The relationship between sand size and beach face slope; Trans. Amer. Geophys. Union, 32, 866-874.

Bowen, A. J., and Inman, D. L., 1971, Edge waves and crescentic bars; Jour. Geophys. Res., 76, 8662-8671.

Loring, D. H., and Nota, D. J. G., 1973, Morphology and sediments of the Gulf of St. Lawrence; Fish Res. Board Canada, Bull. No. 182, 147 p.

Owens, E. H., 1975, Barrier beaches and sediment transport in the southern Gulf of St. Lawrence; Proc. 14th Coastal Engr. Conf., Copenhagen, June 1974, A.S.C.E., N.Y., 1177-1193.

Owens, E. H., 1977, Temporal variations in beach and nearshore dynamics; Jour. Sediment. Petrol., v. 47 (in press).

Owens, E. H., and McCann, S. B., in preparation, The coastal geomorphology of the Magdalen Islands, Quebec.

Suhayda, J. N., 1974, Standing waves on beaches; Jour. Geophys. Res., 79, 3065-3071.

Wright, L. D., and Coleman, J. M., 1972, River delta morphology: wave climate and the role of the subaqueous slope; Science, 176, 282-284.

Unclassified
Security Classification

DOCUMENT CONTROL DATA - R & D

(Security classification of title, body of abstract and indexing annotation must be entered when the overall report is classified)

1. ORIGINATING ACTIVITY (Corporate author)	2a. REPORT SECURITY CLASSIFICATION
Coastal Studies Institute Louisiana State University Baton Rouge, Louisiana 70803	Unclassified 2b. GROUP Unclassified

3. REPORT TITLE

PROCESS AND MORPHOLOGY CHARACTERISTICS OF TWO BARRIER BEACHES IN THE MAGDALEN ISLANDS, GULF OF ST. LAWRENCE, CANADA

4. DESCRIPTIVE NOTES (Type of report and inclusive dates)

5. AUTHOR(S) (First name, middle initial, last name)

Edward H. Owens

6. REPORT DATE	7a. TOTAL NO. OF PAGES	7b. NO. OF REFS
December 1977	17	8

8a. CONTRACT OR GRANT NO.	9a. ORIGINATOR'S REPORT NUMBER(S)
N00014-75-C-0192 b. PROJECT NO. NR 388 002 c. d.	Technical Report No. 245 9b. OTHER REPORT NO(S) (Any other numbers that may be assigned this report) A043 720

10. DISTRIBUTION STATEMENT

Approved for public release; distribution unlimited.

11. SUPPLEMENTARY NOTES	12. SPONSORING MILITARY ACTIVITY
Reprint from: Proceedings, 15th Coastal Eng. Conf., Honolulu, Hawaii, July 11-17, 1976, pp. 1975-1991 (Amer. Soc. Civil Engr.).	Geography Programs Office of Naval Research Arlington, Virginia 22217

13. ABSTRACT

Detailed field investigations of barrier beach morphology and processes at adjacent sites in the Magdalen Islands, Gulf of St. Lawrence, show that the two beaches are in distinctly different morphodynamic environments. The differences are expressed in terms of wave energy levels, sediment dispersal patterns, and nearshore, littoral, and dune geomorphology. The exposed west-facing coast has a steeper offshore gradient, is a zone of sediment bypassing, and has a complex sequence of three nearshore bars. Wave energy levels are lower on the sheltered east coast, and this is a zone of sediment redistribution and deposition with a single, linear nearshore bar. The different morphological characteristics of the two barriers are attributed to the spatial variation in energy levels and to the differences in offshore gradients on the two coasts. Computed wave energy values, derived from data monitored during two study periods (August and November, 1974), indicate that the mean wave energy levels were greater on the west coast as compared to the east coast by factors of 2.25 in summer and 2.95 in winter. This is due primarily to the dominance of winds out of the westerly quadrant throughout the year.

14. KEY WORDS	LINK A		LINK B		LINK C	
	ROLE	WT	ROLE	WT	ROLE	WT
Gulf of St. Lawrence, Canada barrier beaches Magdalen Islands beach morphology beach processes						

Unclassified Distribution List
Reports of Contract N00014-75-C-0192,
Project NR 388 002

Office of Naval Research
Geography Programs
Code 462
Arlington, Virginia 22217

Defense Documentation Center
Cameron Station
Alexandria, Virginia 22314

Director, Naval Research Lab
Attn: Technical Information Officer
Washington, D.C. 20375

Director
Office of Naval Research Branch Office
1030 East Green Street
Pasadena, California 91101

Director
Office of Naval Research Branch Office
536 South Clark Street
Chicago, Illinois 60605

Director
Office of Naval Research Branch Office
495 Summer Street
Boston, Massachusetts 02210

Commanding Officer
Office of Naval Research Branch Office
Box 39
FPO New York 09510

Chief of Naval Research
Asst. for Marine Corps Matters
Code 100M
Office of Naval Research
Arlington, Virginia 22217

Office of Naval Research
Operational Applications Div.
Code 200 Arlington, Virginia 22217

Office of Naval Research
Scientific Liaison Officer
Scripps Inst. of Oceanography
La Jolla, California 92038

Director, Naval Research Lab
Attn. Library, Code 2628
Washington, D.C. 20375

Commander
Naval Oceanographic Office
Attn. Library, Code 1600
Washington, D.C. 20374

Naval Oceanographic Office
Code 3001
Washington, D.C. 20374

Chief of Naval Operations
OP 987P1
Department of the Navy
Washington, D.C. 20350

Oceanographer of the Navy
Hoffman II Building
200 Stovall Street
Alexandria, Virginia 22322

Naval Academy Library
U.S. Naval Academy
Annapolis, Maryland 21402

Commanding Officer
Naval Coastal Systems Laboratory
Panama City, Florida 32401

Librarian
Naval Intelligence Support Center
4301 Suitland Road
Washington, D.C. 20390

Office of Naval Research
Code 480
National Space Technology Lab
Bay St. Louis, MS 39520

Commanding Officer
Naval Civil Engineering Lab
Port Hueneme, California 93041

Officer in Charge
Environmental Prediction Research Facility
Naval Post Graduate School
Monterey, California 93940

Dr. Warren C. Thompson
Dept. of Meteorology and Oceanography
U.S. Naval Post Graduate School
Monterey, California 93940

Director
Amphibious Warfare Board
U.S. Atlantic Fleet
Naval Amphibious Base
Norfolk, Little Creek, Va. 23520

Commander, Amphibious Force
U.S. Pacific Fleet
Force Meteorologist
COMPHIBPAC CODE 25 5
San Diego, California 92155

Commanding General
Marine Corps Development and Educational Command
Quantico, Virginia 22134

Dr. A. L. Slafkosky
Scientific Advisor
Commandant of the Marine Corps
Code MC-RD-1
Washington, D.C. 20380

Defense Intelligence Agency
Central Reference Division
Code RDS-3
Washington, D.C. 20301

Director
Coastal Engineering Res. Center
U.S. Army Corps of Engineers
Kingman Building
Fort Belvoir, Virginia 22060

Chief, Wave Dynamics Division
USAE-WES
P.O. Box 631
Vicksburg, Miss. 39180

Commandant
U.S. Coast Guard
Attn: GECV/61
Washington, D.C. 20591

Office of Research and Development
c/o DS/62
U.S. Coast Guard
Washington, D.C. 20591

National Oceanographic Data Center c/o D764
Environmental Data Services
NOAA
Washington, D.C. 20235

Central Intelligence Agency
Attn: OCR/DD-Publications
Washington, D.C. 20205

Dr. Donald Swift
Marine Geology and Geophysics Laboratory
AOML - NOAA
15 Rickenbacker Causeway
Miami, Florida 33149

Dr. Hsiang Wang
Dept. of Civil Engineering
Dupont Hall
University of Delaware
Newark, Delaware 19711

Ministerialdirektor
Dr. F. Wever
Rue/FO
Bundesministerium der Verteidigung
Hardthoehe
D-5300 Bonn, West Germany

Oberregierungsrat
Dr. Ullrich
Rue/FO
Bundesministerium der Verteidigung
Hardthoehe
D-5300 Bonn, West Germany

Dr. Yoshimi Goda
Director, Wave Research Div.
Port and Harbor Research Inst.
Ministry of Transportation
1-1 Nagase, 3 Chome
Yokosuka, 239 Japan

Mr. Tage Strarup
Defence Research Establishment
Osterbrogades Kaserne
DK-2100 Kobenhavn O, Denmark

Prof. Dr. Rer. Nat. H. G. Gierloff-Emden
Institut F. Geographie
Universitaet Muenchen
Luisenstrasse 37/III
D-800 Muenchen 2, West Germany

Prof. Dr. Eugen Seibold
Geol-Palaeontolog. Institut
Universitaet Kiel
Olshausenstrasse 4-60
D-2300 Kiel, West Germany

Dr. R. Koester
Geo.-Palaeontolog. Institut
Universitaet Kiel
Olshausenstrasse 40-60
D-2300 Kiel, West Germany

Prof. Dr. Fuehrboeter
Lehrstuhl F. Hydromechanik U. Kuestenwasserbau
Technische Hochschule Braunschweig
Beethovenstrasse 51A
D-3300 Braunschweig
West Germany

Prof. Dr. Walter Hansen
Direktor D. Instituts f. Meereskunde
Universitaet Hamburg
Heimhuderstrasse 71
D-2000 Hamburg 13,
West Germany

Prof. Dr. Klaus Hasselmann
Institut F. Geophysik
Universitaet Hamburg
Schuleterstrasse 22
0-2000 Hamburg 13, West Germany

Prof. Dr. Nils Jerlov
Institute for Physical Oceanography
Kobenhavns Universitet
Haraldsgade 6
DK-2200 Kobenhavn, Denmark

Mr. William T. Whelan
Telecommunication Ent. Inc.
Box 88
Burtonsville, MD 20730

Dr. H. J. Schoemaker
Waterloopkundig Laboratorium Te Delft
61 Raam, Delft, Netherlands

Ir. M. W. Van Batenberg
Physisch Laboratorium TNO
Oude Waalsdorper Weg 63, Den Haag
Netherlands

Dr. J. Ernest Breeding, Jr.
Dept. of Oceanography
Florida State University
Tallahassee, Florida 32306

Dr. John C. Kraft
Dept. of Geology
University of Delaware
Newark, Delaware 19711

Dr. Dag Nummedal
Dept. of Geology
University of South Carolina
Columbia, South Carolina 29208

ONR Scientific Liaison Group
American Embassy
Room A-407
APO San Francisco, CA 96503

Dr. Choule J. Sonu
Tetra Tech, Inc.
630 North Rosemead Blvd.
Pasadena, California 91107

Dr. Richard A. Davis, Jr.
Department of Geology
University of South Florida
Tampa, Florida 33620

Dr. William T. Fox
Department of Geology
Williams College
Williamstown, Mass. 01267

Dr. John Southard
Dept. of Earth and Planetary Sciences
MIT
Cambridge, Massachusetts 02139

Dr. John T. Kuo
Henry Krumb School of Mines
Seeley W. Mudd Building
Columbia University
New York, New York 10027

Dr. Edward B. Thornton
Department of Oceanography
Naval Postgraduate School
Monterey, California 93940

Prof. C. A. M. King
Department of Geography
University of Nottingham
Nottingham, England

Dr. Douglas L. Inman
Scripps Institute of Oceanography
La Jolla, California 92037

Prof. Toshiyuki Shigemura
Civil Engineering Dept.
National Defense Academy
1-10-20 Hashirimizu
Yokosuka 239, Japan

Prof. Yuji Iwagaki
Civil Engineering Dept.
Kyoto University
9 Shimogamo Zenbucho, Sakyo-Ku
Kyoto, Japan

Prof. Kiyoshi Horikawa
Dept. of Civil Engineering
University of Tokyo
7-3-1, Hongo, Bunkyo-Ku
Tokyo 113, Japan

Dr. William W. Wood
Department of Geosciences
Purdue University
Lafayette, Indiana 47907

Dr. Alan W. Niedoroda
Director, Coastal Research Center
University of Massachusetts
Amherst, Mass. 01002

Dr. Benno M. Brenninkmeyer, S.J.
Dept. of Geology & Geophysics
Boston College
Chestnut Hill, Mass. 02167

Dr. Omar Shemdin
JPL-CALTECH
Mail Stop 183-501
4800 Oak Grove Drive
Pasadena, California 91103

Dr. Lester A. Gerhardt
Rennsselaer Polytechnic Inst.
Troy, New York 12181

Mr. Fred Thomson
Environmental Research Inst.
P.O. Box 618
Ann Arbor, Michigan 48107

Dr. Thomas K. Peucker
Simon Fraser University
Department of Geography
Burnaby 2, B.C., Canada

Dr. Robert Dolan
Department of Environmental Sciences
University of Virginia
Charlottesville, VA 22903

Revised 12-12-77